Universidade de Aveiro Departamento de Engenharia Cerâmica e do Vidro
2009

ANDREIA FILIPA GOUVEIA MACHADO

SÍNTESE E CARACTERIZAÇÃO DE MEMBRANAS DE FAUJASITE
SYNTHESIS AND CHARACTERIZATION OF FAUJASITE MEMBRANES

Universidade de Aveiro Departamento de Engenharia Cerâmica e do Vidro
2009

ANDREIA FILIPA GOUVEIA MACHADO

SYNTHESIS OF FAUJASITE MEMBRANES

Dissertação apresentada à Universidade de Aveiro para cumprimento dos requisitos necessários à obtenção do grau de Mestre em Ciência e Engenharia dos Materiais, realizada sob a orientação científica do Dr. Zhi Lin, Investigador Auxiliar do Centro de Investigação em Materiais Cerâmicos e Compósitos (CICECO) no Departamento de Química da Universidade de Aveiro e do Prof. Dr. Tito Trindade, Professor Associado com Agregação no Departamento de Química da Universidade de Aveiro.
A dissertation presented to the University of Aveiro in partial fulfillment of the requirements for the awarding of the master degree in Materials Science and Engineering carried out under the supervision of Dr. Zhi Lin, Auxiliary Researcher at Research Center for Ceramic and Composite Materials (CICECO) of the University of Aveiro, and Dr. Tito Trindade, Associate Professor with Aggregation at Chemistry Department of University of Aveiro.

Apoio financeiro do POCTI no âmbito do III Quadro Comunitário de Apoio.

Apoio financeiro da FCT no âmbito do III Quadro Comunitário de Apoio.

o júri

presidente

Prof. Dr. Ana Cavaleiro
Professora Catedrática da Universidade de Aveiro

Dr. Stanislav Ferdov
Investigador Auxiliar da Universidade do Minho

Prof. Dr. Tito Trindade
Professor Associado com Agregação da Universidade de Aveiro

Dr. Zhi Lin
Investigador Auxiliar do CICECO, Universidade de Aveiro

acknowledgements

I would like to express my sincere gratitude to all those who gave me the possibility to complete this thesis.

I am sincerely indebt to my supervisors Dr. Tito Trindade and Dr. Zhi Lin, who were always willing to listen, discuss and give advice and for the encouragement throughout this thesis. I wish to thank Dra. Rosário Soares for XRD analysis, Engª Marta Ferro for the help on SEM characterization and Celeste Azevedo for the assistance in the utilization of equipments and providing material when needed.

I would like to thank the collaboration of Professor Adélio Mendes group from FEUP, who helped to enrich the content of this thesis, especially Miguel Teixeira for the permeability and selectivity measurements. I wish to acknowledge FCT for the financial support through the project POCI/EQU/59344/2004.

I am grateful to the members of Chemistry Department for sharing scientific knowledge and making friendly environment, namely Dra. Paula Brandão, Dr. Duarte Ananias, Dr. Fanian Shi and Rita Craveiro.

I would like to acknowledge Prof. Margarida Almeida for her constant encouragement. I would like to thank all my friends from Erasmus Mundus Materials Science, especially Liliana, Amit and Asif for their friendship and motivation.

And last, I wish to thank my family and friends for their endless support and understanding.

palavras-chave

zeólitos, faujasite, membranas, síntese hidrotérmica, caracterização, separação, permuta iónica, prata

resumo

Os processos de separação usando membranas são cada vez mais frequentes para aplicações industriais devido à superioridade técnica e económica deste tipo de metodologia. Os zeólitos são candidatos promissores para membranas de elevado desempenho porque combinam as vantagens das membranas inorgânicas, tais como estabilidade a elevadas temperaturas, resistência a meios agressivos e fácil modificação catalítica, com as características únicas de peneiro molecular, permuta iónica, adsorpção selectiva e catálise típica dos zeólitos. Entre os vários zeólitos, a faujasite é particularmente atractiva porque apresenta a estrutura mais aberta de todos os zeólitos conhecidos. Os seus poros largos (~7.4Å) podem ser usados para aplicações envolvendo moléculas maiores comparativamente com as que podem ser acomodadas em outros zeólitos. O objectivo desta tese consiste na síntese de membranas de faujasite para separação de olefinas/parafinas. Para esta aplicação, o revestimento do suporte e a eliminação de defeitos que criam percursos intrazeolíticos são fundamentais. Desta forma, a optimização das condições de síntese e o conhecimento do efeito de cada variável na microstrutura e qualidade do material são essenciais. As membranas de faujasite foram sintetizadas hidrotermicamente em suportes tubulares de α-Al_2O_3 pelo método de crescimento secundário a partir de géis e soluções. Os suportes foram revestidos por imersão numa suspensão aquosa de cristais de zeólitos e subsequente tratamento a 150ºC. Em seguida, os suportes foram colocados no gel ou solução contendo os precursores de aluminosilicatos e o sistema foi tratado a diferentes temperaturas e em tempos variáveis. As amostras resultantes foram caracterizadas por difracção de raios X e microscopia de varrimento electrónico. A permeabilidade e a selectividade das amostras para misturas de propano/propeno foram também analisadas. Os efeitos da composição da mistura reaccional, tempo e temperatura, repetição das sínteses e cristais usados para revestimento foram também estudados.

Foram obtidas membranas de faujasite de elevado grau de cristalização com uma espessura de 10 μm quando se usaram géis e de 12 μm quando se partiu de uma solução.

Até ao momento, o processo mais usado para a separação de olefinas/parafinas é baseado na destilação criogénica, que envolve elevados recursos energéticos e elevados custos de operação. Neste contexto, o objectivo deste estudo consiste na preparação de uma nova classe de membranas ultramicroporosas com transportadores fixos para serem usadas como uma alternativa para a separação de misturas de propano/propeno. O mecanismo é baseado no efeito sinérgico de adsorpção selectiva, devido à complexação-π entre as olefinas e um ião de um metal (nomeadamente, Ag^+), e de peneiro molecular, uma vez que a prata pode alterar o tamanho dos poros ou a entrada dos mesmos. A combinação destes efeitos pode resultar em membranas com elevada selectividade para as olefinas e, consequentemente, com elevada eficiência em separações de olefinas/parafinas. Os pós de faujasite permutada com prata provaram ser excelentes sorbentes para uma elevada quantidade de processos de purificação incluindo a remoção de dienos das olefinas. Por isso, foram inseridos iões de prata nos poros de membranas de faujasite por permuta em solução aquosa de $AgNO_3$. Como a capacidade de permuta catiónica depende da razão Si/Al na estrutura dos zeólitos, foram testadas membranas de faujasite com diferentes razões Si/Al. As membranas permutadas com prata apresentaram um aumento na selectividade de propano/propeno (1.7-6.3) relativamente às membranas sem prata incorporada (1.0-1.9). Modificando a composição da mistura de alimentação resultou num aumento da selectividade das membranas para misturas de propano/propeno e foi obtido um valor máximo de 8.0. Como resultado, as membranas de faujasite modificadas por permuta iónica com prata são uma promissora alternativa para a separação de misturas de olefinas/parafinas.

keywords

zeolites, faujasite, membranes, hydrothermal synthesis, characterization, separation, ion-exchange, silver

abstract

Membrane processes are increasingly being used in industrial applications due to the technical and economical superiority of this type of method. Zeolite is a promising candidate for a high performance membrane because it combines the general advantages of inorganic membranes such as long-term stability at high temperatures, resistance to harsh environments and easy catalytic modification with the unique characteristics of molecular sieving, ion-exchange, selective adsorption and catalysis typical of zeolites. Among zeolite materials, faujasite is particularly attractive since it has the most open framework of all known zeolites. Their large pores (~7.4Å) can be used for applications involving larger molecules compared to those that can be accommodated in other zeolites. The aim of this thesis consists in the synthesis of faujasite membranes for olefin/paraffin separations. For this application, it is fundamental the coverage of the support and the elimination of defects that creates intrazeolitic pathways. Therefore, the optimization of the synthesis conditions and understanding the effect of each parameter in the final microstructure and quality of the material is crucial. Faujasite membranes have been hydrothermally synthesized on porous α-Al_2O_3 tubular supports by the seeding and secondary growth method from gels and clear solutions. The supports were first seeded using a water suspension containing zeolite crystals by dip coating and dried at 150 ºC. Then, the seeded supports were placed in previously prepared aluminosilicate precursor gels and the whole system was treated at different temperatures with variable times. The obtained samples were characterized by X-ray diffraction and scanning electron microscopy. The samples were also evaluated by permeability and selectivity of a binary mixture of propane/propene. The effects of the composition of the starting mixture, synthesis time and temperature, synthesis repetition and crystals used as seeds have been studied.

High crystalline faujasite membranes have been obtained with a thickness of ca. 10 μm when using a gel and ca. 12 μm when using a clear solution.

To date, the most common process employed for olefin/paraffin separation is based on cryogenic distillation, which involves large energy requirements and high operating costs. In this context, the purpose of this study consists in the preparation a new class of ultramicroporous membranes with fixed carriers used as an alternative approach for the separation of propane/propylene mixtures. The mechanism is based on a synergetic effect of selective adsorption, due to the π-complexation between olefins and a metallic ion (namely, Ag^+), and molecular sieving effects, since silver loading may change pore size or pore entrances. The combination of these effects may result in membranes with improved selectivity to olefins and, consequently, with increased efficiency in olefin/paraffin separations. Silver-exchanged faujasite powder has shown to be an excellent sorbent for a number of purification process including the removal of dienes from olefins. Therefore, silver ions were loaded into the pores of the synthesized faujasite membranes via ion-exchange in $AgNO_3$ solution. Since the cation exchange capacity depends on the framework Si/Al ratio, faujasite membranes with different Si/Al ratio have been tested. Silver ion-exchanged membranes resulted in an increase in the selectivity of propane/propene (1.7-6.3) comparatively to simple faujasite (1.0-1.9). Changing the composition of the feed mixture resulted in an improvement in the selectivity of the membranes for propane/propylene mixtures and a value as high as 8.0 was obtained. Therefore, faujasite membranes modified by ion-exchanged with silver are a promising alternative for the separation of olefin/paraffin mixtures.

TABLE OF CONTENTS

Resumo	**i**
Abstract	**iii**
List of Symbols	vii
List of Abbreviations	viii
List of Figures	ix
List of Tables	xiii

1 Introduction

1.1 Zeolites	1
1.1.1 Structure	1
1.1.2 Properties	3
1.1.3 Applications	6
1.2 Synthesis of zeolites	7
1.2.1 Reaction mechanism during hydrothermal treatment	8
1.2.1.1 Nucleation	12
1.2.1.2 Crystal growth	13
1.3 Zeolitic membranes	13
1.3.1 Synthesis of zeolite membranes	15
1.3.2 Experimental factors affecting the properties of zeolite membranes	17
1.4 Aims of research	18
1.5 References	19

Chapter 2 Faujasite membranes derived from a gel

2.1 Faujasite	23
2.2 Faujasite membranes	24
2.3 Experimental	26
2.4 Results and discussion	28
2.4.1 XRD analysis	29
2.4.2 SEM analysis	31
2.4.2.1 Seeding effect	32
2.4.2.2 Effect of reaction time	34
2.4.2.3 Effect of gel chemical composition	36
2.4.2.4 Synthesis repetition	41
2.4.2.5 Effect of synthesis repetition with gels and clear solutions	43
2.4.2.6 Effect of the support	44

2.5 Conclusions 46
2.6. References 47

Chapter 3 Faujasite membranes grown from clear solution

3.1 Clear solutions 48
3.2 Experimental 48
3.3 Results and discussion 50
3.3.1 XRD analysis 50
3.3.2 SEM analysis 50
3.3.2.1 Effect of seeding 52
3.3.2.2 Effect of time 52
3.3.2.3Effect of repeat synthesis 53
3.3.2.4 Effect of support 56
3.3.2.5 Effect of composition 57
3.3.2.6 Effect of temperature 59
3.4 Conclusions 60
3.5. References 61

Chapter 4 Ion-exchanged membranes

4.1 Ion-exchange theory 62
4.2 Ion-exchanged faujasite for separation applications 64
4.3 Olefins/metal complexation 66
4.4 Silver redox behavior 68
4.5 Separation mechanisms 69
4.5.1 Diffusion 70
4.5.2 Diffusion in zeolites 71
4.6 Experimental 73
4.7 Results 75
4.7.1 SEM 75
4.7.2 EDS 76
4.7.3 Permeability and selectivity 77
4.7.3.1 Effect of Ag^+ on bi-component selectivity 78
4.8 Conclusions 80
4.9 References 81

Chapter 5 General conclusions and future work *83*

List of Symbols

a	term associated to molecular diffusion
b	term associated with Knudsen diffusion
α_B^A	separation factor for ion-exchange
$\alpha_{A/B}$	selectivity for separation
A_s	equivalent fraction of cation A in solution
A_z	equivalent fraction of cation A in zeolite
B_s	equivalent fraction of cation B in solution
B_z	equivalent fraction of cation B in zeolite
C	concentration
C_A	molar fraction of component A
C_B	molar fraction of component B
D_K	coefficient of diffusivity
ΔP_A	pressure difference
l	thickness
L_g	total permeance
L_K	permeability due exclusively to Knudsen diffusion
L_v	permeability due exclusively to molecular diffusion
M	molecular weight
m_{A_z}	molality of cation A in zeolite
m_{B_z}	molality of cation B in zeolite
M_{A_S}	number of cation A per unit volume of the solution
M_{B_S}	number of cation B per unit volume of the solution
μ_m	dynamic viscosity
N_A	normalized flux
N_K	Knudsen flux
N_v	viscous flow
P_A	permeability coefficient
P_h	partial pressure of the gas in the feed side
P_l	partial pressure of the gas in the permeate side
R	gas constant
r_p	radius of the pore
T	temperature
z	length
z_A	charge of cation A
z_B	charge of cation B

List of Abbreviations

BFLM	bulk flow liquid membrane
CHA	chabazite
CVD	chemical vapor deposition
EDS	energy dispersive X-ray spectroscopy
ERI	erionite
FAU	faujasite
FER	ferrierite
GIS	gismondine
GME	gmelinite
IZA	International Zeolite Association
LTA	Linde Type A
LTL	Linde Type L
MOR	mordenite
MRI	magnetic resonance imaging
MTBE	methyl tert-butyl ether
OFF	offretite
PDMS	polydimethylsiloxane
SBU	secondary building unit
SEM	scanning electron microscopy
STI	stilbite
STP	standard temperature and pressure
TEA	triethanolamine
TMA	tetramethylammonium
XRD	X-ray diffraction

List of Figures

Figure 1.1 – Secondary building units (SBUs) in zeolites. The corner of the polyhedral represents T atoms [7].

Figure 1.2 - Univalent cations in zeolites (e.g. Na^{+}) [9].

Figure 1.3 - Divalent cations in zeolites (e.g. Ca^{2+}) [9].

Figure 1.4 - Acidic sites in zeolites.

Figure 1.5 – Molecular sieving effect.

Figure 1.6 – Three examples of zeolite framework and pore system: MFI (left), LTA (centre) and MOR (right) topologies [10].

Figure 1.7 - Zeolite synthesis under hydrothermal condition. The starting materials are transformed in aqueous medium into the crystalline product whose microporosity is determined by their crystal structure.

Figure 1.8 – Steps involved in the synthesis of zeolites from a Na_2O-Al_2O_3-SiO_2-H_2O system [21].

Figure 1.9 – Equilibrium of the starting mixture to establish a partly ordered intermediate (secondary amorphous phase) and a characteristic distribution of solution species [20].

Figure 1.10 - The evolution of order, from the primary amorphous phase (a) through the secondary amorphous phase (b) to the crystalline product (c) [20].

Figure 1.11 – Events taking place upon hydrothermal treatment and in the presence of seeds [86].

Figure 1.12 - Framework structure of a FAU-type zeolite [3].

Figure 1.13 – Flow chart of the synthesis procedure of faujasite membranes.

Figure 1.14 – XRD patterns collected from a powder sample (a); the inside (b) and outside (c) of a membrane synthesized at condition G49 in table 2.1. Stars depict the reflections from the α-alumina support.

Figure 1.15 – XRD patterns collected from a powder sample of (a) faujasite and (b) zeolite P; and (c) the inside of a membrane synthesized at condition G4 in table 2.1. Stars depict the reflections from the α-alumina support.

Figure 1.16 – XRD patterns collected from a powder sample (a); the inside (b) and outside (c) of a membrane synthesized at condition G60 in table 2.1. Stars depict the reflections from the α-alumina support.

Figure 1.17 – Micrograph of the inside surface of the membrane synthesized at condition G46 (left) and G2 (right) in table 2.1.

Figure 1.18 – Top view (left) and cross-section (right) of the outside surface of the faujasite membrane synthesized at condition G49 in table 2.1.

Figure 1.19 – Top view (left) of the inside surface and cross-section (right) of the outside surface of the faujasite membrane synthesized at condition G54 in table 2.1.

Figure 1.20 – The inside surface of the faujasite membrane synthesized at conditions G25 (left) and G40 (right) in table 2.1.

Figure 1.21 – The inside surface of the faujasite membrane synthesized at conditions G50 (top left) and and G51 (bottom left) in table 2.1, using 20 wt.% X seeds, and G53 (top right) and G52 (bottom right) using 20 wt.% Y seeds.

Figure 1.22 – The inside surface of the faujasite membranes synthesized at conditions (from top) G25, G40 and G6 (left images), using 20 wt.% X seeds; G26, G39 and G5 (centre), using 20 wt.% Y seeds and G27, G38 and G4 (right images) using 5 wt.% Y seeds.

Figure 1.23 – The inside surface of the membranes synthesized at conditions G51 (top), G64 (middle left), G65 (middle right), G66 (bottom left) and G67 (bottom right) in table 2.1, corresponding to 5, 24, 48, 72, and 96h, respectively.

Figure 1.24 – The inside surface of the membranes synthesized at conditions G27 (left) and G28 (right) in table 2.1, corresponding to 5 and 8h, respectively.

Figure 1.25 – The inside surface of the faujasite membranes synthesized at conditions G2 (left), corresponding to a molar ratio of $1Al_2O_3:10SiO_2:14Na_2O:829H_2O$, and G38 (right) of a molar ratio $1Al_2O_3:19SiO_2:25Na_2O:1575H_2O$, in table 2.1.

Figure 1.26 – The inside surface of the faujasite membranes synthesized at conditions G6 (left), corresponding to a molar ratio of $1Al_2O_3:10SiO_2:14Na_2O:829H_2O$, and G41 (right) of a molar ratio $1Al_2O_3:19SiO_2:25Na_2O:1575H_2O$, in table 2.1.

Figure 1.27 – The inside surface of the faujasite membranes synthesized at conditions G25 (left), corresponding to a molar ratio of $1Al_2O_3:10SiO_2:12Na_2O:829H_2O$, and G49 (right) of a molar ratio $1Al_2O_3:5SiO_2:7Na_2O:415H_2O$, in table 2.1.

Figure 1.28 – The inside surface of the faujasite membranes synthesized at conditions G29 (top left), G26 (middle left) and G30 (bottom left), corresponding to a molar ratio of $1Al_2O_3:10SiO_2:12Na_2O:829H_2O$, and G56 (top right), G54 (middle left) and G62 (bottom left) of a molar ratio $1Al_2O_3:5SiO_2:7Na_2O:415H_2O$, in table 2.1.

Figure 1.29 – The inside surface of the faujasite membranes synthesized at conditions G46 (top left), corresponding to a molar ratio of $1Al_2O_3:5SiO_2:7Na_2O:415H_2O$, and G2 (right) of a molar ratio $1Al_2O_3:10SiO_2:14Na_2O:829H_2O$, in table 2.1.

Figure 1.30 – The inside surface of the faujasite membranes synthesized at conditions G55 (left), corresponding to a molar ratio of $1Al_2O_3:5SiO_2:7Na_2O:415H_2O$, and G5 (left) of a molar ratio $1Al_2O_3:10SiO_2:14Na_2O:829H_2O$, in table 2.1.

Figure 1.31 – The inside surface of the faujasite membranes synthesized at conditions G62 (left), corresponding to a molar ratio of $1Al_2O_3:5SiO_2:7Na_2O:415H_2O$, and G42 (right) of a molar ratio $1Al_2O_3:19SiO_2:25Na_2O:1575H_2O$, in table 2.1.

Figure 1.32 – The inside surface of the faujasite membranes synthesized at conditions G56 (top left) and G54 (bottom left), corresponding to a molar ratio of $1Al_2O_3:5SiO_2:7Na_2O:415H_2O$, and G41 (top right) and G39 (bottom right) of a molar ratio $1Al_2O_3:19SiO_2:25Na_2O:1575H_2O$, in table 2.1.

Figure 1.33 – The inside surface of the faujasite membranes synthesized at conditions G30 (top left), G29 (top right) and G26 (bottom) corresponding to a molar ratio of $1Al_2O_3$:$10SiO_2$:$12Na_2O$:$829H_2O$, in table 2.1.

Figure 1.34 – The inside surface of the faujasite membranes synthesized at conditions G2 (left) and G16 (right) in table 2.1, corresponding to H_2O/Al_2O_3 ratios of 829 and 1086, respectively.

Figure 1.35 – The inside surface of the faujasite membranes synthesized at conditions G40 (left), G43 (centre) and G44 (right) in table 2.1, corresponding to H_2O/Al_2O_3 ratios of 1575, 1723 and 5000, respectively.

Figure 1.36 – The inside surface of the faujasite membranes synthesized at conditions G25 (top left) and G40 (bottom left) corresponding to one synthesis, and G29 (top right) and G41 (bottom right) in table 2.1, corresponding two syntheses.

Figure 1.37 – The inside surface of the faujasite membranes synthesized at conditions G31 (left) and G34 (right) in table 2.1, corresponding to one and two synthesis, respectively.

Figure 1.38 – The inside surface of the faujasite membranes synthesized at conditions G54 (left) and G55 (right) in table 2.1, corresponding to one and two synthesis, respectively.

Figure 1.39 – The inside surface of the faujasite membranes synthesized at conditions G49 (left) and G57 (right) in table 2.1, corresponding to one and four synthesis, respectively.

Figure 1.40 – The inside surface of the faujasite membrane synthesized at condition G61 (right) in table 2.1.

Figure 1.41 – The inside surface of the faujasite membranes synthesized at conditions G58 (top left) and G57 (bottom left) in table 2.1, corresponding to four synthesis with gel, and G60 (top right) and G62 (bottom right) in table 2.1, corresponding to four synthesis with both gels and clear solutions.

Figure 1.42 – The top view (left) and cross-section (right) of the faujasite membranes synthesized at conditions G54 (top), G52 (middle) and G53 (bottom) on inside surfaces of support tube with 1800, 1000 and 70 nm pores, respectively.

Figure 1.43 – XRD patterns collected from a powder sample (a); the inside (b) and outside (c) of a membrane synthesized at condition C18 in table 3.1. Stars depict the reflections from the α-alumina support.

Figure 1.44 – The inside surfaces of the faujasite membranes synthesized at condition C19 (left) and C24 (right) in table 3.1.

Figure 1.45 – The outside surfaces of the faujasite membranes synthesized at condition C21 (left) and C28 (right) in table 3.1.

Figure 1.46 – The cross-section of the inside surface of the faujasite membrane synthesized at condition C22 (left) and C20 (right) in table 3.1.

Figure 1.47 – The inside surface of the faujasite membranes synthesized at conditions C18 (left) and C28 (right) in table 3.1.

Figure 1.48 – The inside surface of membranes synthesized at conditions C5 (left), C3 (middle) and C4 (right).

Figure 1.49 – The inside surface of membranes synthesized at conditions C1 (5h, left) and C15 (7h, right).

Figure 1.50 – The inside surface of a membrane synthesized at condition C16 (24h, left) and C25 (48h, right).

Figure 1.51 – The inside surface of membranes synthesized with different repletion times at conditions C1 (1 time, top left), C5 (2 times, top right), C7 (4 times, middle left) and C11 (6 times, middle right) and C14 (8 times, bottom). Each synthesis is 5h.

Figure 1.52 – The inside surfaces of membranes synthesized at conditions C16 (24h, top), C17 (24+5h, middle left), C18 (24+24h, middle right), C21 (3 times 24h, bottom left) and C24 (4 times 24h, bottom right).

Figure 1.53 – Internal cross-section view of the membranes synthesized at conditions C18 (top), C21 (bottom left) and C24 (bottom right) corresponding, respectively, to 2, 3 and 4 repetitions of 24h each.

Figure 1.54 – The cross-sections of inside surface of membranes C18 and C21 (top images), C20 and C23 (middle images) and C19 and C22 (bottom images), corresponding to a support with 1800, 1000 and 70 nm pore, respectively.

Figure 1.55 – The inside surfaces of membranes prepared at condition C1 (left) and with a lower sodium content at condition C31 (right).

Figure 1.56 – The inside surfaces of membranes prepared at condition C33 (top), C34 (bottom left) and C35 (bottom right) corresponding to a H_2O/Al_2O_3 ratio of 3000, 2000 and 1000, respectively.

Figure 1.57 – The inside surface of membranes synthesized at condition C5 (left) and C30 (right), corresponding to 80°C and 100°C, respectively.

Figure 1.58 - Schematic representation of the C_2H_4-Ag interactions by π-complexation, showing (A) donation of the π-electrons of ethylene to the 5s orbital of Ag (B) backdonation of electrons from the d_{yz} orbitals of Ag to the antibonding π^* orbitals of ethylene, and (C) redistribution. C also depicts the possible electron redistribution from the $4d_{z2}$ orbitals (the dumbbell and doughnut-shaped orbitals) to the $4d_{yz}$ orbitals [17].

Figure 1.59 - Effect of pore size on the diffusivity and activation energy of diffusion [32].

Figure 4.3 – Flow chart of the synthetic procedure of silver ion-exchanged faujasite membranes.

Figure 4.4 - The outside surface of a faujasite membrane prepared at condition S3 in Table 4.1 before (left) and after (right) ion-exchange with silver in a 0.1M $AgNO_3$solution.

Figure 4.5 - The cross-section of outside surface of a faujasite membrane prepared at condition S3 in Table 4.1 before (left) and after (right) ion-exchange with silver in a 0.1M $AgNO_3$solution.

Figure 4.6 – EDS of sample S20.

Figure 4.7 – EDS of sample S20 after ion-exchange with 0.1M $AgNO_3$.

Figure 4.8 – EDS of sample S20 after ion-exchange with 0.1M $AgNO_3$ with less Ag content.

List of Tables

Table 1.1- Pore structure of zeolites [8]

Table 1.2 – Summary of principal proposals for zeolite synthesis mechanism, 1959-2004 [20]

Table 1.3 – Advantages and disadvantages of inorganic membranes [2]

Table 1.4 – Synthesis conditions for the membrane prepared from a gel

Table 1.5 – Synthesis conditions for the membrane prepared from a clear solution

Table 4.1 – Synthesis conditions of the membranes for permeability measurements

Table 4.2 – Summary of the results for some of the most promising faujasite membranes synthesized without silver exchange.

Table 4.3 – Bi-component selectivity (C_3H_6/C_3H_8) results for faujasite membrane before and after silver ion-exchange, at 25°C.

Table 4.4 – Bi-component selectivity (C_3H_6/C_3H_8) results of silver functionalized membranes for a feed composition of 10%C_3H_6/10%C_3H_8/1%O_2/79%He, at 25°C.

1 Introduction

1.1 Zeolites

Zeolites are a class of materials which name derives from the classical Greek word meaning “boiling stones”. This name was primarily assigned by the Swedish mineralogist Axel Fredrick Cronstedt who, in 1756, discovered that stilbite, a natural mineral, visibly lost water when heated. Although the origin of this material appeared for a long time only in the last past decades they have received considerable attention and turned into essential commercial materials.

Zeolites are a class of crystalline microporous materials with crystallographically well-defined channels and cavities in the molecular range of 0.3 to about 1.5 nm [1]. The zeolite structure consists of a three-dimensional network of TO_4 tetrahedra (T = Si, Al) linked to each other by shared oxygen atoms forming cavities or channels that can be connected by ring or pore openings of defined size and shape [2]. An isolated tetrahedral SiO_4 unit would carry a formal charge of -4, but the overall zeolite framework formed from SiO_4 units is neutral, because each oxygen atom is shared by two T atoms (where T is a tetrahedrally coordinated atom). On the other hand, the net formal charge of the AlO_4 units is -5, so that the overall zeolite framework containing AlO_4 units is negatively charged [3]. Due to this, most zeolites contain water, organic molecules or exchangeable cations in their channels to balance the anionic charge of the framework. The crystalline structure comprised of various combinations of tetrahedral SiO_4 or AlO_4 enables the zeolite to have monodisperse pore size distribution and better mechanical strength compared with amorphous materials [4].

The general empirical formula of zeolites is:

$$M_{x/m}Al_xSi_{2-x}O_4 \cdot nH_2O$$

where *m* is the valence of cations *M*, *n* the water content and $0 \leq x \leq 1$ [5].

1.1.1 Structure

The attractive properties of zeolites are mainly related to their structure. Due to the lack of proper identification techniques the determination of structures was hindered for a long time, and only with the discovery of X-ray diffraction at the beginning of the 20th century, systematic studies were initiated on zeolite identification. Although originally defined as aluminosilicates with anionic frameworks, the definition of zeolites has, sometimes, expanded to include silicates, aluminophosphates, silicoaluminophosphates, gallosilicates, titanosilicates, metallosulfides, metallo-oxides, etc. Some of these new members of the zeolite family have neutral frameworks [6]. The International Zeolite Association provides the classification by framework type which is available in IZA website or in the Atlas

of Zeolite Framework Types. Until March 2009, 191 framework types have been accepted by this commission.

The zeolites frameworks are comprised of assemblies of TO_4, which share vertices to form secondary building units (SBUs). The simplest of these are the n-rings, e.g. 4-rings, 8-rings, and 12-rings, where n is the number of T atoms in a ring. There are presently 23 SBUs (figure 1.1). They are interconnected to form a wide range of polyhedra which in turn connect to generate the infinitely extended frameworks of the various specific crystal structures.

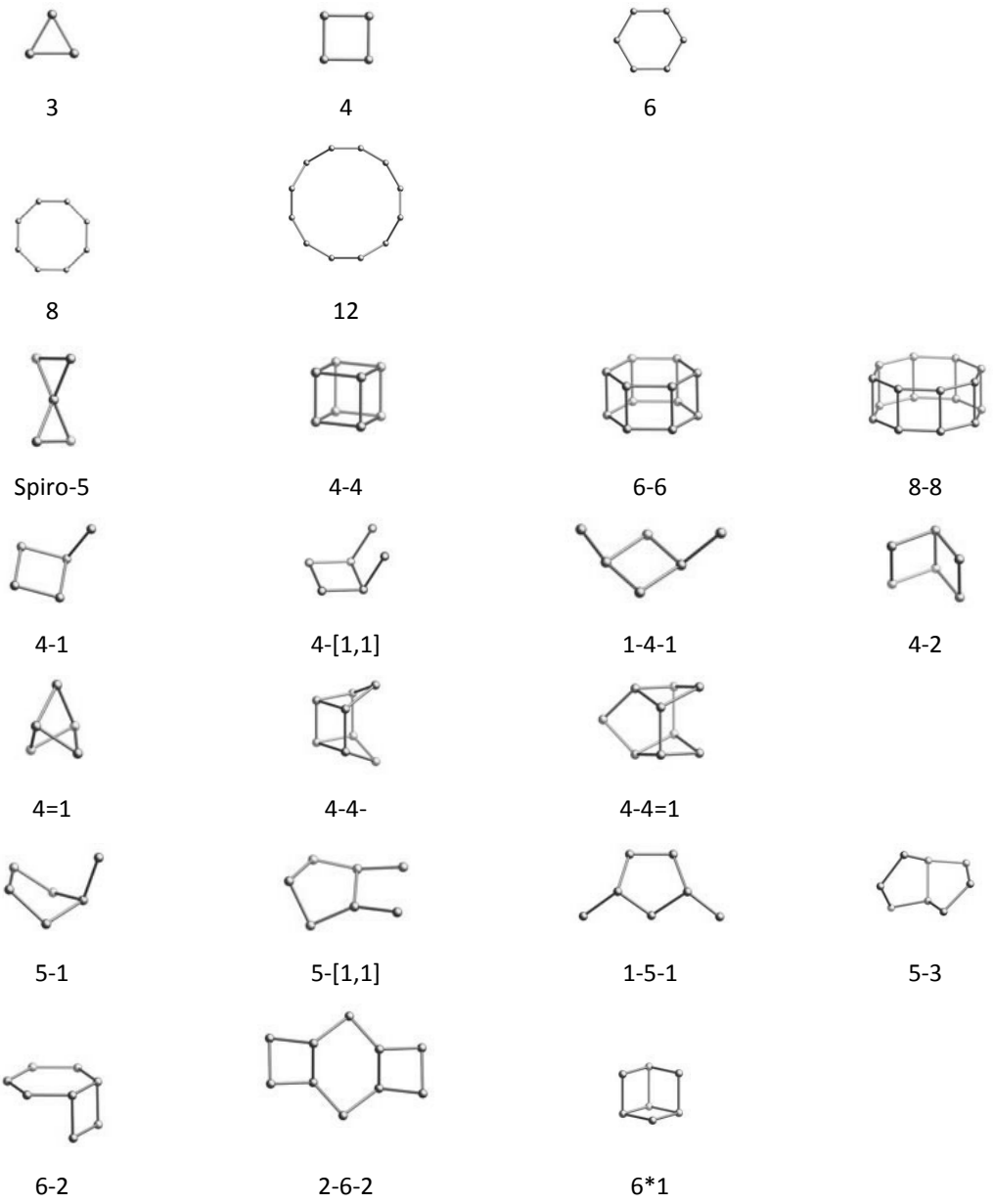

Figure 1.1 – Secondary building units (SBUs) in zeolites. The corner of the polyhedral represents T atoms [7].

Another way to classify zeolites is to take into account their pore openings and the dimensionality of their channels. Thus, one distinguishes small pore zeolites (6-, 8-, and 9-membered rings), medium pore zeolites (10-membered rings), large pore zeolites (12-membered-rings), and ultralarge pore structures (14-, 18- or 20-membered rings). Table 1.1 describes some pore structures of zeolites using pore openings and dimensions. This classification simplifies comparisons in terms of adsorptive, molecular sieving and catalytic properties.

Table 1.1- Pore structure of zeolites [8]

Type Code	Name	Pore system	Pore dimensions (Å)
CHA	Chabazite	8	3.8 × 3.8
ERI	Erionite	8	3.6 × 5.1
FAU	Faujasite (X,Y)	12	7.4
FER	Ferrierite	10; 8	4.2 × 5.4; 3.5 × 4.8
GIS	Gismondine	8	3.1 × 4.5; 2.8 × 4.8
GME	Gmelinite	12; 8	7.0 ; 3.6 × 3.9
LTA	Linde Type A	8	4.1
LTL	Linde Type L	12	7.1
MEL	ZSM-11	10	5.1 × 5.5
MFI	ZSM-5	10	5.4 × 5.6; 5.1 × 5.5
MOR	Mordenite	12 ; 8	6.5 × 7.0; 2.6 × 5.7
OFF	Offretite	12 ; 8	6.7 × 6.8; 3.6 × 4.9
RHO	Rho	8	3.9 × 5.1
STI	Stilbite	10; 8	4.7 × 5.0; 2.7 × 5.6

1.1.2 Properties

Several properties account for the extensive use of zeolites and their importance in a wide range of applications. They have a high internal surface area, high thermal stability, ion exchange properties and the ability to separate molecules based on shape or size. In addition, the zeolite frameworks can be modified by synthesis with T-metal cations other than aluminum and silicon in the framework (isomorphous substitution) or by dealumination (to increase the hydrophobicity of the zeolite). These changes imply an irreversible change of their ion exchange, catalytic or adsorption properties [3]. All the factors mentioned make zeolites unique materials. The most important properties are briefly described in detail.

❖ **Ion exchange**

The presence of negative charges in the framework of zeolites must be balanced by extraframework uni- or divalent cations (figures 1.2-1.3), the amount of which is determined by the Si/Al ratio of the framework. These extraframework cations can be exchanged by other cations provided they are excluded from the pores, which changes the stability, adsorption behavior and selectivity, catalytic activity and other physical properties. Therefore, through ion-exchange it is possible to tune the zeolitic properties for specific applications.

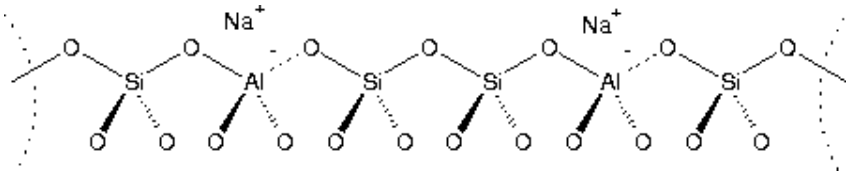

Figure 1.2 - Univalent cations in zeolites (e.g. Na^{+}) [9].

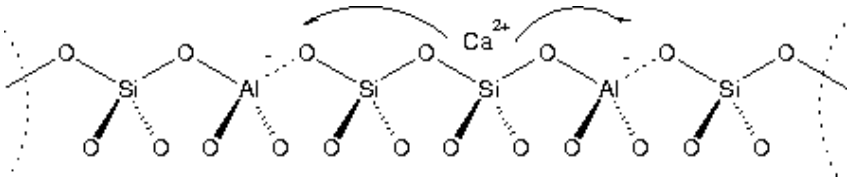

Figure 1.3 - Divalent cations in zeolites (e.g. Ca^{2+}) [9].

The cation exchange behavior of zeolites depends upon several factors, namely, the nature of cation species, the cation size and cation charge, the temperature, the concentration of the cations species in solution, the anion species associated with the cation in solution, the solvent and the structural characteristics of the zeolite.

❖ **Acidity**

The presence of cations that preserves the solid neutrality creates an acid site if protons act as counterions. Figure 1.4 represents typical zeolite acidic sites. Proton compensates the negative charge of the framework. This confers the zeolite a very strong acidity, about 1000 stronger than that of amorphous aluminosilicates [5], with important consequences that in part explain their large use in catalytic applications.

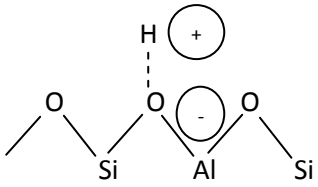

Figure 1.4 - Acidic sites in zeolites.

❖ **Molecular sieving**

One of the most important properties of zeolites is their ability to perform separation of molecules based on their size and shape. While molecules with dimension smaller than the pore size can pass through, bigger molecules are rejected, as shown schematically in figure 1.5:

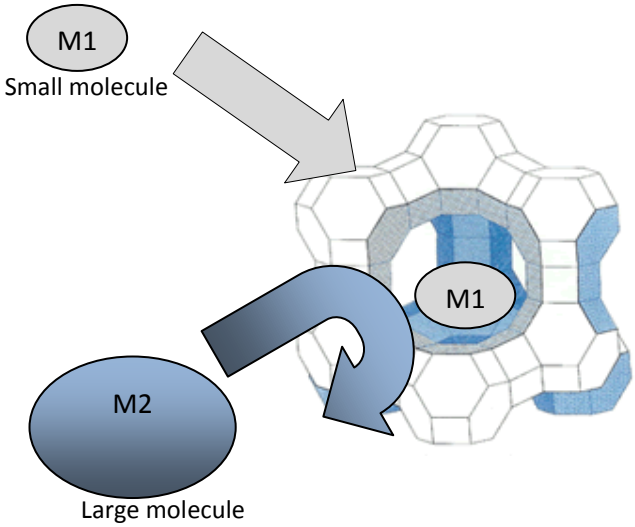

Figure 1.5 – Molecular sieving effect.

The discrimination can occur so sharply that the molecules with even sub-Å size difference can be separated by zeolites, which are crystalline materials. This molecular sieving effect is a unique and inherent characteristic of zeolites and related the crystal structure of the materials [4]. This is explained by their pore systems that contain pores of different sizes in the order of molecular dimension (from about 0.3 to 1.2 nm) and can be one, two or three-dimensional, which is determined by the crystal structure. The variability in pore dimensions (figure 1.6) as well as the very high internal surface area (>500 m^2/g) are responsible for catalytic shape selectivity of zeolites. The reactions within zeolites can be inhibited if certain molecules and a sterically confined environment allowing conversion of reactants are not matched each other.

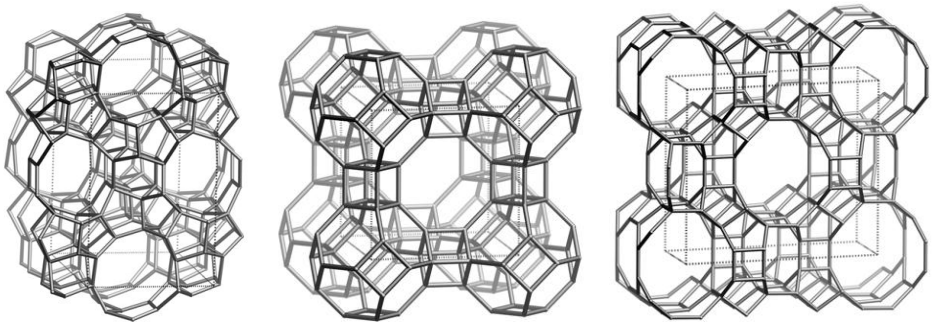

Figure 1.6 – Three examples of zeolite framework and pore system: MFI (left), LTA (centre) and MOR (right) topologies [10].

Shape selectivity in zeolites was first observed by Weisz and Frilette in 1960. Since then this phenomenon has been thoroughly documented in literature. The molecular shape selectivity in zeolites can occur through different mechanisms [11]:

Reactant selectivity: some molecules preferentially enter the pores of zeolites and diffuse freely within the intracrystalline volume of the zeolite, while others are rejected due to diffusion constraints, selective sorption, or molecular sieving effects. This type of selectivity is observed in processes such as molecular shape-selective cracking, hydrocracking and selectoforming.

Product selectivity: some reaction products or intermediates are too bulky to diffuse. They can be either converted to smaller molecules or deactivate the catalyst due to the pore blocking. After reaction has occurred, products must diffuse away from the micropores which results in a kind of molecular traffic control. It is important in processes, such as, the selective production of para-aromatic compounds over ZSM-5 zeolite based catalysts.

Transition state selectivity: it is observed when local configuration constraints (space around the catalytic active sites) prevent or decrease the occurrence probability of a given transition state. Transition state selectivity can be observed in processes such as isomerization reactions of alkyl-benzenes.

1.1.3 Applications

Zeolites are widely used for different applications. Several properties account for their commercial use: they are good adsorbents, excellent solid catalysts and show a very high selectivity. They are utilized in the recovery of our environment, such as the removal of radioactive Sr^{2+} and Cs^{+} from contaminated waste solutions [12]; removal of carbon dioxide [13] and sulfur compounds [14] from natural gas; removal of atmospheric pollutants such as sulphur dioxide [15]; removal of heavy metals from the environment, e.g., cobalt, zinc, copper and manganese ions [16]. As examples of medical applications, Hemosorb and Quikclot are zeolite-based commercial products, applied to wounds to cease bleeding, or in kidney dialysis machines to absorb ammonia from blood and prevent it from accumulation [17-18]. Zeolites are the most widely used water softening agents in the detergent industry due to their ion-exchange capability. The ability to separate water or small molecules contributes to desiccation and gas purification. Due to the molecular sieving effect, zeolites can separate molecules with very small size difference, such as n-alkanes from branched alkanes [19]. They are used as heterogeneous acid catalysts in many commercial processes such as catalytic cracking, hydrocracking, selectoforming, hydroisomerization, dewaxing, alkylation, methanol to gasoline conversion, NO_x reduction, etc. Moreover, they can be used for shape selective catalysis, e.g., in the transalkylation reaction of 1,3-dimethylbenzene, in which the methyl group cannot access 5-position carbon benzene

(the part with no methyl groups) due to spatial confinement inside the pore. Hence, only 1,3,4-trimethylbenzene is formed instead of 1,3,5-trimethylbenzene. The application of zeolitic materials has been actively expanded into new fields during the last decade. Various morphologies of zeolites, such as self-standing films, fibers, and micropatterns, have been synthesized. Especially, zeolite-based films are expected to have high potential as separation devices, membrane reactors, chemical sensors, and host for guest species in optical applications. Zeolitic materials have also been developed as contrast agents for magnetic resonance imaging (MRI). Gd^{+} is an excellent contrast agent for MRI, but its toxicity forbids its use. When Gd^{+} is impregnated in zeolites, the composite shows benign toxicity. In addition, zeolite can be used as a reactor for single-walled carbon nanotubes. The synthesized tube with 0.4 nm diameter shows superconductivity [4]. This diversity in zeolite applications makes it a particularly interesting material to study and enlighten the attention devoted to this type of materials.

1.2 Synthesis of zeolites

The synthesis of zeolites has been extensively reviewed in several books and the literature on this topic is vast. Usually, it is carried out under hydrothermal conditions. An aluminate and a silicate solution are mixed in an alkaline medium, and then treated at temperatures above ambient (usually between 60-180°C) and under autogeneous pressures during hours or days, as shown in figure 1.7.

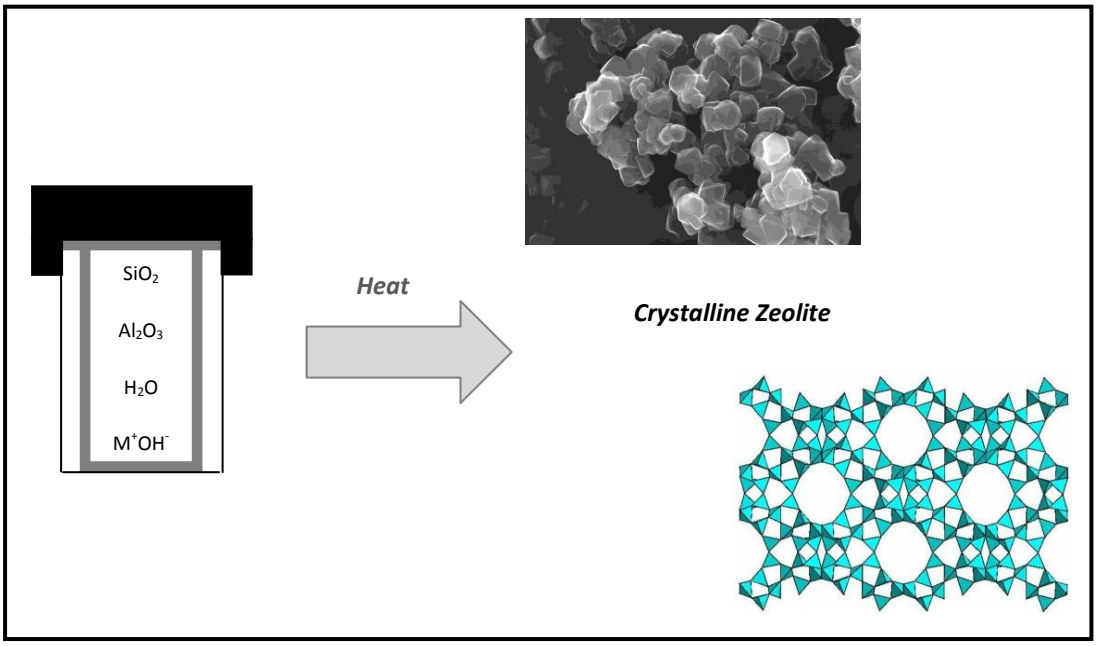

Figure 1.7 - Zeolite synthesis under hydrothermal condition. The starting materials are transformed in aqueous medium into the crystalline product whose microporosity is determined by their crystal structure.

The main steps involving the Na_2O-Al_2O_3-SiO_2-H_2O system which is used in synthesizing zeolites of types A, X and Y, are shown in figure 1.8:

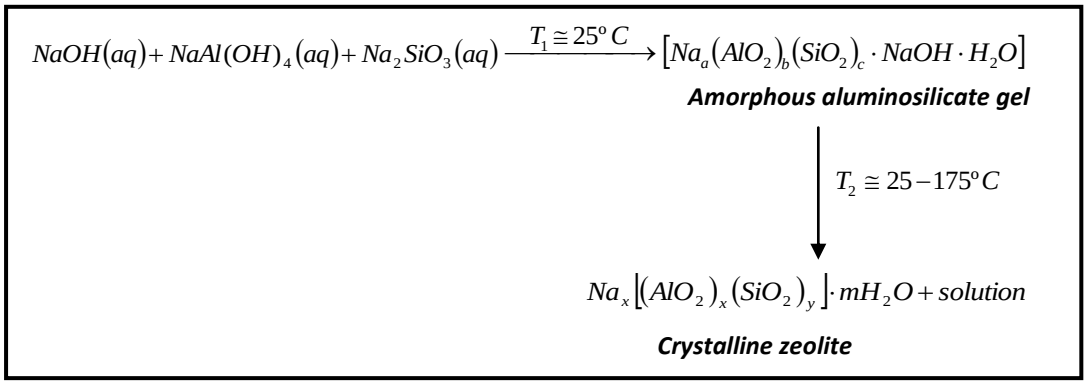

Figure 1.8 – Steps involved in the synthesis of zeolites from a Na_2O-Al_2O_3-SiO_2-H_2O system [21].

Usually, the original mixture becomes viscous shortly after mixing, due to the formation of an amorphous phase, i.e., an amorphous aluminosilicate gel. The gel formation is probably due to the copolymerization of the silicate and aluminate species by a condensation-polymerization mechanism. As the synthesis proceeds at elevated temperature, nucleation of zeolite crystals occurs first, and these zeolite nuclei extend the structure by consuming aluminosilicate material from the solution phase. At the same time, the amorphous gel phase is dissolved to replenish the solution with aluminosilicate species. As a result of the transformation of amorphous gel to crystalline zeolite, by transport of material through the solution phase, the amount of zeolite crystals relative to amorphous gel increases as the synthesis proceeds [22]. This is a simplified model since in the real crystallization process, different Si and Al species exist in solution, the crystallization process does not take place at an identical condition and different zeolite phases as well as nonporous materials can form at different period of synthesis time. Moreover, the different species in precursor do not exist independently from each other. The sum of all silicate, aluminosilicate, aluminate, alkali and template species form a pH- and temperature-dependent precursor. During nucleation and crystal growth, certain species are consumed from the solution. This leads to pH and concentration changes and to the establishment of new equilibriums until a lower concentration limit of precursors in solution is reached and crystal growth stops [23]. Zeolites crystallize easily due to the high reactivity of the gel, the concentration of the alkali hydroxide, and the high surface activity due to the small particle size of the solid phases concerned [24].

1.2.1 Reaction mechanism during hydrothermal treatment

The formation mechanism of zeolite under hydrothermal condition is complex and involves several steps, such as, molecular level self-organization, nucleation and growth [25].

Several studies have been performed on the kinetics and mechanism of zeolite formation, particularly, on the synthesis of zeolite A, faujasite, and more recently on ZSM-5 and mordenite. The

most important studies are described in Table 1.2. At the beginning these studies have been controversial. Barrer et al. [26] suggested a solution transport mechanism and proposed that the nucleation was the result of the polymerization of aluminate, silicate and possibly more complex ions in the liquid phase. The gel dissolution was responsible for the continuous supply of ions necessary for polymerization. Zhdanov [27] in a detailed review proposed a solution-mediated transport mechanism and showed that the nuclei of zeolite crystals begin to form in the liquid phase of precursors or at the interface of gel phase. The growth of crystal nuclei proceeds at the consumption of aluminosilicate hydrated anions (different combinations of Si-O and Al-O tetrahedra) present in the solution. The solution mechanism was also supported by Kerr [28] who reported on a study of the rate of crystallization of zeolite A. The crystallization occurred rapidly after an induction period, which was concluded to be due to the formation of nuclei, and the crystal growth occurred by deposition of some dissolved sodium aluminosilicate species on the crystal surface.

McNicol et al. [29-30] proposed a solid phase transformation mechanism for zeolites A and faujasite formations, involving zeolite crystallization in the solid gel phase via condensation between hydroxylated Si-Al tetrahedra. Polak et al. [31-32], who studied the formation of zeolites X and Y, was in agreement with the solid phase transformation. A similar mechanism was proposed by Flanigen [33] who considered the reordering of the hydrogel to an ordered crystalline state via surface diffusion in the absence of liquid phase transport. Derouane et al. [34-35] studied the synthesis of zeolite ZSM-5 and concluded that both the liquid phase ion transportation mechanism and solid hydrogel phase transformation mechanism are important, depending on the silica source and the gel formulation used. In the former mechanism only a few nuclei are formed, yielding large crystallites, whereas the latter involves numerous nuclei yielding polycrystalline aggregates. However, by using a combination of chemical analyses, Raman spectroscopy, XRD, sorption and particle size measurements, Angell and Flank [36] reached the opposite conclusion. They demonstrated that the mechanism involved formation and subsequent dissolution of an amorphous aluminosilicate intermediate, with solution transport from the gel to the growth surface of the crystallite. This view was reinforced by two further synthetic studies. Culfaz and Sand [37] examined crystallization rates for mordenite, zeolite X and zeolite A. From considerations of rate limitations by diffusion and seed crystal surface area, they deduced that crystal growth in these cases occurred from solution. Kacirek and Lechert [38] used detailed kinetic studies on seeded faujasite syntheses to develop further the solution growth model, concluding that the rate-determining step was the connection of silicate species to the surface of the crystal. They also pointed out that, under their conditions, the solution phase would contain essentially only monomers and dimers during the crystallization of zeolite X, and higher oligomers (perhaps up to Si20) present in the synthesis of the more siliceous Y-types.

Table 1.2 – Summary of principal proposals for zeolite synthesis mechanism, 1959-2004 [20]

Author(s) [Ref.]	Principal system studied	Main features of mechanism	Schematic summary
Barrer [26,39]	Various low-silica phases	Condensation polymerisation of polygonal and polyhedral anions	
Flanigen and Breck [40-42]	Na-A, Na-X	Linkage of polyhedral (formed by M^+-assisted arrangement of anions): crystal growth mainly in the solid phase	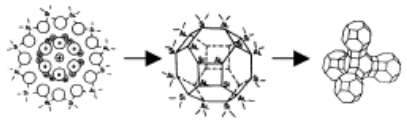
Kerr [28,43]	Na-A	Crystal growth from solution species	$\text{Amorphous solid} \xrightarrow{\text{fast}} \text{soluble species(S)}$ $\text{(S)} + \text{nuclei(or zeolite crystals)} \xrightarrow{\text{slow}} \text{zeolite A}$
Zhdanov [27]	Na-A, Na-X	Solid ⟷ liquid solubility equilibrium, nuclei from condensation reactions, crystal growth from solution	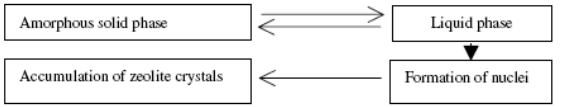
Derouane, Detremmerie, Gabelica and Blom [34-35]	Na,TPA-ZSM-5	Synthesis "A": liquid phase ion transportation. Synthesis "B": solid hydrogel phase transformation	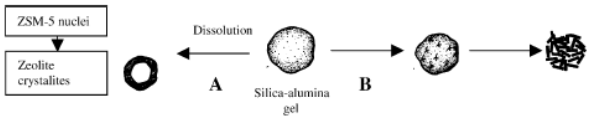
Chang and Bell [44]	Na,TPA-Si-ZSM-5	Embryonic clathrate TPA-silicate units, ordered into nuclei through OH^--mediated Si-O-Si cleavage/recombination	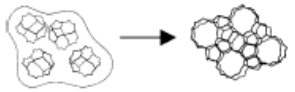
Burkett and Davis [45-47]	TPA-Si-ZSM-5	Pre-organised inorganic-organic composites, nucleation through aggregation, crystal growth layer-by-layer	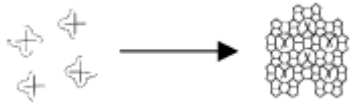
Leuven Group [48-54]	TPA-Si-ZSM-5	Oligomers ⟶ precursor "trimer" (33Si) ⟶ ×12 ⟶ "nanoslabs", growth by aggregation	

Several groups of authors have commented upon the existence of the secondary amorphous phase. Angell and Flank [36] reported that the initial gel is converted via solution transport to an apparently amorphous aluminosilicate intermediate, which is later converted to crystalline zeolite via dissolution by the basic medium. Fahlke et al. [55] observed an immediate precipitation of a silica-rich primary gel, followed by its slow dissolution and then the precipitation of a secondary gel having a similar Si/Al ratio to that of the zeolite product. At the point where the synthesis reactants are initially mixed together, a visible gel is frequently formed. This will be referred to as the primary amorphous phase. In some cases (''clear solution'' syntheses), this primary phase is colloidal, and thus invisible to the naked eye, but its function and behavior are essentially the same. The primary amorphous phase represents the initial and immediate product from the reactants and is a non-equilibrium and probably heterogeneous product containing (for example) (a) precipitated amorphous aluminosilicates, (b) coagulated silica and alumina precipitated from starting materials due to the destabilization induced by the change in pH and increase in salt content and (c) raw reactants. After some time, either on standing, or—more rapidly— on heating at reaction temperature, the above mixture undergoes changes due to the equilibration reactions which occur and is converted into a pseudo-steady-state intermediate, the secondary amorphous phase. Concurrently, the relationship between the solid and solution phases approaches equilibrium and a characteristic distribution of silicate and aluminosilicate anions is established (figure 1.9).

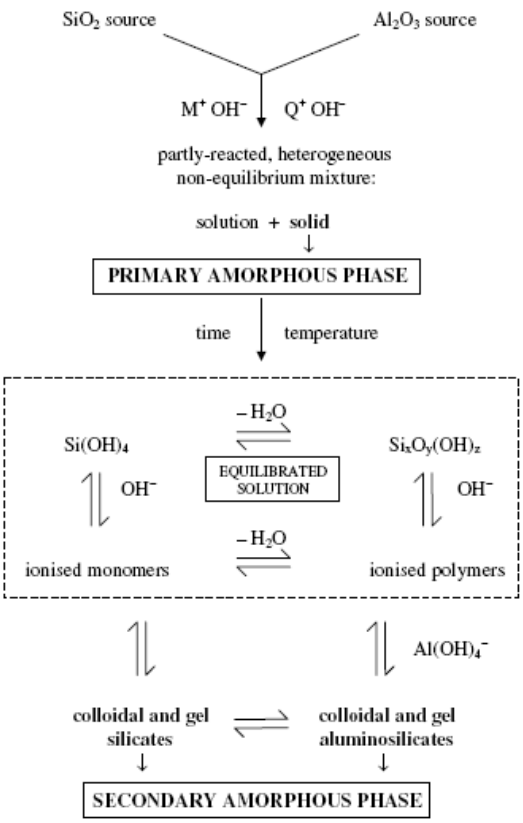

Figure 1.9 – Equilibrium of the starting mixture to establish a partly ordered intermediate (secondary amorphous phase) and a characteristic distribution of solution species [20].

In the final stage of the synthesis (usually at elevated temperature for a prolonged period), the secondary amorphous phase is converted into the crystalline zeolite product (figure 1.10). The concept of an equilibrated intermediate phase is clearly expressed in Zhdanov's representation of the synthesis process [27] and is also implied in the type-A and type-B schemes of Derouane et al. [34].

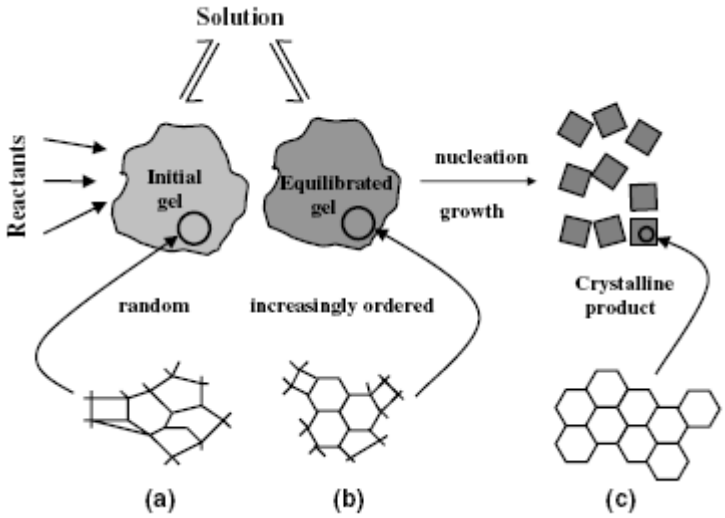

Figure 1.10 - The evolution of order, from the primary amorphous phase (a) through the secondary amorphous phase (b) to the crystalline product (c) [20].

1.2.1.1 Nucleation

The nucleation is the process by which the periodic zeolite lattice is established and is able to propagate. It basically consists in:

(a) the mixture of the reactants to give a non-equilibrate, inhomogeneous starting material (primary amorphous phase),

(b) its equilibrium for the creation of a semi-organized precursor (secondary amorphous phase),

(c) the formation of sufficient regular structure which is propagated (the nucleation step itself),

(d) the onset of crystal growth on the established nuclei.

For the formation of these ordered structures several nucleation mechanisms can be followed in liquid-solid systems. They have been divided into several categories as follows:

1. **Primary nucleation** characterized as being driven by the solution itself, either strictly within the solution (homogeneous nucleation), or catalyzed by extraneous material in the solution (heterogeneous nucleation).

2. **Secondary Nucleation** is catalyzed by the presence of parent crystals of the same phase. The seed crystals might be added at the beginning of a synthesis (initial breeding) or might be generated in the system by fluid shear, collision breeding or fracture [56].

1.2.1.2 Crystal growth

Most crystallization processes involve assimilation of material from simple species in solution. The crystalline region is extended from nucleus by the acquisition of growth units from solution. These are replenished by the adjustment of solution equilibrium and the dissolution of amorphous (or less ordered) material. A debate has arisen regarding what species are added to the crystal surface to promote growth and whether an agglomeration mechanism plays a role in zeolite crystal growth. Schoeman [57] postulated that the agglomeration will not be possible in silicate synthesis solution and that the crystal growth was sustained by the addition of low molecular weight species, most likely the monomer. However, Kirschhock, et al. [52] showed that the agglomeration in crystal surfaces was possible. They noted that the nanoparticles should be at about 7 Å near the crystal surface in a potential well, and have enough time to orient and chemically bond to the surface. More recently, Nikolakis, et al. [58] analyzed silicalite crystal growth and the energy of nanoparticle-crystal interactions using atomic force microscopy. They have also concluded that zeolite crystal growth by nanoparticle addition was possible, even though their total potential energy curves showed no potential wells or negative values at distances greater than a fraction of an angstrom. The related studies are still going on. Thus, growth by addition of monomers, low molecular weight species, or nanoparticles cannot be ruled out. The growth in different crystal systems and under different synthesis conditions could follow different mechanisms.

1.3 Zeolitic membranes

Membrane processes are increasingly being used in industrial applications due to the technical and economical superiority of this type of method. Their characteristics, which includes low capital investment, simplicity and ease of installation and operation, low maintenance and energy requirements, low weight and space requirements, high process flexibility, high selectivity and permeability for the transport of specific components, easy control and scale-up, and environment compatibility, explain the advantages relative to other competing technologies [59]. These properties make them used on a large scale to produce potable water from sea and brackish water, to clean industrial effluents and recover valuable constituents, to concentrate, purify, or fractionate macromolecular mixtures in the food and drug industries, and to separate gases and vapors in petrochemical processes. They are also key components in energy conversion and storage systems, in chemical reactors, in artificial organs, and in drug delivery devices [60].

During the last decades a lot of effort and dedication has been devoted to the development of stable inorganic membranes, the characteristics of which are exhibited in Table 1.3. Their advantages encouraged increasing studies in order to overcome the disadvantages in the application of the membrane processes. Among the inorganic materials, zeolite is a promising candidate for a high performance membrane because it combines the general advantages of inorganic membranes with the unique characteristics of zeolite crystals such as molecular sieving, ion-exchange, selective adsorption and catalysis [61]. They are attractive for a variety of reasons, namely, steady-state operation, tailored selectivity, low energy consumption, and potential for combined reaction-separation systems [62]. These properties make them useful in applications such as separation processes, chemical synthesis and sensor devices [25]. They can perform difficult separations, such as, in mixtures of compounds with close boiling-points, similar molecular weight or even species that form azeotropes. The use of zeolite membranes in reactors has been promoted in different functions, namely, the selective removal of products (e.g., removal of hydrogen from dehydrogenation systems) and selective addition of reactants (e.g., controlled addition of oxygen to oxidative decomposition system of methane) [63]. Furthermore, due to their intrinsic catalytic properties it is possible to conceive reactors where the membrane performs the reaction and separation functions, improving the reaction conversion or selectivity [64]. The discrimination between subnanometer molecules made them useful for the separation of gas mixtures under severe conditions where organic membranes do not functionalize [65].

Table 1.3 – Advantages and disadvantages of inorganic membranes [2]

Advantages	**Disadvantages**
Long-term stability at high temperatures	High capital
Resistance to harsh environments	Brittleness
Resistance to high pressure drops	Low membrane surface per module volume
Inertness to microbiological degradation	Difficulty in achieving high selectivities in large-scale microporous membranes
Easy regeneration after fouling	Generally low permeability of the highly selective (dense) membranes at medium temperatures
Easy catalytic modification	Difficult membrane-to-module sealing at high temperatures

The first zeolite membrane preparation was patented by Suzuki in 1987. Since then, small-pore (A-type), medium-pore (MFI-, MEL-, and FER-type) and large-pore (MOR- and Y-type) zeolite membranes have been prepared mainly on stainless steel and alumina supports [66]. Falconer et al. [67] prepared silicalite zeolite membranes on a porous, tubular, α-alumina support. Bakker et al. [68] prepared a silicalite-1 membrane on a metal support and studied the permeation behavior of several gases, such as, hydrogen and methane through the membrane. Matsukata et al. [69] synthesized defect-free mordenite membranes on porous alumina supports, with a separation factor of benzene/p-xylene higher than 160.

Matsukata et al. [70] also prepared mordenite membranes on the outer surface of a porous α-alumina tube by seed-assisted crystallization. The membranes were highly water-selective achieving separation factors more than 250 for the separation of water/acetic acid mixtures. Morooka et al. [71] prepared an A-type zeolite membrane on porous substrate by a hydrothermal process. The membranes were polycrystalline and the thickness was in the range 0.4-3.8 μm. They achieved a maximum separation factor of 4.8 for a mixed H_2-N_2 feed. Gavalas et al. [72] prepared defect-free, single-crystal ferrierite membranes. Albers [73] patented the synthesis of zeolites X, Y, and A membranes using supports such as glass, silicon, alumina, aluminum silicone, and others. Yamazaki and Tsutsumi [74] prepared an A zeolite membrane on Si/SiO_2, quartz by using Na_2SiO_3 and aluminum hydroxide as a source of T elements of the framework. Faujasite-type zeolite membranes with a variety of low Si/Al ratios were prepared on the outer surface of porous α-alumina tubes. They exhibited a CO_2 permeability of (0.4-2.5)×10^{-6} mol·$m^{-2}s^{-1}Pa^{-1}$ and a selectivity of CO_2/N_2 of 20–50. The Na-X-type faujasite showed lower permeability and higher selectivity values [75]. More recently, Sato et al. [76] prepared tubular NaY zeolite membranes for industrial purposes. The membranes showed a separation factor for water(10%)/ethanol(90%) mixtures of 190-220. They can be applied to dehydration of aqueous ethanol and products could be purified up to 98.5 wt.%.

In order to prepare zeolite membranes, the crystals must be interconnected to form a continuous layer on the substrate. In this way, the only available transport pathways are through the zeolite pores. It must also be mechanically durable but sufficiently thin to provide good permeance. Therefore, they are usually grown on some supports, such as a flat plate or tube [77]. As will be discussed the crystal size of zeolites is also an important property in building up zeolite catalysts.

1.3.1 Synthesis of zeolite membranes

The syntheses of zeolite films and membranes are completely different from that of crystalline zeolite powders and require new strategies coupled to simple hydrothermal treatment for various specific aims. Basically, its synthesis can be divided into four categories:

1. Pre-treatment of the supports, which can involve thermal and plastic treatment, chemical treatment (preparation of siloxane monolayers to anchor zeolitic crystals, silicon adsorption and thermal treatment, hydroxide treatment), and mechanical treatment
2. Synthetic methodology, including in-situ synthesis on supports (gel or clear solution), seeding, nanosized crystals, synthesis at the interface between two phases, selective etching, seed-film, electro-trapping, pressurized sol-gel coating, binding, electrical orientation, microwave, isomorphous substitution of framework atoms
3. Impregnation of the supports, where the volume of the autoclave relative to the synthetic mixture is important. For the preferential growth of membranes on asymmetrical tubular supports the protection, pressure and sealing of both ends are relevant factors.

4. Elimination of small defects, which can be achieved by CVD of silica (by reaction with silicon alkoxide or other silylation agents) or by selective coking [3].

There are mainly three methods for the preparation of zeolite membranes: in situ or direct crystallization, vapor phase transformations and methods involving seeding of the substrate surface prior to film synthesis [78].

For a long time, the direct crystallization was the common approach, which consists of placing a porous support, such as ceramics or stainless steel, in contact with a synthesis solution or gel under proper hydrothermal conditions [79]. This will result in nucleation and subsequent growth of zeolite crystals on the surface of the support forming a continuous membrane [62]. Several mechanisms for the growth of zeolite membrane layers on a mesoporous ceramic or metal-support surface under hydrothermal condition have been discussed. Myatt et al. [80] suggested that the growing seed crystallites are directly attached to the surface first, whereupon microcrystals grow in the voids between them forming finally a continuous layer. Jansen et al. [81] proposed that first a gel film forms on the support. Crystal nuclei are then formed at the interface between the gel and the solution, growing through the gel into the direction of the support. Sano et al. [82] proposed the simultaneous occurrence of different mechanisms with nuclei formed in the solution phase or directly on the surface and with nutrients for growth from either the solution phase or from the attached gel phase. The wide application of this method is based on its simplicity, since it is a one-step process where the requirement for specially designed substrates (e.g. organic-functionalized or microstructured) as well as a seeding step by dip- or spin-coating is eliminated. Moreover, it produces excellent adhesion to a wide variety of substrates and can easily coat surfaces of complex shape and in confined spaces [83]. The major challenge in this approach is to optimize the synthesis conditions in order that the zeolite crystals nucleate and grow in an interlocking fashion minimizing the non-selective interzeolitic porosity, while avoiding competitive nucleation and growth of the crystals in the solution phase [79]. The disadvantages of this method are that a considerable film thickness (several micrometers) is often necessary to obtain compact films and that the surface chemistry of the substrate highly determines the zeolite formation mechanism [84].

Nowadays, the secondary seeded growth has become the prominent method for the preparation of zeolite membranes and is the most versatile and flexible approach. It is based on the pre-deposition of a closely packed layer of zeolite crystals from a colloidal suspension onto the substrate surface, which in subsequent hydrothermal reaction grows to fill the interparticle voids [85]. The possible events taking place in solution and on a substrate during hydrothermal treatment are summarized schematically in the figure 1.11 [86]:

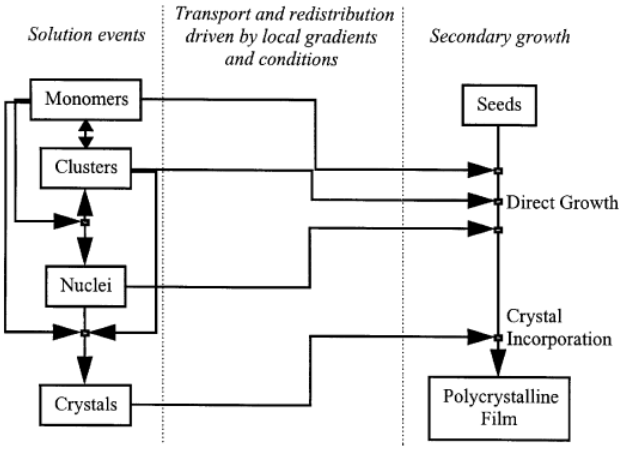

Figure 1.11 – Events taking place upon hydrothermal treatment and in the presence of seeds [86].

The employment of seed crystals may be a way to reduce the membrane thickness and to increase the permeation rate, while also controlling the crystal orientations [23]. Moreover, the inclusion of this seeding step is a suitable way of avoiding the complex processes that occur in the early stages of the zeolite crystal growth and has several advantages over the other synthesis methods:

- the nucleation and growth steps are independent from each other, which add improved flexibility in tailoring the zeolite film microstructure. This means that there is a wider range of conditions for the development of a continuous membrane [79];
- the need for heterogeneous nucleation is eliminated;
- reduction of the influence of the surface chemistry of the support on the zeolite membrane formation. Therefore, it has potential advantages in terms of reproducibility and control of the membrane microstructure as compared to the in situ synthesis method [87];
- zeolite top layers could grow on the seeded supports at lower temperatures and in shorter periods of time than those required when using unseeded supports. The induction time needed for zeolite nucleation is eliminated [25] and, therefore, seeding the support will increase the rate of zeolite growth. This is favorable to form a continuous and defect-free zeolite top layer.

1.3.2 Experimental factors affecting the properties of zeolite membranes

Several parameters influence the structure and quality of the crystalline layer. The nature of the support is an important factor. The chemical constitution of a nonporous substrate can influence crystal growth by releasing selected compounds into the solution, by adsorbing amorphous precursor particles or smaller nuclei, and by providing sites e.g. –OH groups, for crystal adhesion. With porous substrates pore size is the major property although the chemical constitution of the material remains important for the same reasons as for nonporous substrates. The gel composition is also a crucial factor

controlling not only the type of zeolite crystallized but also the quality of the zeolite layer. Some synthesis solutions yield a continuous layer of intergrown and interlocking crystals while other compositions give rise to layers macroscopically continuous but containing mesoporous transmembrane pathways or even originate isolated crystal patches with much of the surface remaining uncovered. The important variables in the synthesis of zeolite membranes include crystallization temperature and time as well as the rotation, and gel aging [88]. All these factors interact each other in a complicated manner that result in a narrow range of operation conditions for obtaining a well-intergrown, defect-free membrane covering the whole surface of the support. The optimization of these favorable conditions is crucial for the quality and morphology of the final product and requires intensive studies [85].

1.4 Aims of research

Although zeolite membranes have appeared for a long time the factors affecting the synthesis of zeolite membrane have not been fully understood yet. The mechanisms for zeolite membrane formation depend on a wide number of parameters which make difficult to predict the final result. Therefore, a deep insight in the influence of the several synthesis variables is required investigation in the control of this type of materials. This was the main motivation for the research reported here.

Faujasite membranes were selected as the object of study due to its pore opening suitable for the separation of olefin and paraffins, which is currently one of the most important and costly operations in the petrochemical industry. In this context, faujasite membranes were prepared by using gels or clear solutions as the precursors. The differences of the final properties of the material according to the synthesis batch was evaluated and the effect of each synthesis parameters was also investigated, namely, type of seeds used, time and temperature, gel composition and synthesis repetition. This could provide information about the most suitable reaction mixture for the preparation of high-quality, defect-free membranes of pure faujasite phase. The characterization of the membranes was performed by X-ray diffraction and scanning electron microscopy.

For the separation of a gas mixture of propane and propylene, the most promising membranes prepared here were then silver ion-exchanged, taking advantage of π-complexation reactions between silver ions and olefins. The effect of silver ion-exchange was analyzed by permeability and selectivity measurements of propane/propylene mixtures. All the silver ion-exchanged faujasite membranes were also characterized using techniques such as scanning electron microscopy, energy dispersive X-ray spectroscopy and X-ray diffraction.

1.5 References

[1] S. Mintova, N. H. Olson, T. Bein, Angew. Chem. Int. Ed. 38 (1999) 3201-3204

[2] F. Schuth, K. S. W. Sing, J. Weitkamp, *Handbook of Porous Solids*, Vol. 4, Wiley-VCH, Germany, 2002

[3] A. Tavolaro, E. Drioli, Adv. Mater. 11 (1999) 975-996

[4] H. Lee, *A New Strategy for Synthesizing Zeolites and Zeolite-like Materials*, California Institute of Technology, Pasadena, California, 2005

[5] C.J.Y. Houssin, *Nanoparticles in Zeolite Synthesis***,** Universiteitsdrukkerij Technische Universiteit Eindhoven, 2003

[6] T. Sun, K. Seff, Chem. Rev. 94 (1994) 857-870

[7] http://izasc.ethz.ch/fmi/xsl/iza-sc/SBUList.htm

[8] Ch. Baerlocher, W.M. Meier, D.H. Olson, *Atlas of zeolite framework types*, 5th revised edition, Elsevier, 2001

[9] F. Keller, L. Körner, *Zeolites*, University of Wisconsin – Madison

[10] http://www.iza-structure.org

[11] F. Roozeboorn, H.E. Robson, S.S. Chan in: F.R. Ribeiro, A.E. Rodrigues, L.D. Rollmann, C. Naccache, *Zeolite Science and Technology*, NATO ASI Series, Series E: Applied Sciences Nº 80, Martinua Nijhoff Publishers, 1984, USA, pp. 306-309

[12] J.K. Hofstetter, G.H. Hite, Sep Sci Technol 18 (1983) 1747–1764

[13] V. Sebastián, I. Kumakiri, R. Bredesen, M. Menéndez, J. Membr. Sci. 292 (2007) 92-97

[14] S. Satokawa, Y. Kobayashi, H. Fujiki, App. Catal. B: Environmental 56 (2005) 51–56

[15] E. Ivanova, B. Koumanova*, J. Hazard. Mat.(2009) article in press*

[16] E. Erdem, N. Karapinar, R. Donat, J. Coll. Interf. Sci. 280 (2004) 309–314

[17] Andersson, S., Grenthe, I. & Jonsson, E. (1975) German Patent 2,512,212.

[18] Ash, S. R. (1986) U.S. Patent 4,581,141.

[19] S.K. Gade, V.A. Tuan, C.J. Gump, R.D. Noble, J.L. Falconer, Chem. Commun. (2001) 601–602

[20] C.S. Cundy, P.A. Cox, Micropor. Mesopor. Mater. 82 (2005) 1–78

[21] Ralph T. Yang, *Adsorbents: Fundamentals and Applications*, John Wiley & Sons, Inc., USA, 2003

[22] H.G. Karge, J. Weitkamp, *Molecular Sieves Science and Technology*, Vol. 1 Springer, Germany, 1998

[23] F. Schuth, K.S.W. Sing, J. Weitkamp, *Handbook of Porous Solids*, Vol. 2, Wiley-VCH, Germany, 2002, pp. 744

[24] D.W. Breck, *Zeolite Molecular Sieves*, John Wiley & Sons Inc, New York & London, 1974

[25] W.C. Wong, L.T.Y. Au, C.T. Ariso, K.L. Yeung, J. Membr. Sci. 191 (2001) 143-163

[26] R.M. Barrer, J.W. Baynham, F.W. Bultitude, W.M. Meier, J. Chem. Soc. (1959) 195.

[27] S.P. Zhdanov, in: E.M. Flanigen, L.B. Sand (Eds.), Molecular Sieve Zeolites—I, ACS Adv. Chem. Ser., vol. 101, 1971, p. 20.

[28] G.T. Kerr, J. Phys. Chem. 70 (1966) 1047

[29] B.D. McNicol, G.T. Pott, K.R. Loos, N. Mulder, J. Phys. Chem 76 (1972) 3388

[30] B.D. McNicol, G.T. Pott, K.R. Loos, N. Mulder, Advan. Chem. Ser. 121 (1972)

[31] F. Polak, A. Cichocki, Advan. Chem. Ser. 121 (1973) 209

[32] F. Polak, E. Stobiecka, Bull. Acad. Pol. Sci., 26 (1978) 899

[33] E.M. Flanigen, Adv. Chem. Ser. 121 (1973) 119

[34] E.G. Derouane, S. Detremmerie, Z. Gabelica, N. Blom, Appl. Catal. 1 (1981) 201.

[35] Z. Gabelica, N. Blom, E.G. Derouane, Appl. Catal. 5 (1983) 227.

[36] C. L. Angell, W.H. Flank, in: J.R. Katzer (Ed.), Molecular Sieves – II, ACS Symp. Ser., Vol. 40 (1977) p. 194

[37] A. Culfaz, L.B. Sand, in W.M. Meier, J.B. Uytterhoeven (Eds.), Molecular Sieves, ACS Adv. Chem. Ser. Vol. 121 (1973), p. 140

[38] H. Kacirek, H. Lechert, J. Phys. Chem. 80 (1976) 1291

[39] R.M. Barrer, Chem. Brit. (1966) 380

[40] E.M. Flanigen, D.W. Breck, 137th Meeting of the ACS, Division of Inorganic Chemistry, Cleveland, OH, April 1960, Abstracts, p. 33-M.

[41] E.M. Flanigen, D.W. Breck, 137th Meeting of the ACS, Division of Inorganic Chemistry, Cleveland, OH, April 1960, Paper No. 82: Crystalline zeolites, V—Growth of zeolite crystals from gels

[42] D.W. Breck, J. Chem. Ed. 41 (1964) 678

[43] G.T. Kerr, Zeolites 9 (1989) 451

[44] C.D. Chang, A.T. Bell, Catal. Lett. 8 (1991) 305.

[45] S.L. Burkett, M.E. Davis, J. Phys. Chem. 98 (1994) 4647.

[46] S.L. Burkett, M.E. Davis, Chem. Mater. 7 (1995) 920.

[47] S.L. Burkett, M.E. Davis, Chem. Mater. 7 (1995) 1453.

[48] R. Ravishankar, C. Kirschhock, B.J. Schoeman, P. Vanoppen, P.J. Grobet, S. Storck, W.F. Maier, J.A. Martens, F.C. De Schryver, P.A. Jacobs, J. Phys. Chem. B 102 (1998) 2633.

[49] R. Ravishankar, C.E.A. Kirschhock, P.-P. Knops-Gerrits, E.J.P. Feijen, P.J. Grobet, P. Vanoppen, F.C. De Schryver, G. Miehe, H. Fuess, B.J. Schoeman, P.A. Jacobs, J.A. Martens, J. Phys. Chem. B 103 (1999) 4960.

[50] C.E.A. Kirschhock, R. Ravishankar, F. Verspeurt, P.J. Grobet, P.A. Jacobs, J.A. Martens, J. Phys. Chem. B 103 (1999) 4965.

[51] C.E.A. Kirschhock, R. Ravishankar, L. Van Looveren, P.A. Jacobs, J.A. Martens, J. Phys. Chem. B 103 (1999) 4972.

[52] C.E.A. Kirschhock, R. Ravishankar, P.A. Jacobs, J.A. Martens, J. Phys. Chem. B 103 (1999) 11021.

[53] C.E.A. Kirschhock, V. Buschmann, S. Kremer, R. Ravishankar, C.J.Y. Houssin, B.L. Mojet, R.A. van Santen, P.J. Grobet, P.A. Jacobs, J.A. Martens, Angew. Chem. Int. Ed. 40 (2001) 2637. [73] C.E.A.

Kirschhock, S.P.B. Kremer, P.J. Grobet, P.A. Jacobs, J.A. Martens, J. Phys. Chem. B 106 (2002) 4897.

[54] C.E.A. Kirschhock, S.P.B. Kremer, P.J. Grobet, P.A. Jacobs, J.A. Martens, J. Phys. Chem. B 106 (2002) 4897

[55] B. Fahlke, P. Starke, V. Seefeld, W. Wieker, K.-P. Wendlandt, Zeolites 7 (1987) 209

[56] H. Robson, *Verified Syntheses of Zeolitic Materials*, 2nd Revised Edition, Elsevier Science, 2001

[57] B.J. Schoeman, Micropor. Mesopor. Mater., 22 (1998) 9

[58] V. Nikolakis, F. Kokkoli, M. Tirrell, M. Tsapatsis, D. G. Vlachos, Chem. Mater. 12 (2000) 845

[59] Y. Li, Tai-Shung Chung, S. Kulprathipanja, AIChE J. 53 (2007) 610-616

[60] H. Strathmann, L. Giorno, E. Drioli, *An Introduction to Membrane Science and Technology*, Consiglio Nazionale Delle Richerche, 2006

[61] H. Kita, K. Fuchida, T. Horita, H. Asamura, K. Okamoto, Sep. Purif. Technol. 25 (2001) 261-268

[62] S. Nair, Z. Lai, V. Nikolakis, G. Xomeritakis, G. Bonilla, M. Tsapatsis, Micropor. Mesopor. Mater. 48 (2001) 219-228

[63] Y. Hasegawa, K. Kusakabe, S. Morooka, J. Membr. Sci. 190 (2001) 1-8

[64] M.P. Bernal, J. Coronas, M. Menéndez, J. Santamaria, J. Membr. Sci. 195 (2002) 125-138

[65] A. Takahashi, R.T. Yang, C.L. Munson, D. Chinn, Langmuir 17 (2001) 8405-8413

[66] S. Li, V.A. Tuan, J.L. Falconer, R.D. Noble, Micropor. Mesopor. Mater. 53 (2002) 59-70

[67] H.H. Funke, A.M. Argo, J.L. Falconer, R.D. Noble, Ind. Eng. Chem. Res. 36 (1997) 137-143

[68] W.J.W. Bakker, L.J.P. van den Broeke, F. Kapteijn, J.A. Moulijn, AIChE J. 43 (1997) 2203-2214

[69] N. Nishiyana, K. Ueyana, M. Matsukata, Micropor. Mater. 7 (1996) 299-308

[70] G. Li, E. Kikuchi, M. Matsukata, Sep. Purif. Technol. 32 (2003) 199-206

[71] K. Aoki, K. Kusakabe, S. Morooka, J. Membr. Sci. 141 (1998) 197-205

[72] J. E. Lewis, G. R. Gavalas. M.E. Davis, AIChE J. 43 (1997) 83-90

[73] E. Albers, G. C. Edwards, U.S. Patent No. 3 730 910, 1973

[74] S. Yamazaki, K. Tsutsumi, Micropor. Mater. 4 (1995) 205-212

[75] S. Morooka, T. Kuroda and K. Kusakabe, in: *Proc. 5th Int. Conf. Inorg. Membr.*, Nagoya (1988) p. 136.

[76] K. Sato, K. Sugimoto, T. Nakane, J. Membr. Sci. 319 (2008) 244-255

[77] Y. Yan, M. Tsapatsis, G.R. Gavalas, M.E. Davis, J. Chem. Soc., Chem. Commum. (1995) 227-228

[78] M. Lassinantti, J. Hedlund, J. Sterte, Micropor. Mesopor. Mater. 38 (2000) 25-34

[79] G. Xomeritakis, S. Nair, M. Tsapatsis, Micropor. Mesopor. Mater. 38 (2000) 61-73

[80] G.J. Myatt, P.M. Budd, C. Price, S.W. Carr, J. Mater. Chem., 2 (1992) 1103-1104

[81] J.C. Jansen, D. Kashchiev, A. Erdem-Senatalar, in Advanced Zeolite Science and Applications, J.C. Jansen, M. Stöcker, H.G. Karge, J. Weitkamp (Eds), Studies in Surface Science and Catalysis, Vol. 85, Elsevier, Amsterdam, 1994, 215-250

[82] T. Sano, F. Mizukami, H. Takaya, T. Mouri, M. Watanabe, Bull. Chem. Soc. Jpn., 65 (1992)146-154

[83] Z. Wang, Y. Yan, Chem. Mater. 13 (2001) 1101-1107

[84] J. Hedlund, S. Mintova, J. Sterte, Micropor. Mesopor. Mater. 28 (1999) 185-194

[85] R. Lai, G.R. Gavalas, Ind. Eng. Chem. Res. 37 (1998) 4275-4283

[86] G. Xomeritakis, A. Gouzinis, S. Nair, T. Okubo, M. He, R.M. Overney, M. Tsapatsis, Chem. Eng. Sci. 54 (1999) 3521-3531

[87] X. Zhang, H. Liu, K.L. Yeung, Mater. Chem. Phys. 96 (2006) 42-50

[88] Y. Yan, M.E. Davis, G.R. Gavalas, Ind. Eng. Chem. Res. 34 (1995) 1652-1661

2 Faujasite membranes derived from a gel

2.1 Faujasite

Faujasite zeolites are aluminosilicates assembled by two independent, though interconnected, three-dimensional networks of cavities. One network consists in a tetrahedral, diamond-type lattice formed by sharing rings (free diameter of about 8Å) of 12 tetrahedra. This gives rise to large cavities with a diameter of about 13Å, called supercages. The other network is created by linking smaller cages, called sodalite cages, in a tetrahedral, diamond-type lattice by joining rings of 6 tetrahedra. Therefore, between sodalite cages, secondary cavities which are hexagonal prisms, are also formed [1]. The framework structure is shown in figure 2.1. Depending on the Si to Al ratio, faujasites are assigned X (Si/Al = 1-1.5) and Y (Si/Al > 2) although topologically they present the same framework [2].

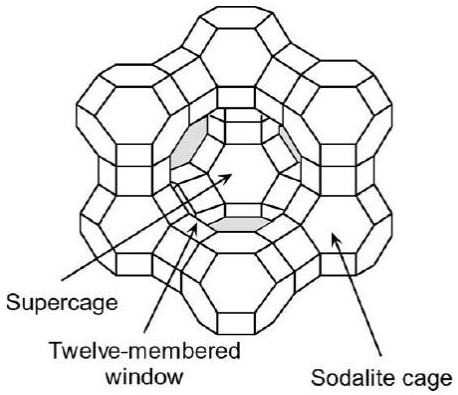

Figure 2.1 - Framework structure of a FAU-type zeolite [3].

In faujasite structure, the negative charges of the framework due to $(AlO_2)^-$ tetrahedra are balanced by charge-compensating, non-framework cations (e.g., Na^+, Li^+, Ca^{2+}) [4]. These extra-framework cations occupy various positions depending on their coordination requirements, ionic radii and on the aluminum distribution in the framework [5]. They are largely responsible for the adsorptive capacity of faujasite zeolites due to van der Waals and Coulombic interactions between them and the adsorbing gas.

The different networks of cavities give this type of materials unusual and interesting features. The sites in the large cages might be expected to exhibit the same selectivity as that exhibited by commercially available resinous-type exchangers because of the higher water content and more open structure, whereas the sites in the network of small cavities might be expected to exhibit a different selectivity, more characteristic of less opened zeolites. Multifunctionality exists in this material [1].

Faujasite has been extensively used in industry since it has the most open framework of traditional zeolites. Their large pores (~7.4Å) can be used for applications involving larger molecules compared to those that can be accommodated in other zeolites. Another feature that makes this kind of

material particularly useful is the high aluminum content, i.e., their hydrophilicity. Zeolite Y can be regarded as the archetype zeolite owing to its remarkable importance in catalysis (hydrocracking of petroleum) due to its high activity and low cost, and its large stable pore structure, which makes it an ideal host for novel composites [6]. Modification of the faujasite crystals, either by ion exchange or de-alumination, can be used to control the adsorption or intracrystalline diffusion properties, providing a method of tailoring the membranes to specific applications [7].

2.2 Faujasite membranes

Faujasite membranes have been synthesized under several different conditions. Giannakopoulos and Nikolakis [8] synthesized faujasite membranes using TEA (triethanolamine) as an organic additive. The starting mixture had a molar composition of 4.17:1.0:10:1.87:460 $Na_2O/Al_2O_3/TEA/SiO_2/H_2O$. The supports were previously seeded with Na-Y crystals using a dip-casting technique. The hydrothermal treatment was performed at 85°C for 7 days. After hydrothermal growth, the membranes were cooled, washed several times with distilled water, and then heat-treated in air at 420°C overnight to free the zeolite pores from remaining TEA or water molecules, under a cooling rate of 2°C min^{-1}. The SEM images revealed that a compact polycrystalline membrane layer, having a thickness of 20 μm, was formed on both surfaces of the support. The membranes showed a maximum separation factor of 13.7 for propylene/propane mixtures. Xu et al. [9] prepared zeolite X membranes by in-situ hydrothermal synthesis on porous ceramic tubes pre-coated with zeolite X seeds or precursor amorphous aluminosilicate. The crystal species were characterized by XRD, and the morphology of the supports subjected to crystallization was characterized by SEM. The membranes have zeolitic top-layers with a thickness of 10-25 μm, and zeolite crystals can be intruded into pores of the supports as deeply as 100 μm. The experimental results indicate that the pre-coating of zeolitic seeds on supports is beneficial to crystallization by shortening the synthesis time and improving the membrane strength. The resulting zeolite X membrane shows permselectivity to tri-n-butylamine over perfluro-tributyl-amine, and a permeance ratio of 57 could be reached at 350°C. Kacirek and Lechert [10] studied the growth of faujasite crystals in the system $Na_2O/Al_2O_3/SiO_2/H_2O$ with varying Si/Al ratios using seed crystals of the zeolite NaX. The kinetics process of the faujasite growth from amorphous aluminosilicate gel was investigated and procedures for the synthesis of faujasites with varying silica contents were described. They showed that the growing of faujasite crystals from nuclei is possible in concentrated ranges where nucleation of this or other species is negligible. Kita et al. [11] synthesized faujasite membranes with a gel of molar composition $1Al_2O_3:10SiO_2:14Na_2O:840H_2O$. The porous cylindrical alumina support was coated by water slurry of seed crystals of NaY zeolite and the membranes were hydrothermally prepared at 100°C for 5h. A zeolite Y membrane with about 20 μm thick, completely covering the support with randomly oriented and intergrown NaY zeolite crystals was obtained. The membranes exhibited high alcohol selectivity (540-7600) for methanol or ethanol from binary mixtures with other organics such as benzene, MTBE, or cyclohexane. The alcohol flux varied from 0.1 to 0.6 kg $m^{-2}\cdot h^{-1}$. The

membranes also showed good selectivity (ca. 125) for water from a water/ethanol mixture. In another investigation, Kita et al. [12] have prepared faujasite membranes on the surface of a porous cylindrical ceramic support also by the seeding and secondary growth method. The aluminosilicate gel had the molar compositions of SiO_2/Al_2O_3 = 3.6–5.3 for zeolite X and 25 for zeolite Y; Na_2O/SiO_2 = 1.2–1.4 for zeolite X and 0.88 for zeolite Y; H_2O/Na_2O = 30–50. The hydrothermal treatment was performed at 90-110°C for different reaction times. The outer-surface of the porous support was completely covered with randomly oriented, intergrown NaX or NaY zeolite crystals and the thickness of the membrane was about 20–30 μm. The zeolite membranes showed high alcohol selectivity for several mixtures with methanol or ethanol. Furthermore, high benzene selectivity was observed for benzene/cyclohexane and benzene/*n*-hexane separation. Kusakabe et al. [13] prepared faujasite zeolite membranes on a porous α-Al_2O_3 tube through a starting gel of molar composition Al_2O_3:SiO_2:Na_2O:H_2O = 1:10:14:798. The outer surface of the tube was rubbed with NaX zeolite particles to implant crystal fragments as nucleation sites and the hydrothermal synthesis was done at 90°C for 24h. A polycrystalline layer of Y-type zeolite was formed on the outer surface of the support. The membrane was about 5 μm thick and the crystals appeared to be randomly oriented by XRD. The crystal size and layer thickness increased with the reaction time. The membranes exhibited a selectivity of CO_2/N_2 between 20 and 100. The high selectivity was obtained for CO_2 at room temperature. This selectivity decreased to 20 at 102°C, indicating that separation was due to the preferential adsorption of CO_2 in the zeolite pore. In another study, Kusakabe et al. [14] synthesized faujasite membranes from a gel with molar composition Al_2O_3:SiO_2:Na_2O:H_2O = 1:12.8:17:975. Porous α-Al_2O_3 tubes were used as support and were seeded with NaX-zeolite particles before hydrothermal treatment at 90°C for 24h. The permeation properties of the membranes were measured and showed a permeance for CO_2 of ~1.3×10^{-6} and N_2 of ~4.9×10^{-8}. The separation factor CO_2/N_2 was between 22-32. Falconer et al. [15] have developed faujasite membranes using a gel molar composition of $4.2Na_2O:1.0Al_2O_3:3.0SiO_2:150H_2O$. A 10 wt% suspension of X-type powder was used for seeding. The membranes were prepared on porous tubes of γ-Al_2O_3, α-Al_2O_3, stainless steel, SiO_2-coated SiC and γ-Al_2O_3 coated SiC. The hydrothermal synthesis was carried out at 100ºC for 6h. They concluded that the best membrane was prepared on γ-Al_2O_3 and it had a tri-isopropyl benzene pervaporation flux of 2.3 $g/m^2 \cdot h$ at 27°C. This membrane separated 1,3-propanediol from glycerol in aqueous mixtures by pervaporation; at 35ºC, the total flux was 2.7 $kg/m^2 \cdot h$, and the 1,3-propanediol/glycerol selectivity was 41.

The faujasite membranes are mainly used for separation purposes. The permeability and selectivity values are strictly dependent on the final microstructure of the zeolite material and the formation of a continuous, defect-free layer is detrimental for the quality of the results. Therefore, the correlation of the synthesis variables and their influence on the final properties of the material is necessary. Their importance makes it the object under investigation in this study.

2.3 Experimental

The zeolite membranes were synthesized in a gel. The general procedure is shown in figure 2.2.

The chemical source used in this work are sodium aluminate (Riedel-de-Haen, Na_2O, 41%; Al_2O_3, 54%), sodium metasilicate (BDH) and sodium hydroxide (Panreac Química, S.A., 98%). Zeolite membranes were hydrothermally synthesized on the surface of porous cylindrical α-Al_2O_3 support tubes (Inocermic) with internal and external diameters of approximately 7 and 10 mm, respectively. The substrates had a mean pore diameter of 70, 1000 and 1800 nm.

Zeolite Y and X crystal powders were synthesized according to the procedure described in the literature [16-17], and used as seeds. The porous support was coated by water slurry of seed crystals of NaY or NaX zeolites, and then dried at 150°C for 20 minutes. The seeded support was put into an autoclave and then the pre-prepared gel was added. In order to improve the quality of the membranes, some samples were prepared by repeating the synthesis, i.e., after a certain time synthesis, the sample was placed into fresh gel and all processes repeated.

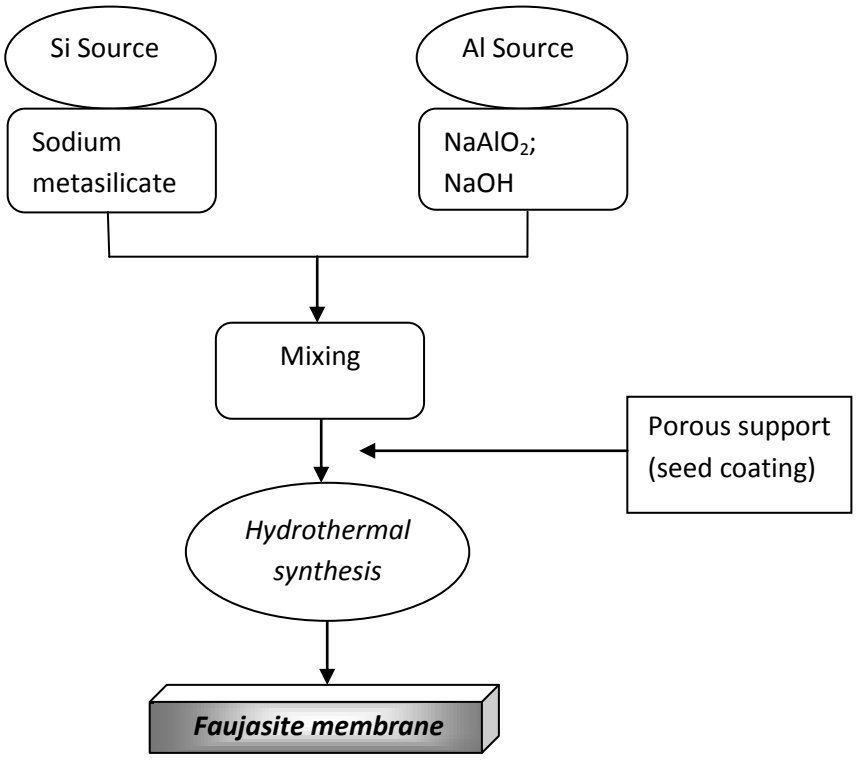

Figure 2.2 – Flow chart of the synthesis procedure of faujasite membranes.

The aluminosilicate gels used in the synthesis were prepared according to the literature [18] and consist in mixing a sodium silicate aqueous solution and an alkaline aluminate aqueous solution. The aluminate solution was made by dissolving sodium aluminate and sodium hydroxide in distilled water,

and the sodium silicate solution was made by dissolving sodium metasilicate in distilled water. Gels with different molar compositions were prepared to optimize the synthesis conditions. Table 2.1 lists the compositions and synthesis conditions used for the preparation of membrane from a gel. After hydrothermal treatment performed at 80-100°C for 5-24 h, the support was taken out, washed and dried at 60°C overnight.

Table 2.1 – Synthesis conditions for the membrane prepared from a gel

Sample	*Compositions (Al_2O_3:SiO_2:Na_2O:H_2O)*	*Time (h)*	*Temperature (°C)*	*Seed Crystals*	*Pore of support (nm)*	*Yield (mg/g)*
G1	1:10:14:829	5	100	X10%	1800	10.10
G2				Y5%		13.89
G3		6				14.48
G4		5+5*				28.62
G5				Y20%		17.17
G6				X20%		19.86
G7		8				23.33
G8		8+8		Y5%	1000	25.81
G9				Y20%		25.34
G10		24		X20%		21.48
G11			90	Y5%	1800	16.02
G12				X20%		29.13
G13		24+24				32.19
G14	1:10:14:829 + 1:9:80:5000	24+5	90 + 80			17.39
G15	1:10:14:1086	5	100			7.89
G16				Y5%		9.90
G17	1:10:14:1379					7.69
G18	1:10:15:829					14.76
G19				X20%	1000	16.06
G20					70	15.03
G21				P20%	1000	7.10
G22	1:9:14:788			X20%	1800	16.62
G23	1:8:12:959			Y5%		17.51
G24	1:10:12:829			X20%	TiO_2	10.80
G25					1800	8.42
G26				Y20%		8.03
G27				Y5%		10.43
G28		8				18.53
G29		5+5		X20%		22.20
G30	1:10:12:829 + 1:9:80:5000	5+5+5+5	100 + 80			20.02
G31	1:12:17:1050	5	100			9.25
G32				Y20%		8.52
G33					1000	16.66
G34		5+5		X20%	1800	14.39
G35					1000	21.87
G36		5+5+5				24.65
G37		24	90		1800	16.06
G38	1:19:25:1575	5	100	Y5%		17.25
G39				Y20%		7.98
G40				X20%		14.01

G41		5+5				20.62
G42	1:19:25:1575 + 1:9:80:5000	5+5+5+5				17.74
G43	1:19:25:1723	5				10.72
G44	1:19:25:5000					1.06
G45			80			2.13
G46	1:5:7:415		100	Y5%		12.73
G47				ZM26 20%		9.47
G48	1:5:7:415 aged 24h			X20%		14.80
G49	1:5:7:415					12.07
G50					70	9.89
G51					1000	10.43
G52				Y20%		16.19
G53					70	11.47
G54					1800	14.96
G55		5+5				12.80
G56				X20%		13.82
G57		5+5+5+5				37.08
G58					1000	50.83
G59[#]						26.36
G60	1:5:7:415 + 1:9:80:5000					23.33
G61					70	18.01
G62					1800	20.82
G63		5+5+5+5 +5+5				24.01
G64	1:5:7:415	24			1000	10.51
G65		48		X20%		23.77
G66		72				16.68
G67		96				12.20

[*] It represents the repeat synthesis; # synthesis with rotation

2.4 Results and discussion

The membranes were studied by X-ray diffraction (XRD) with a Philips X'Pert MPD X-ray diffraction system using Cu-Kα radiation (λ = 1.5405Å). The XRD analysis allows us to identify the type of crystalline material obtained from the membrane synthesis. By comparison with a pattern collected from a faujasite powder sample it was possible to verify if the membranes had the phase required. This powder sample taken as reference was synthesized following the procedure described in the literature [16-17].

The membranes were also studied by scanning electron microscopy (SEM) (Hitachi, S-4100) coupled with energy dispersive X-ray spectroscopy (EDS). The membranes were mounted in a holder using carbon glue and a carbon layer was deposited on the surface by sputtering. The SEM analysis gave the images of the faujasite membranes so it was possible to confirm if they formed a continuous film on the surface of the support and if they possessed the desired morphology.

2.4.1 XRD analysis

The XRD patterns in figure 2.3 are the results obtained from the membrane synthesized at condition G49 in table 2.1. The formation of faujasite membrane can be clearly proved.

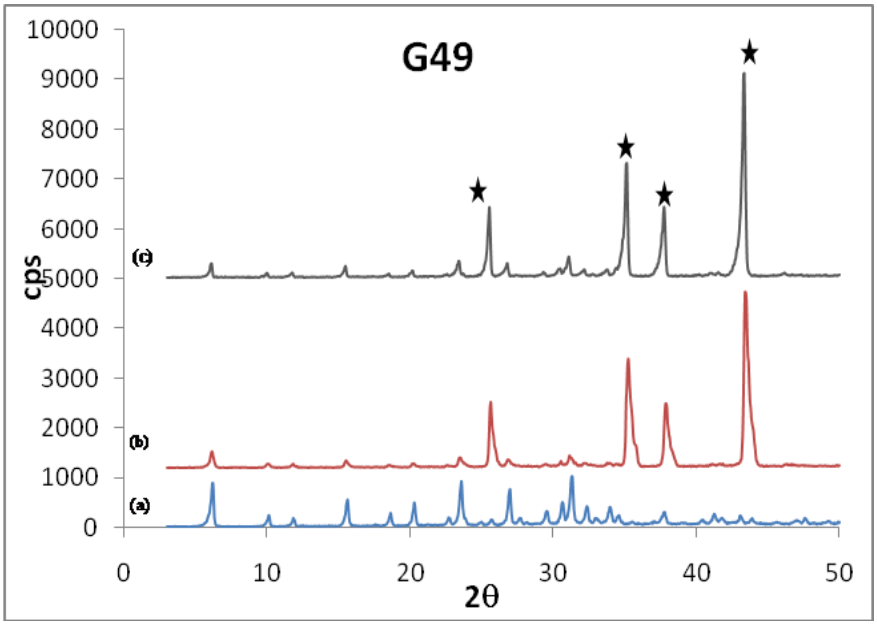

Figure 2.3 – XRD patterns collected from a powder sample (a); the inside (b) and outside (c) of a membrane synthesized at condition G49 in table 2.1. Stars depict the reflections from the α-alumina support.

According to the literature [18-19], this gel initially forms faujasite, but zeolite P is the final stable product. After a prolonged hydrothermal treatment, the growth of zeolite P would be expected, leading to a decrease in the film thickness and changing the properties of permeance and selectivity of the membrane. This reduction in the film thickness might be explained by the growth of zeolite P at the expense of the crystals in the bulk as well as of the crystals constituting the film. Therefore, it is not surprising if, instead of a faujasite, a zeolite P membrane emerges. In fact, a few membranes prepared from gels were a mixture of FAU and zeolite P, as being shown in figure 2.4. However, for most conditions in table 2.1, the control of the synthesis conditions prevented the formation of zeolite P.

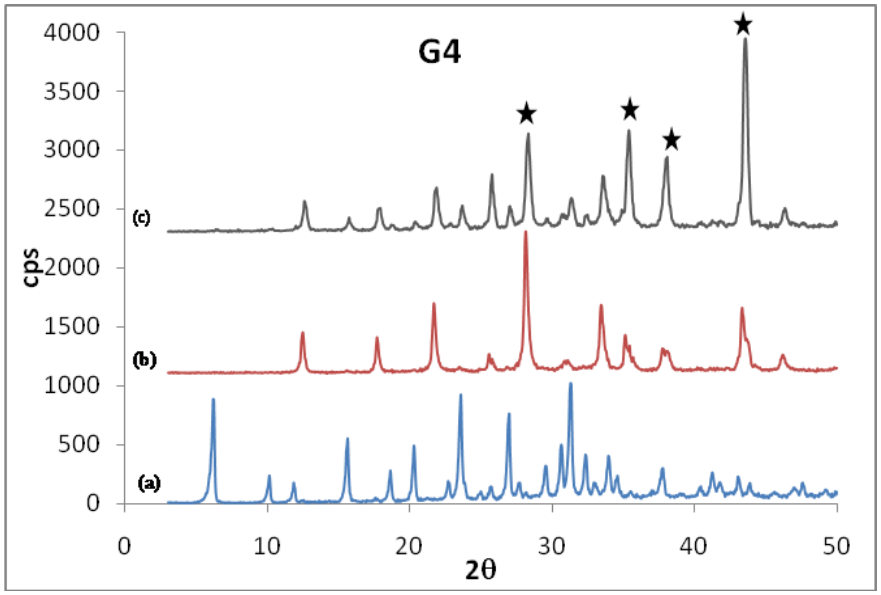

Figure 2.4 – XRD patterns collected from a powder sample of (a) faujasite and (b) zeolite P; and (c) the inside of a membrane synthesized at condition G4 in table 2.1. Stars depict the reflections from the α-alumina support.

A new approach combines the synthesis from a gel and a clear solution (see next chapter), giving a wide range in the control of the membrane formation and preventing the formation of zeolite P even after four time repeated synthesis (figure 2.5). The production of the membrane was carried out using gels or clear solutions as the starting mixture at different steps.

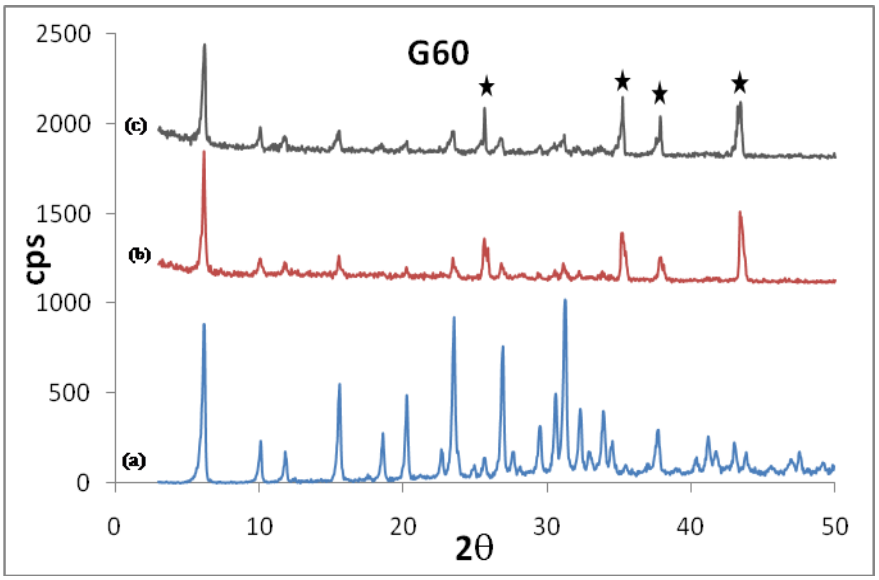

Figure 2.5 – XRD patterns collected from a powder sample (a); the inside (b) and outside (c) of a membrane synthesized at condition G60 in table 2.1. Stars depict the reflections from the α-alumina support.

2.4.2 SEM analysis

Using a gel as a starting mixture sometimes was obtained faujasite layer with a presence of a second phase or even defects, as shown in figure 2.6.

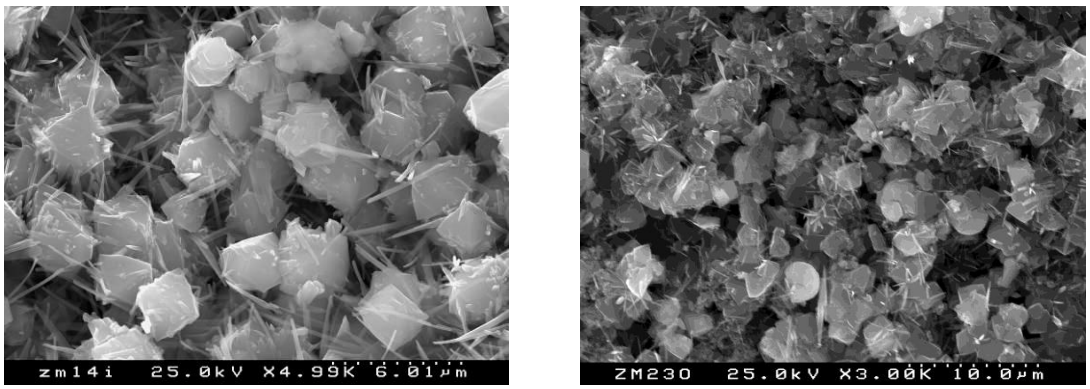

Figure 2.6 – Micrograph of the inside surface of the membrane synthesized at condition G46 (left) and G2 (right) in table 2.1.

Under the optimized synthesis conditions, a continuous layer, covering the porous support tube and with a smooth surface and well defined crystals of faujasite-type zeolites was obtained, as illustrated in figures 2.7-2.9.

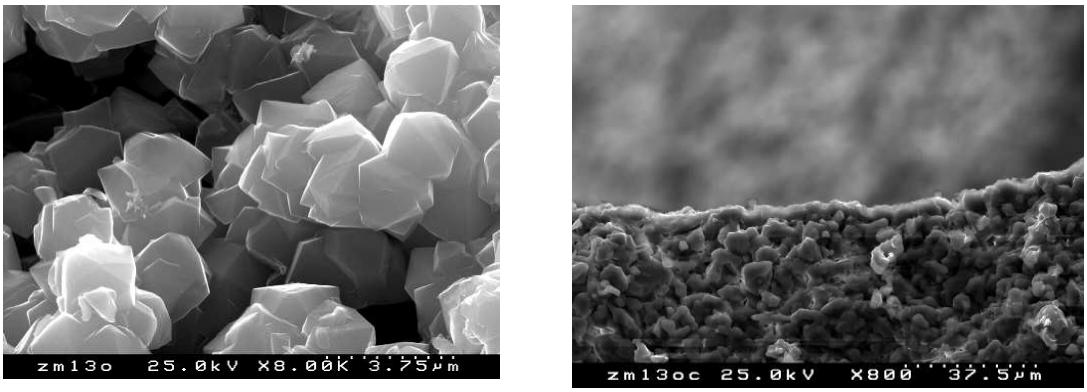

Figure 2.7 – Top view (left) and cross-section (right) of the outside surface of the faujasite membrane synthesized at condition G49 in table 2.1.

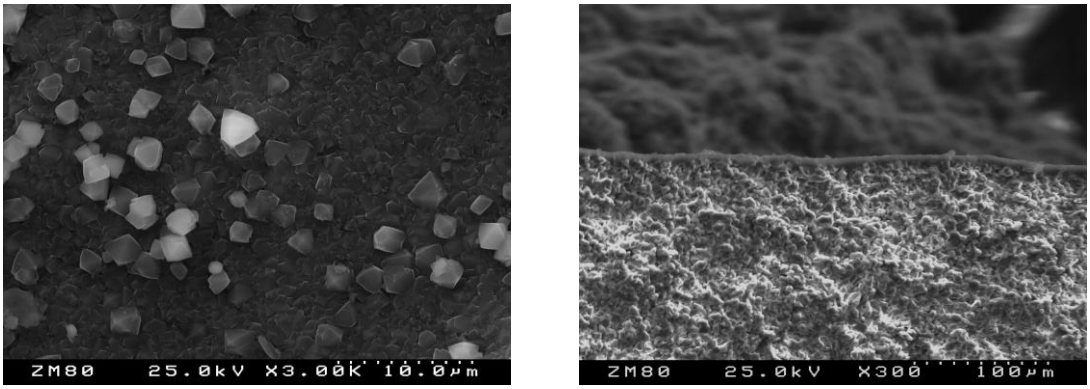

Figure 2.8 – Top view (left) of the inside surface and cross-section (right) of the outside surface of the faujasite membrane synthesized at condition G54 in table 2.1.

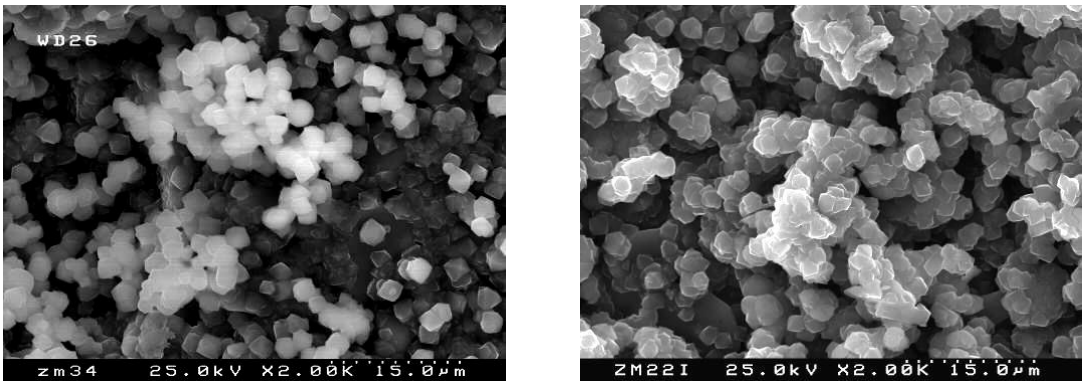

Figure 2.9 – The inside surface of the faujasite membrane synthesized at conditions G25 (left) and G40 (right) in table 2.1.

2.4.2.1 Seeding effect

The use of seeds can be fundamental for the growth of zeolite membranes on supports. Sterte et al. [19] and Morooka et al. [13] investigated the formation of faujasite-type films on α-alumina supports. They concluded that without seeding, no film was formed on the surface of the substrate. Kita et al. [12] pointed out that without coating of seed crystals it is necessary to repeat the preparation procedure several times in order to obtain the membrane with a continuous polycrystalline zeolite fully covering the porous support.

Even though the presence of seeds might not be detrimental for the film formation, it is used to improve the microstructure and strength of the resulting zeolite membrane [9]. When hydrothermal crystallization took place, the seeds provided the crystallization nuclei around which zeolite crystals grew to gradually fill the interstices. Once the seeded support in precursor mixture was at synthesis temperature, the crystal growth could start immediately, which may avoid the nucleation of second phases and therefore eliminate the formation of second phases, and also shorten the synthesis time.

Colloidal suspensions with 20 wt.% zeolite X or Y and 5 wt.% zeolite Y were used in the seeding process. Although these zeolites are topologically the same, they may have different seeding behavior.

In addition, the quantity of crystals used in seeding was also studied to verify if it determines the quality of the final membrane.

In some cases, the surfaces of the membranes when using zeolite Y crystals as seeds are smooth, homogenously covered and the presence of faults and voids are suppressed (figure 2.10).

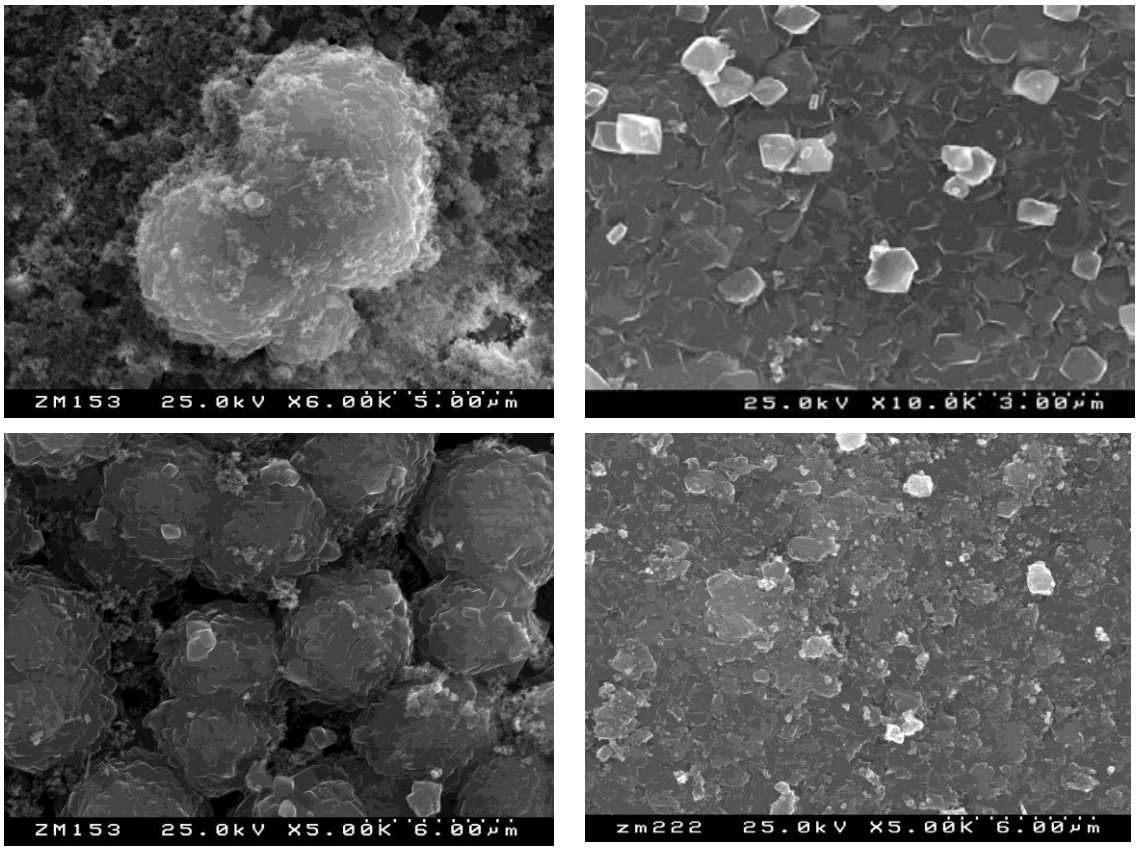

Figure 2.10 – The inside surface of the faujasite membrane synthesized at conditions G50 (top left) and G51 (bottom left) in table 2.1, using 20 wt.% X seeds, and G53 (top right) and G52 (bottom right) using 20 wt.% Y seeds.

However, for support with 1800 nm pore membranes were better when using the zeolite X as seeding, as shown in figures 2.11. Keeping all other parameters unchanged, the zeolite X seeding results in the formation of well-defined crystals, while an inefficient coverage or the presence of a second phase (G4) and defects was common in zeolite Y seeding. Since zeolites X and Y are topologically the same, the difference in their Si/Al ratio and therefore, in their polarizability, might be responsible for the better performance when using zeolite X instead of Y.

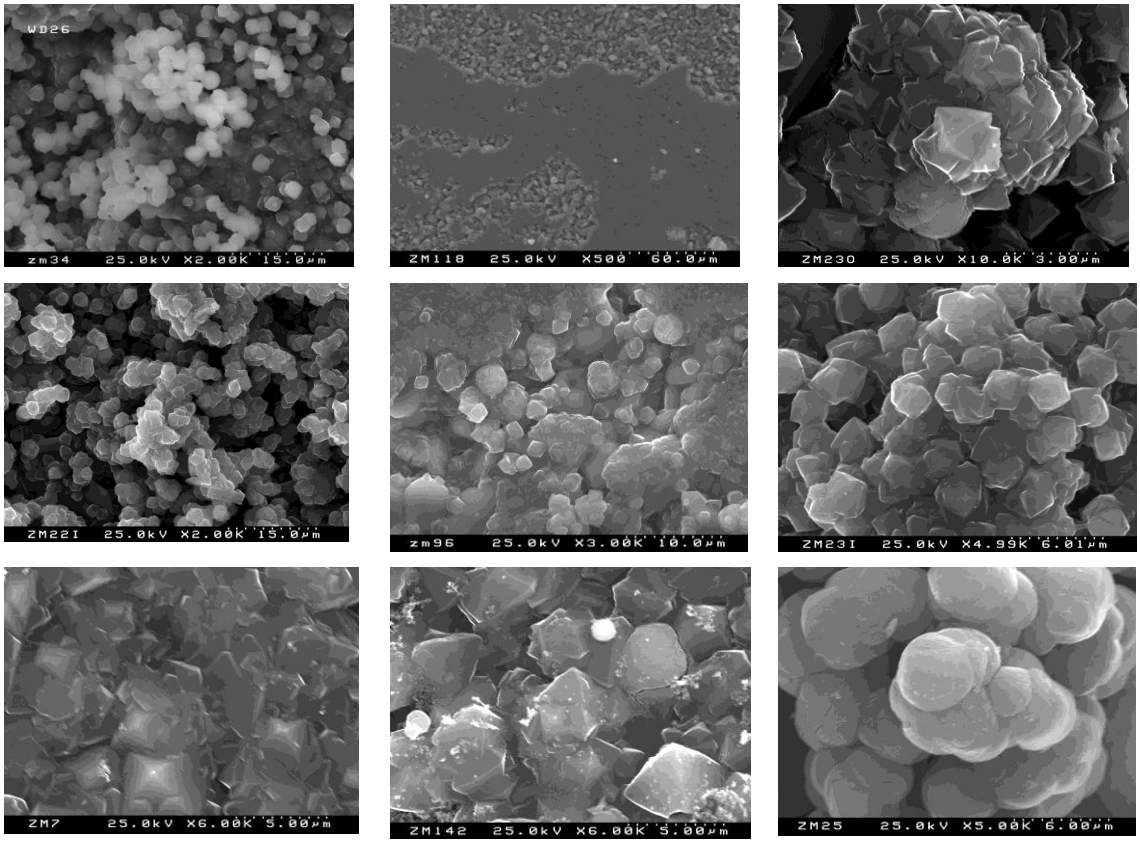

Figure 2.11 – The inside surface of the faujasite membranes synthesized at conditions (from top) G25, G40 and G6 (left images), using 20 wt.% X seeds; G26, G39 and G5 (centre), using 20 wt.% Y seeds and G27, G38 and G4 (right images) using 5 wt.% Y seeds.

2.4.2.2 Effect of reaction time

Increasing the synthesis time, the thickness of the membrane may increase since it will lead to an enlarged quantity of crystals formed. In the crystallization sequence of a faujasite synthesis, the desired phase initially forms but P type zeolite is the final stable product [12]. A prolonged heating in the conventional oven would lead to the formation of zeolite P, using faujasite crystals in the bulk as well as in the constituting film as Si and Al sources. Therefore, the dissolution of the membrane occurs, decreasing the faujasite layer thickness [19-20].

In fact, zeolite P formed in addition to faujasite when the synthesis time was prolonged from 5h to 96 (figure 2.12). In addition, the increase of the synthesis time does not lead to the formation of a well-intergrowth membrane, but instead, to crystal powders dispersed on the support surface. Therefore, 5h is the sufficient time and this was the preferred approach for the preparation of faujasite membranes.

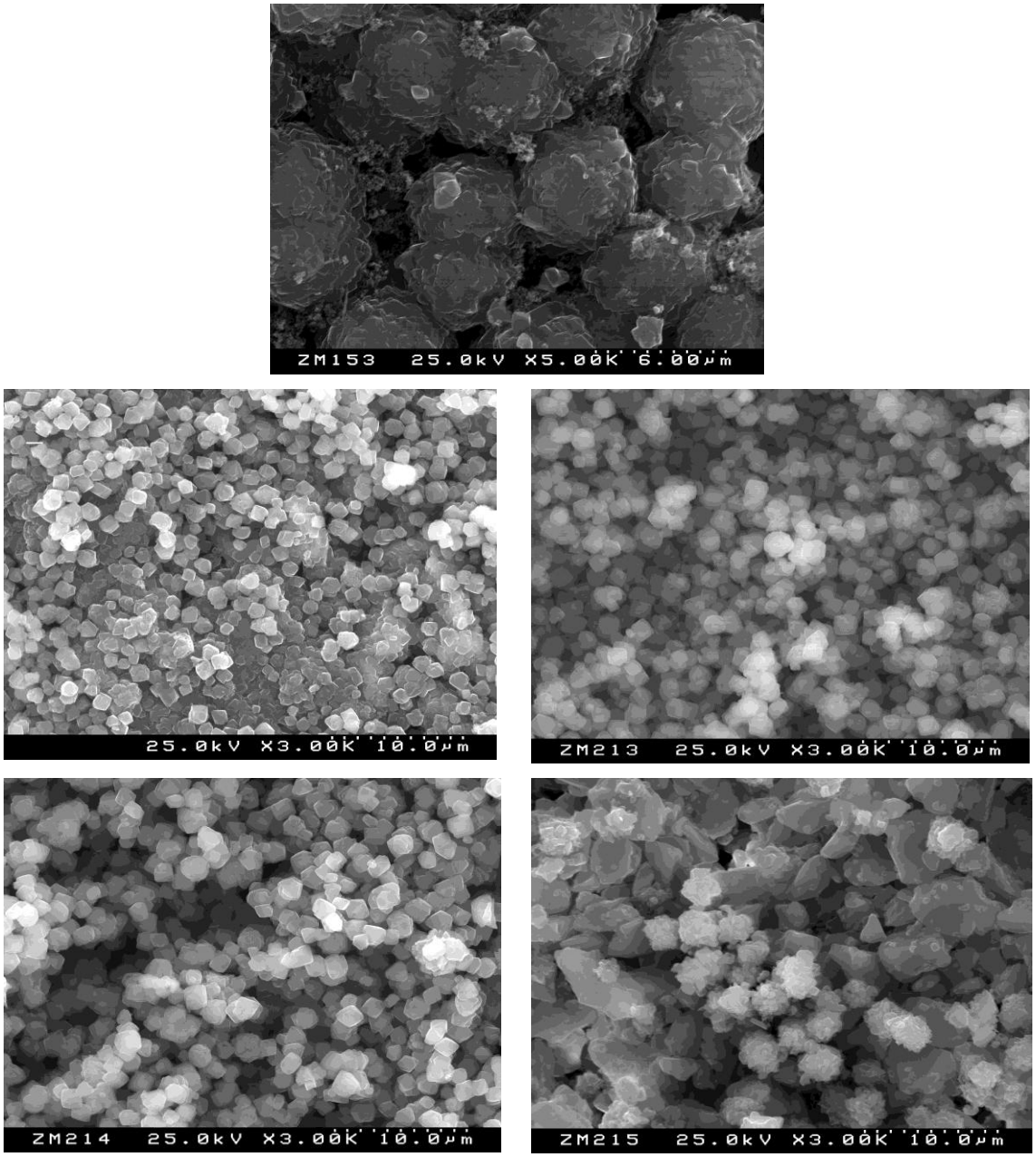

Figure 2.12 – The inside surface of the membranes synthesized at conditions G51 (top), G64 (middle left), G65 (middle right), G66 (bottom left) and G67 (bottom right) in table 2.1, corresponding to 5, 24, 48, 72, and 96h, respectively.

With the different synthesis parameters, the time needed for the formation of zeolite P also changes. For example, when using the conditions G27 and G28 in the table 2.1, zeolite P appears only after 8h with an extensive degree of cracking (figure 2.13). This reassures the use of 5h in the faujasite membrane preparations.

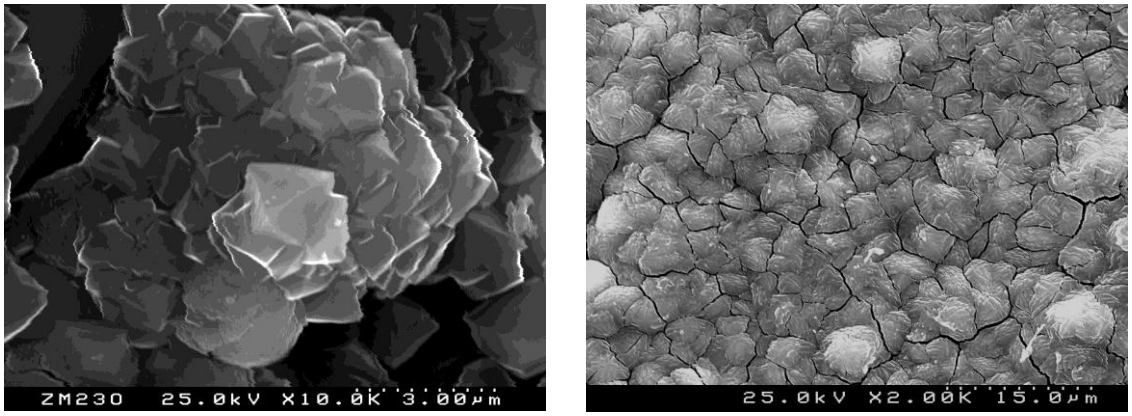

Figure 2.13 – The inside surface of the membranes synthesized at conditions G27 (left) and G28 (right) in table 2.1, corresponding to 5 and 8h, respectively.

In this regard, it was preferred a control of the thickness of the film by performing repeated synthesis.

2.4.2.3 Effect of gel chemical composition

The amount of the components constituting the starting gel was varied in order to understand their influence on the quality of the final membrane. However, no clear trend was found for the morphology change and the presence of defects in the membranes. The influence of the gel composition is strictly dependent on the other parameters involved in the synthesis of zeolite membranes.

For example, a reduction of aluminum from a composition G2 ($1Al_2O_3$:$10SiO_2$:$14Na_2O$:$829H_2O$) to G38 ($1Al_2O_3$:$19SiO_2$:$25Na_2O$:$1575H_2O$) leads to the removal of the second phase (figure 2.14). However, reducing the aluminum content from a composition G6 to G41 increases the amount of defects present in the final product, as shown in figure 2.15.

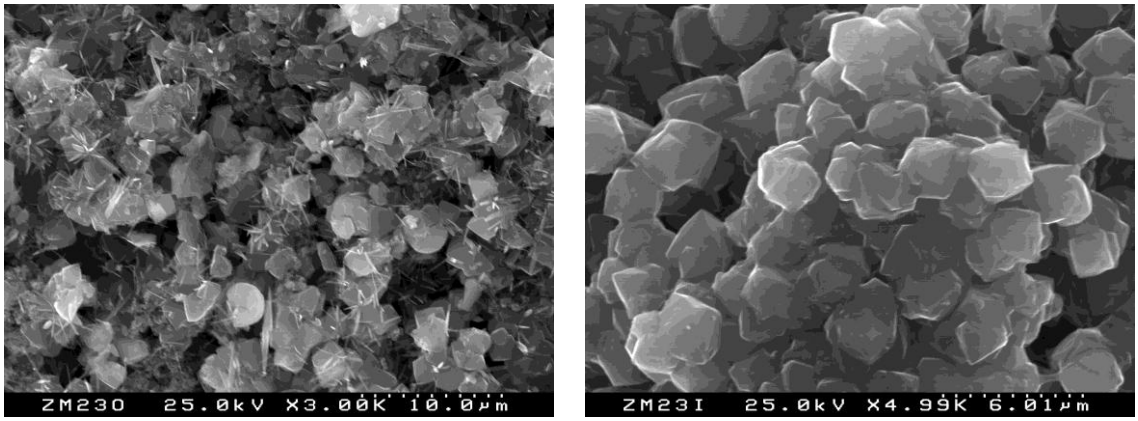

Figure 2.14 – The inside surface of the faujasite membranes synthesized at conditions G2 (left), corresponding to a molar ratio of $1Al_2O_3$:$10SiO_2$:$14Na_2O$:$829H_2O$, and G38 (right) of a molar ratio $1Al_2O_3$:$19SiO_2$:$25Na_2O$:$1575H_2O$, in table 2.1.

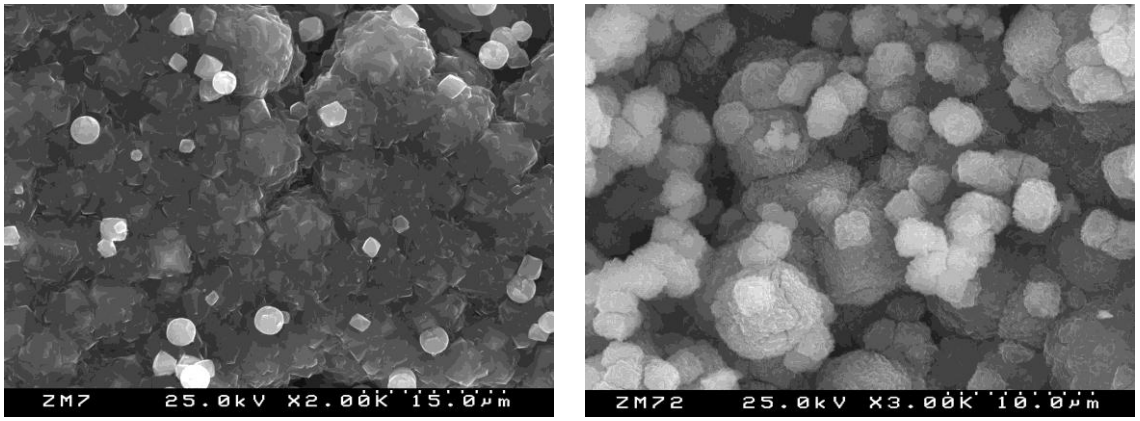

Figure 2.15 – The inside surface of the faujasite membranes synthesized at conditions G6 (left), corresponding to a molar ratio of $1Al_2O_3$:$10SiO_2$:$14Na_2O$:$829H_2O$, and G41 (right) of a molar ratio $1Al_2O_3$:$19SiO_2$:$25Na_2O$:$1575H_2O$, in table 2.1.

However, increasing the aluminum, from a molar ratio $1Al_2O_3$:$10SiO_2$:$12Na_2O$:$829H_2O$ to $1Al_2O_3$:$5SiO_2$:$7Na_2O$:$415H_2O$, improves the final properties of the membranes, for all the membranes tested (figures 2.16-2.17). Therefore, this composition is the most suitable for the preparation of faujasite membranes under the conditions specified.

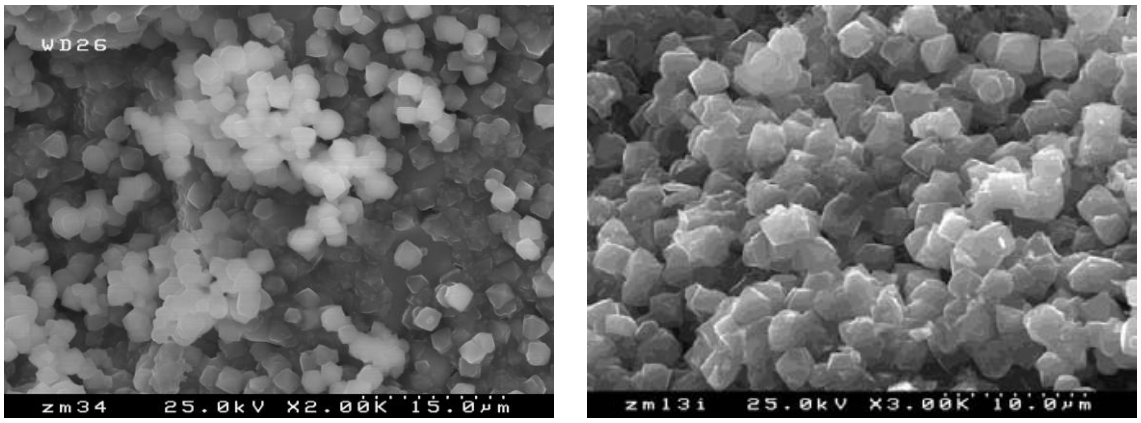

Figure 2.16 – The inside surface of the faujasite membranes synthesized at conditions G25 (left), corresponding to a molar ratio of $1Al_2O_3$:$10SiO_2$:$12Na_2O$:$829H_2O$, and G49 (right) of a molar ratio $1Al_2O_3$:$5SiO_2$:$7Na_2O$:$415H_2O$, in table 2.1.

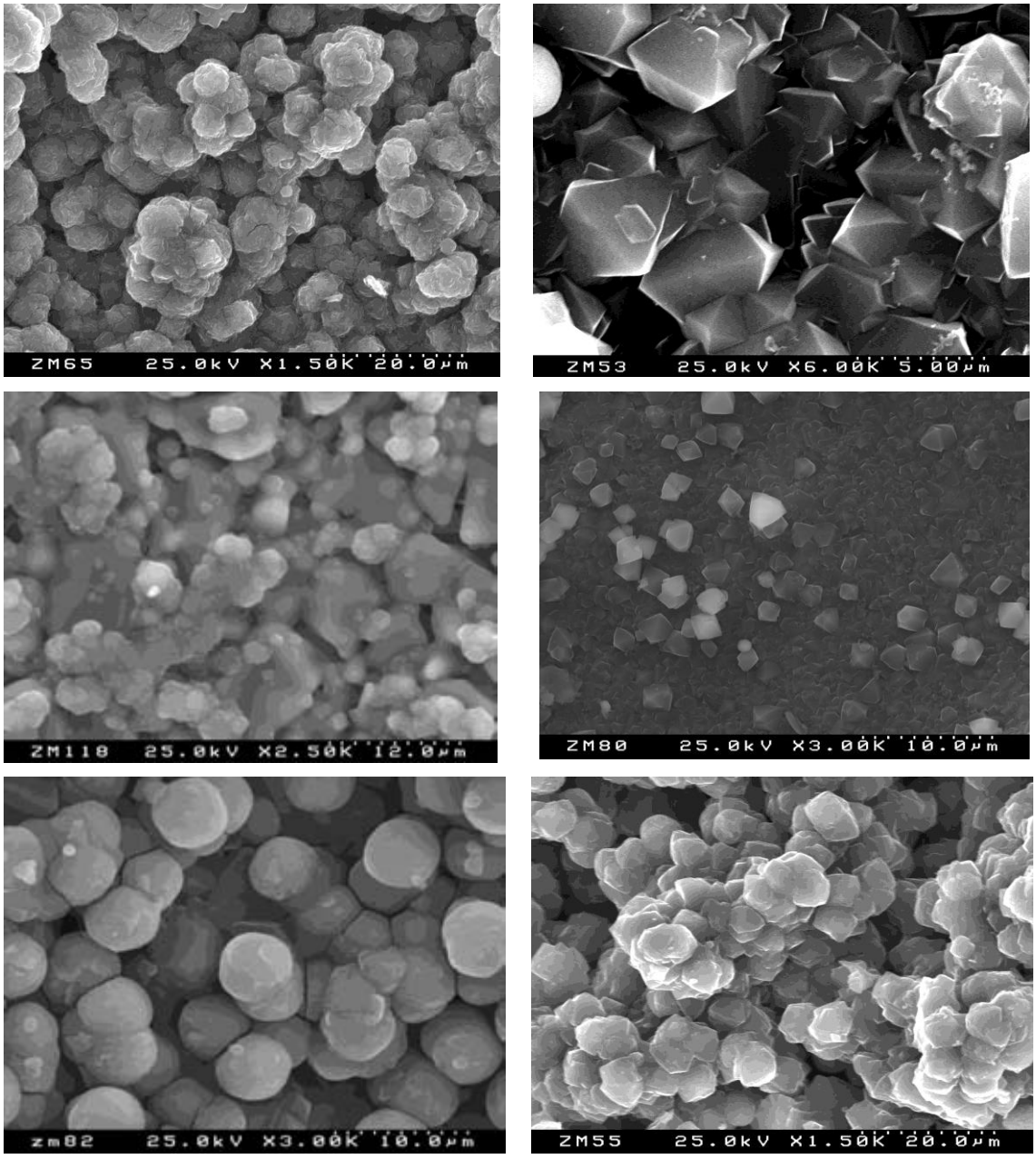

Figure 2.17 – The inside surface of the faujasite membranes synthesized at conditions G29 (top left), G26 (middle left) and G30 (bottom left), corresponding to a molar ratio of $1Al_2O_3$:$10SiO_2$:$12Na_2O$:$829H_2O$, and G56 (top right), G54 (middle left) and G62 (bottom left) of a molar ratio $1Al_2O_3$:$5SiO_2$:$7Na_2O$:$415H_2O$, in table 2.1.

Although, in the majority of the samples the ratio $1Al_2O_3$:$5SiO_2$:$7Na_2O$:$415H_2O$ is the best, there are also contradictious results. For instance, the membrane prepared under the conditions G46 in table 2.1 shows a second phase, as evidenced in figure 2.18. Comparing with $1Al_2O_3$:$10SiO_2$:$14Na_2O$:$829H_2O$, $1Al_2O_3$:$5SiO_2$:$7Na_2O$:$415H_2O$ produces a better final material (figure 2.19). This may be related to the amount of seeds used.

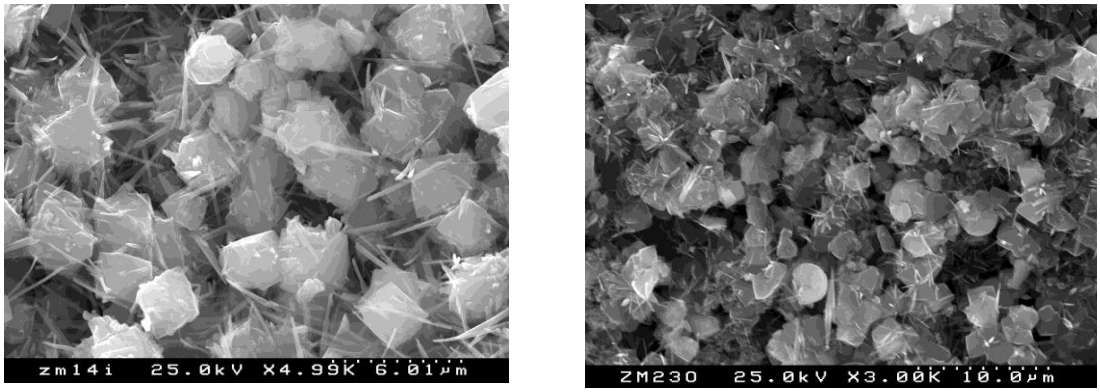

Figure 2.18 – The inside surface of the faujasite membranes synthesized at conditions G46 (top left), corresponding to a molar ratio of $1Al_2O_3$:$5SiO_2$:$7Na_2O$:$415H_2O$, and G2 (right) of a molar ratio $1Al_2O_3$:$10SiO_2$:$14Na_2O$:$829H_2O$, in table 2.1.

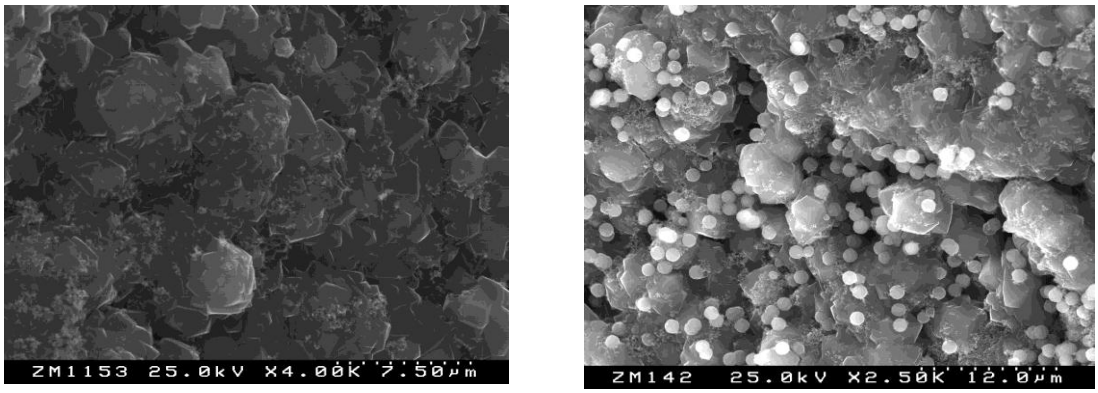

Figure 2.19 – The inside surface of the faujasite membranes synthesized at conditions G55 (left), corresponding to a molar ratio of $1Al_2O_3$:$5SiO_2$:$7Na_2O$:$415H_2O$, and G5 (right) of a molar ratio $1Al_2O_3$:$10SiO_2$:$14Na_2O$:$829H_2O$, in table 2.1.

When the ratio was changed from $1Al_2O_3$:$5SiO_2$:$7Na_2O$:$415H_2O$ to $1Al_2O_3$:$19SiO_2$:$25Na_2O$:$1575H_2O$ it was also observed that the best results occur for the first composition, as shown in figures 2.20-2.21.

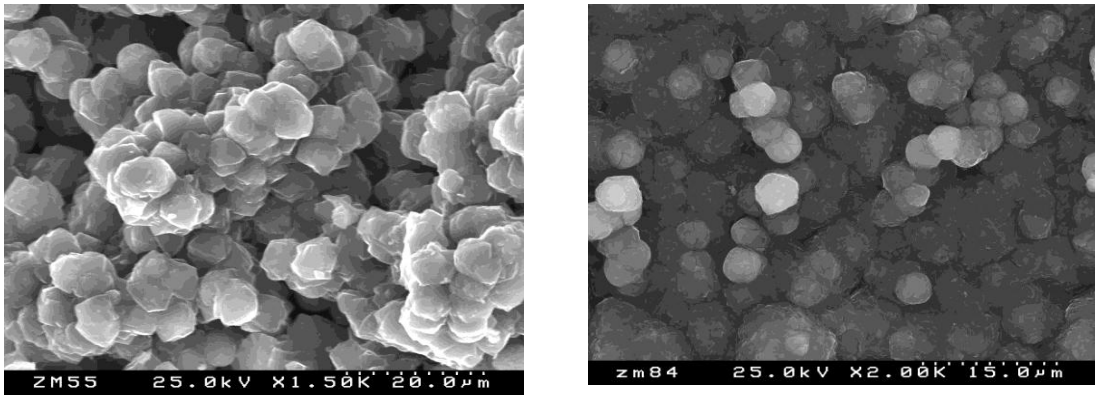

Figure 2.20 – The inside surface of the faujasite membranes synthesized at conditions G62 (left), corresponding to a molar ratio of $1Al_2O_3$:$5SiO_2$:$7Na_2O$:$415H_2O$, and G42 (right) of a molar ratio $1Al_2O_3$:$19SiO_2$:$25Na_2O$:$1575H_2O$, in table 2.1.

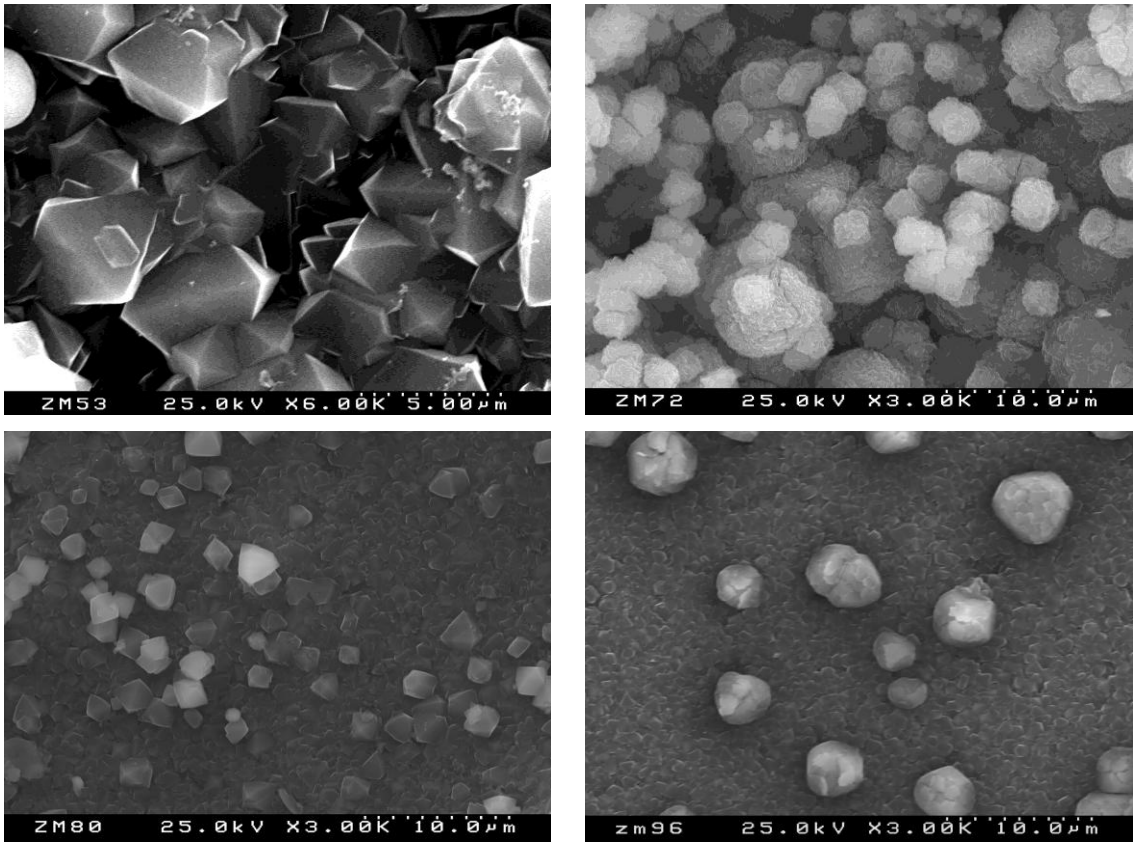

Figure 2.21 – The inside surface of the faujasite membranes synthesized at conditions G56 (top left) and G54 (bottom left), corresponding to a molar ratio of $1Al_2O_3$:$5SiO_2$:$7Na_2O$:$415H_2O$, and G41 (top right) and G39 (bottom right) of a molar ratio $1Al_2O_3$:$19SiO_2$:$25Na_2O$:$1575H_2O$, in table 2.1.

The SEM images obtained for samples G42, G41 and G39 with a molar ratio $1Al_2O_3$:$19SiO_2$:$25Na_2O$:$1575H_2O$ presented in the figure 2.20-2.21 can be compared with G30, G29 and G26 (figure 2.22), respectively, with a molar composition of $1Al_2O_3$:$10SiO_2$:$12Na_2O$:$829H_2O$. There is no clear trend for the results obtained, maybe because their water contents were also different.

Figure 2.22 – The inside surface of the faujasite membranes synthesized at conditions G30 (top left), G29 (top right) and G26 (bottom) corresponding to a molar ratio of $1Al_2O_3$:$10SiO_2$:$12Na_2O$:$829H_2O$, in table 2.1.

By changing the water amount, the final membranes present different properties. A small change can sometimes lead to the presence of a second phase, as shown in figure 2.23, while a very high amount of water can prevent the membrane formation and no material is attached to the substrate (figure 2.24).

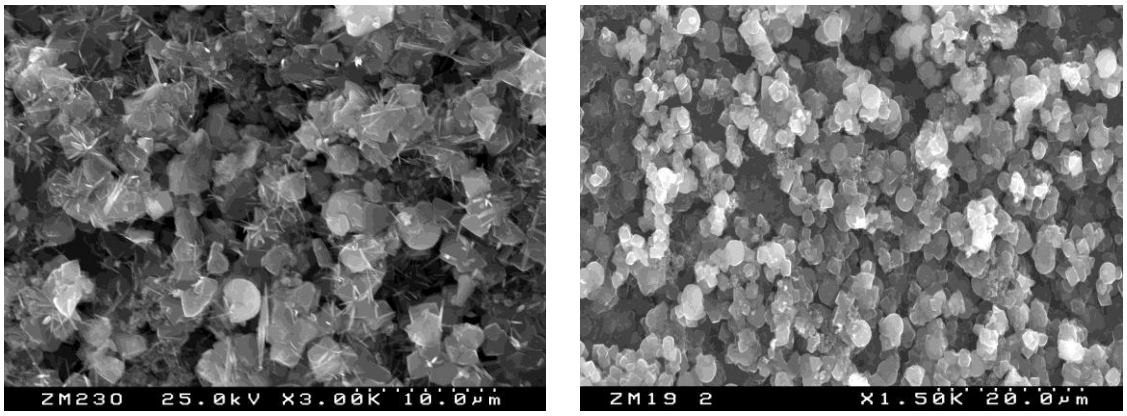

Figure 2.23 – The inside surface of the faujasite membranes synthesized at conditions G2 (left) and G16 (right) in table 2.1, corresponding to H_2O/Al_2O_3 ratios of 829 and 1086, respectively.

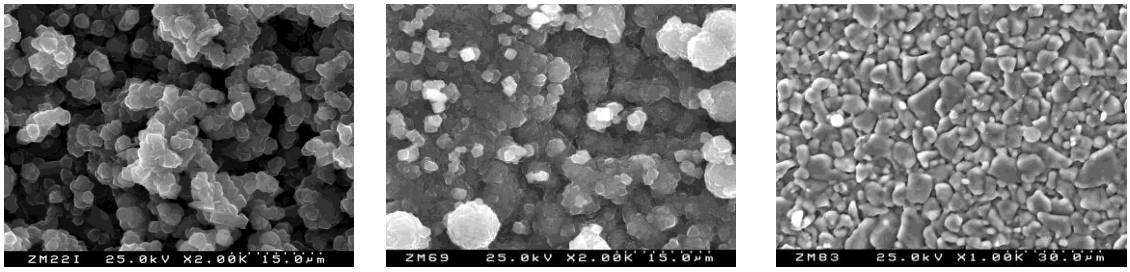

Figure 2.24 – The inside surface of the faujasite membranes synthesized at conditions G40 (left), G43 (centre) and G44 (right) in table 2.1, corresponding to H_2O/Al_2O_3 ratios of 1575, 1723 and 5000, respectively.

According to the previous results, the quality of the final membrane depends on the interaction of several parameters. No clear systematic relationship was found between synthesis conditions and the final microstructure of membranes. Nevertheless, it was possible to conclude that the composition $1Al_2O_3{:}5SiO_2{:}7Na_2O{:}415H_2O$ is the most favorable conditions through which a high quality membrane can be synthesized.

2.4.2.4 Synthesis repetition

Repeating the synthesis is sometimes used to make a defect-free zeolite membrane. However, since there are several factors that affect their structure and quality, the results obtained with repeat synthesis depend on the combination of all these parameters. Some of the membranes were composed

of a mixture of FAU and P, as shown in figure 2.25. However, at certain compositions, such as G31 and G54, the transformation of the FAU phase to zeolite P did not occur and the membranes were comprised of typical bipyramidal crystals, randomly oriented and well intergrown (figures 2.26 and 2.27).

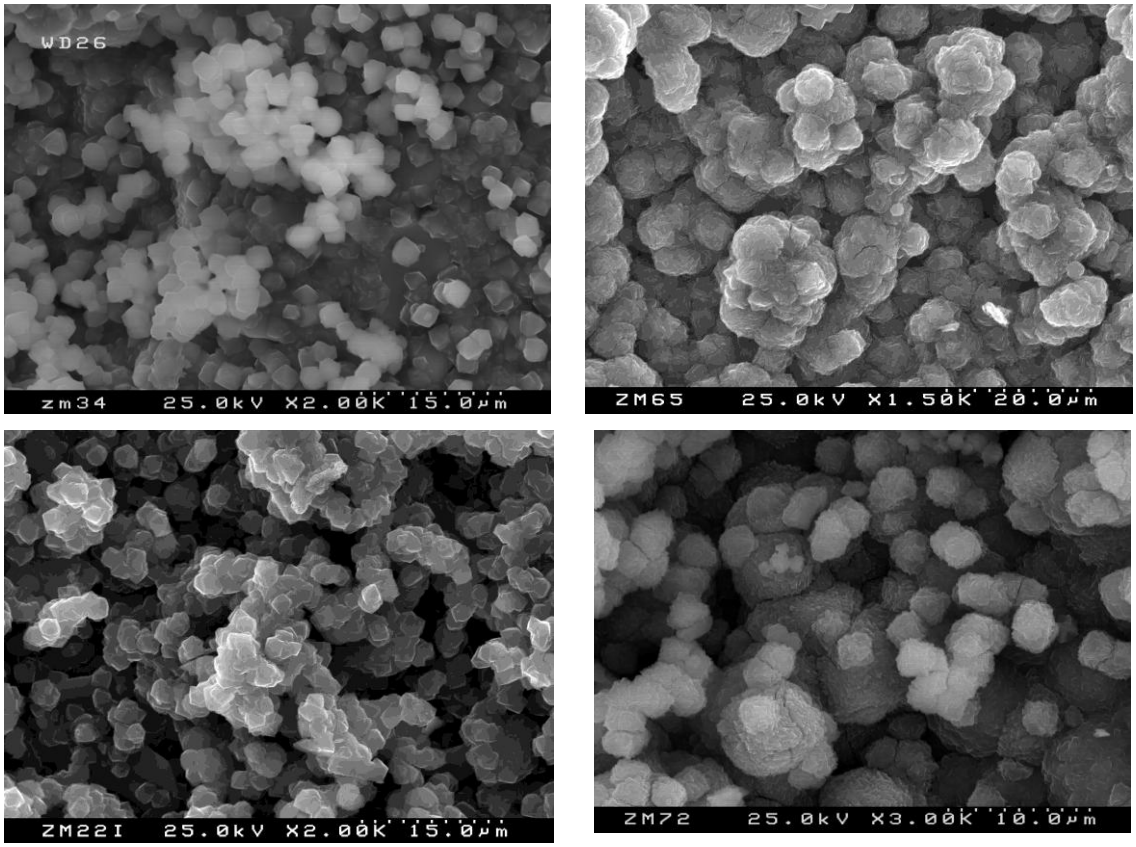

Figure 2.25 – The inside surface of the faujasite membranes synthesized at conditions G25 (top left) and G40 (bottom left) corresponding to one synthesis, and G29 (top right) and G41 (bottom right) in table 2.1, corresponding two syntheses.

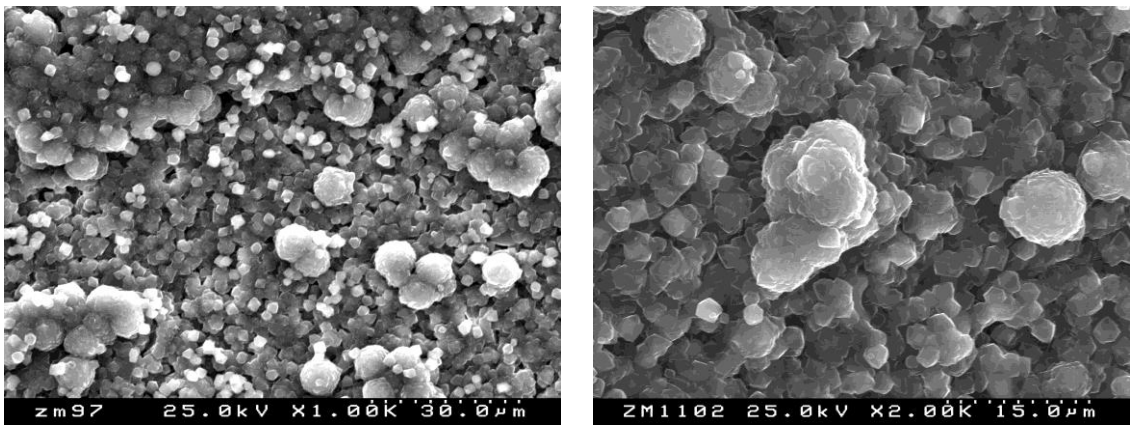

Figure 2.26 – The inside surface of the faujasite membranes synthesized at conditions G31 (left) and G34 (right) in table 2.1, corresponding to one and two synthesis, respectively.

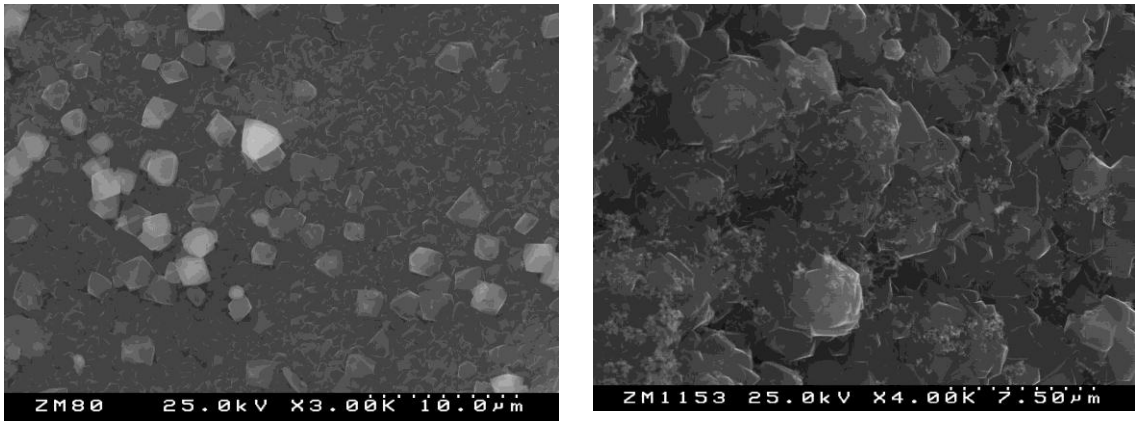

Figure 2.27 – The inside surface of the faujasite membranes synthesized at conditions G54 (left) and G55 (right) in table 2.1, corresponding to one and two synthesis, respectively.

Therefore, the repeat synthesis seems to give a better way to control the phase formation than increasing the synthesis time. This could be due to the lack of zeolite P nuclear centre in fresh nutrients. According to SEM results the film thickness was doubled with the repetition of the synthesis. However, repeat synthesis more than two times results in a mixture of zeolite P and FAU again (figure 2.28), which was also identified by XRD results.

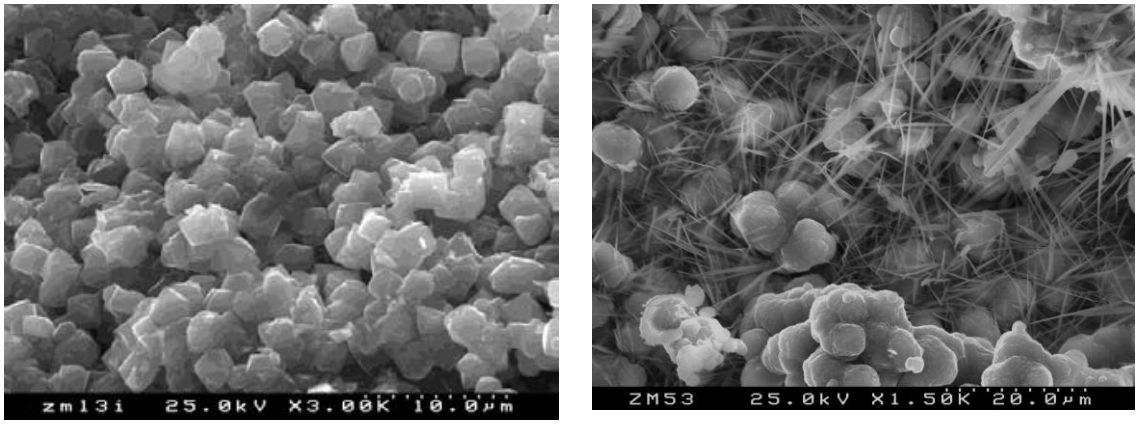

Figure 2.28 – The inside surface of the faujasite membranes synthesized at conditions G49 (left) and G57 (right) in table 2.1, corresponding to one and four synthesis, respectively.

2.4.2.5 Effect of synthesis repetition with gels and clear solutions

A new way to control the formation of faujasite membranes consists in the combination of gels and clear solutions (see next chapter) as the starting mixture. Some membranes were prepared with two syntheses made from a gel and another two with a clear solution. Through this way, it is possible to obtain a good surface coverage of single FAU phase (figure 2.29).

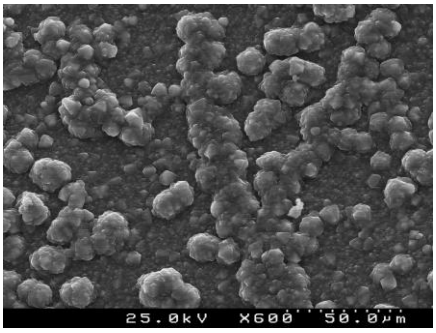

Figure 2.29 – The inside surface of the faujasite membrane synthesized at condition G61 (right) in table 2.1.

This is a better way to control the phase of the final membrane relatively to the repeat synthesis with only gels by reducing the defects and increasing the surface coverage or eliminating second phases (figure 2.30).

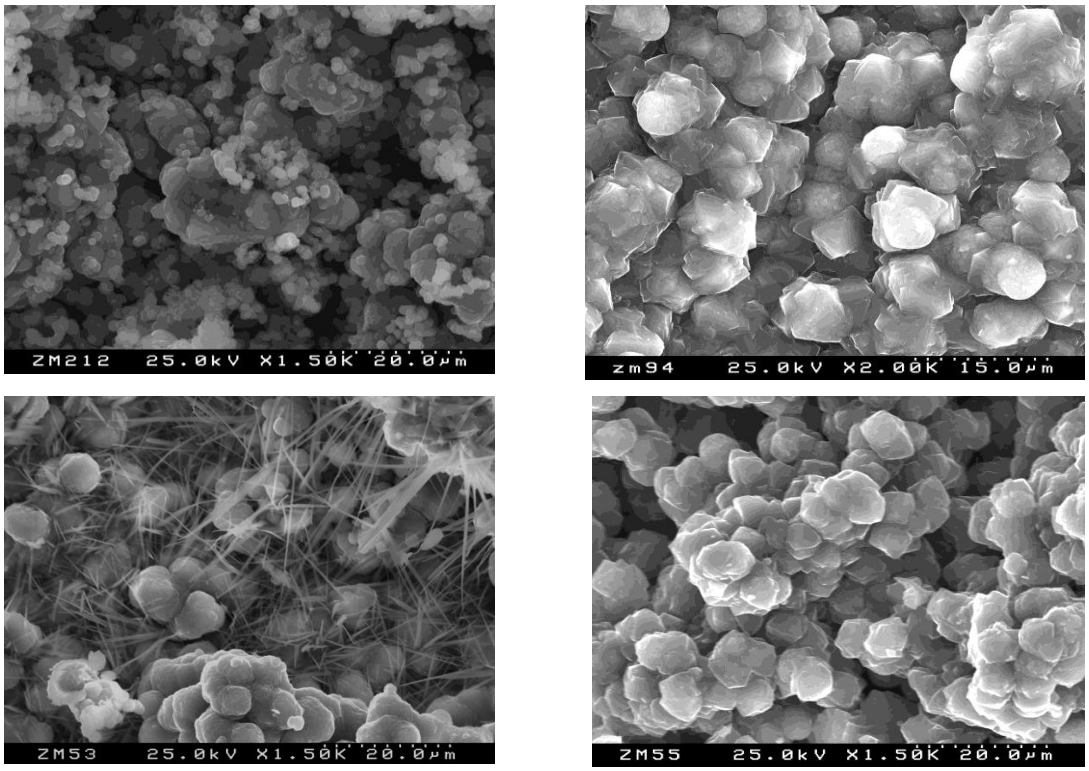

Figure 2.30 – The inside surface of the faujasite membranes synthesized at conditions G58 (top left) and G57 (bottom left) in table 2.1, corresponding to four synthesis with gel, and G60 (top right) and G62 (bottom right) in table 2.1, corresponding to four synthesis with both gels and clear solutions.

2.4.2.6 Effect of the support

The characteristic of the macroporous support is critical for the quality of the membrane itself. Defects and irregularities of the support surface, such as pores much larger than the average pore

diameter of the support or grains broken out of the support, usually produce defects in the layer grown on it. Rough surfaces exclude the formation of defect-free thin and smooth layers in a single step. Finally the wetting behavior of the surface is also important in layer formation processes. Severe local changes in wettability result in pinhole formation. Consequently, high quality supports should be smooth, have constant and homogeneous surface characteristics (wettability) and preferably have a relatively narrow pore size distribution. They should have sufficient mechanical strength which does not decrease with time [21]. In this study, α-Al_2O_3 tubes were selected as the support for the growth of faujasite membranes. The influence of different porosities, namely, 70, 1000 and 1800 nm, on the final microstructure was tested. The best results were obtained for the samples using supports with 70 and 1000 nm pores, since the zeolite layer was thicker, forming a continuous and flat film, as shown in figures 2.31, and a maximum layer thickness of ca. 10 μm was obtained when using the 70 nm support.

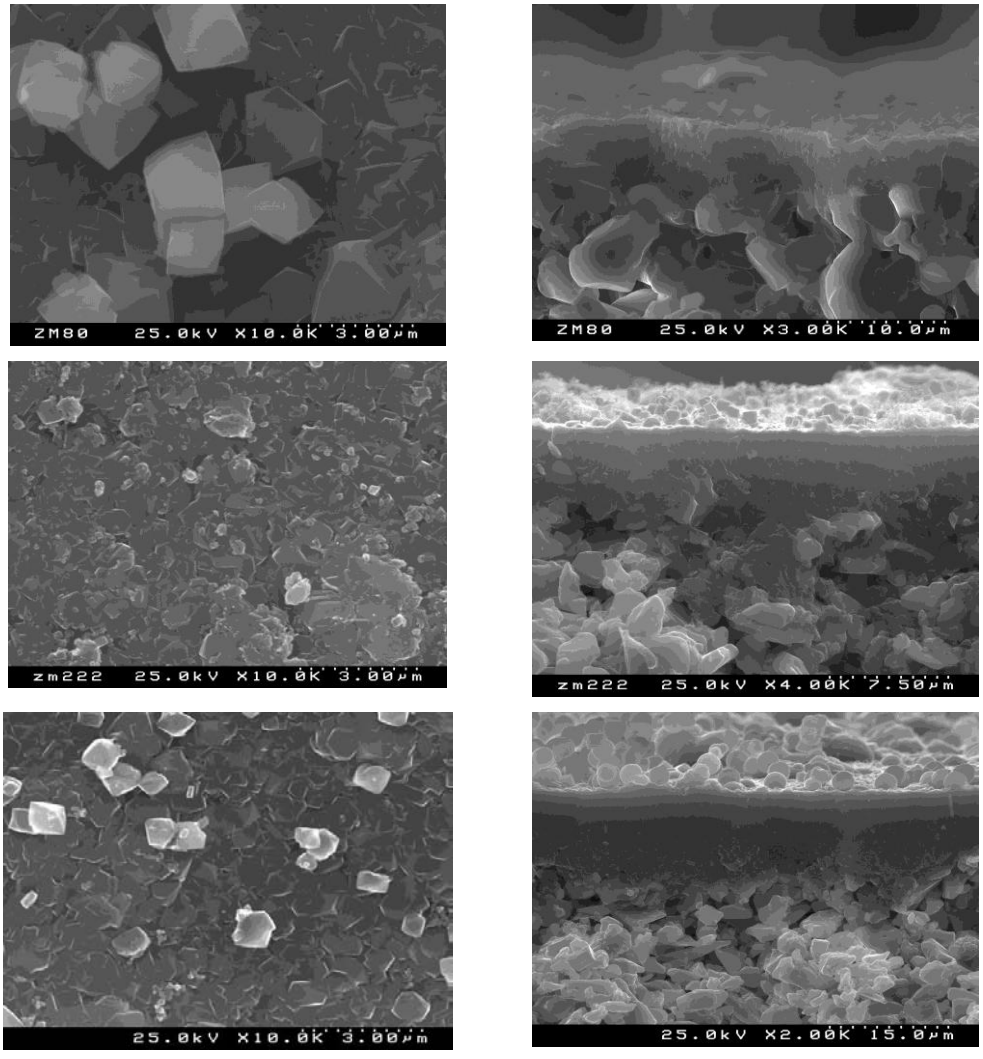

Figure 2.31 – The top view (left) and cross-section (right) of the faujasite membranes synthesized at conditions G54 (top), G52 (middle) and G53 (bottom) on inside surfaces of support tube with 1800, 1000 and 70 nm pores, respectively.

2.5 Conclusions

Several faujasite membranes were prepared under different conditions in order to optimize the synthesis procedure. Pure faujasite membranes were obtained with well-defined and intergrown crystals covering the alumina support tube. According to the results obtained, it is possible to conclude that several parameters determine the final microstructure and properties of the faujasite membranes, namely, type of seed crystals used, support, time and temperature, gel composition and amount of synthesis performed for the same membrane.

A suspension of 20% zeolite X crystals was considered to be better for seeding instead of zeolite Y, which might be explained by the different Si/Al ratio of these zeolites.

Better and thicker membranes were produced when using supports of 70 and 1000 nm relatively to 1800 nm due to the lower porosity, which is adequate for the preparation of a homogeneous and continuous layer.

The effect of each component in the gel was not clearly identified since it is strictly dependent on the other parameters used. No clear trend was found but the composition $1Al_2O_3{:}5SiO_2{:}7Na_2O{:}415H_2O$ resulted in a wider range of variable conditions for the production of defect-free, well intergrown, faujasite membranes.

A prolonged hydrothermal treatment would lead to the formation of zeolite P. Therefore, a suitable time and temperature of synthesis must be selected in order to avoid its formation and produce pure faujasite membranes. A better way to control the layer thickness and phase formation consists in repeating the synthesis. When using only gels, no more than two syntheses could be performed without the presence of zeolite P. However, when using mixed gels and clear solutions at least four syntheses could be performed with an increase in the layer thickness and without reducing the quality and purity of the membrane.

2.6 References

[1] H.S. Sherry, J. Phys. Chem. 70 (1966) 1158-1168

[2] V. Nikolakis, G. Xomeritakis, A. Abibi, M. Dickson, M. Tsapatsis, D.G. Vlachos, J. Membr. Sci. 184 (2001) 209-219

[3] M.R. Antonio, D.T. Tsou, Ind. Eng. Chem. Res. 32 (1993) 273-278

[4] N.D. Hutson, B.A. Reisner, R.T. Yang, B.H. Toby, Chem. Mater. 12 (2000) 3020-3031

[5] T. Sun, K. Seff, Chemical Reviews 94 (1994) 857-870

[6] S. Mintova, N.H. Olson, T. Bein, Angew. Chem. Int. Ed. 38 No 21 (1999) 3201-3204

[7] S. Nair, Z. Lai, V. Nikolakis, G. Xomeritakis, G. Bonilla, M. Tsapatsis, Micropor. Mesopor. Mater. 48 (2001) 219-228

[8] I.G. Giannakopolous, V. Nikolakis, Ind. Eng. Chem. Res. 44 (2005) 226-230

[9] Z. Xu, Q. Chen, G. Lu, J. Natur. Gas Chem. 11 (2002) 171-179

[10] H. Kacirek, H. Lechert, J. Phys. Chem. 79 (1975) 1589-1593

[11] H. Kita, T. Inoue, H. Asamura, K. Tanaka, K. Okamoto, Chem. Commun. (1997) 45-46

[12] H. Kita, K. Fuchida, T. Horita, H. Asamura, K. Okamoto, Sep. Purif. Technol. 25 (2001) 261-268

[13] K. Kusakabe, T. Kuroda, A. Murata, S. Morooka, Ind. Eng. Chem. Res. 36 (1997) 649-655

[14] Y. Hasegawa, K. Kusakabe, S. Morooka, Chem. Eng. Sci. 56 (2001) 4273-4281

[15] S. Li, V.A. Tuan, J.L. Falconer, R.D. Noble, Micropor. Mesopor. Mater. 53 (2002) 59-70

[16] H. Robson, K.P. Lillerud, *Verified Syntheses of Zeolitic Materials*, Second Revised Edition, Elsevier Science B.V. (2001) p. 150-152

[17] H. Robson, K.P. Lillerud, *Verified Syntheses of Zeolitic Materials*, Second Revised Edition, Elsevier Science B.V. (2001) p. 156-158

[18] R. Bulánek, B. Wichterlová, Z. Sobalík, J. Tichý, Appl. Catal. B: Environmental 31 (2001) 13-25

[19] M. Lassinantti, J. Hedlund, J. Sterte, Micropor. Mesopor. Mater. 38 (2000) 25-34

[20] K. Weh, M. Noack, I. Sieber, J. Caro, Micropor. Mesopor. Mater. 54 (2002) 27-36

[21] A. J. Burggraaf, L. Cot, *Fundamentals of Inorganic Membrane Science and Technology*, Membrane Science and Technology Series, 4, Elsevier 1996

3 Faujasite membranes grown from clear solutions

3.1 Clear solutions

In the preparation of zeolite membranes, one of the desired processes is to synthesize them from a clear solution. The advantages include: producing less waste chemicals, consuming less source materials and easier control of crystallization.

There is little information available in the literature about the synthesis of zeolites from clear solutions. They are mainly used for the preparation of zeolite nanoparticles such as silicalite [1-2] and zeolite Y [3]. The use of clear solutions for the synthesis of zeolite membranes is not widely expanded and few information is found in the literature. Kyotani et al. [4] prepared and characterized zeolite LTA membranes on tubular porous alumina from clear solutions of different molar compositions. Frontera et al. [5] prepared zeolite LTA on silicon wafer using tetramethylammonium (TMA) hydroxide as a structure directing agent by hydrothermal treatment at 100°C during 4h. High quality oriented zeolite LTA membranes were obtained and the effect of aging time on layer thickness and orientation was studied. Yan et al. [6] prepared oriented continuous zeolite MFI thin films (< 0.4 μm) on stainless steel substrates by direct in-situ crystallization and the influence of the compositions on the orientation was investigated. Yang et al. [7] synthesized high quality hydroxysodalite zeolite membranes on α-Al_2O_3 supports with layer thicknesses of 6-7 μm by microwave-assisted hydrothermal synthesis method. Gas permeation results showed a hydrogen/n-butane permselectivity larger than 1000. Therefore, these membranes are promising candidates for the separation of hydrogen from gas mixtures and important for the emerging hydrogen energy fuel system. The use of clear solutions in the preparation of faujasite membranes, however, is even rare. To date, only Kumakiri et al. [8] prepared faujasite membranes on the surface of α-alumina disks, using zeolite Y as seeds. The membranes had a thickness of about 5 μm. By repeating the synthesis, there was no phase transformation from faujasite to other material. The zeolite crystals increased in size with synthesis time and formed a continuous membrane on the porous substrate. The selectivities also increased with repeating the synthesis.

Due to the lack of information and research on the development of zeolite membranes from clear solution, a comprehensive study is required and is the subject of this chapter. The experimental procedure and the results obtained are described in the following sections.

3.2 Experimental

The faujasite membranes crystallized in a clear solution follow the same general procedure shown in figure 2.2.

An aluminate solution was made by dissolving sodium aluminate and sodium hydroxide in distilled water, and a silicate solution was made by dissolving sodium metasilicate in distilled water. After being stirred at 70°C for 1h, the silicate solution was added to the aluminate solution. The aluminosilicate solution was stirred for 5 minutes to produce a clear, homogeneous solution. This clear solution had a molar composition of $80Na_2O:1Al_2O_3:9SiO_2:5000H_2O$. The reaction mixture had a high water content compared with previous reports to avoid any nucleation in the reaction [9]. The hydrothermal synthesis was carried out following two procedures. One involved putting the seeded support into an autoclave, adding the precursor solution and treating it in the oven at 80°C for 5h. The other one consisted in placing the seeded porous support at the bottom of a flask and add the clear solution. This system was then immersed in an oil bath under stirring, fitted with a condenser and a heater. The treatment was also performed at 80°C for 5h. After crystallization, the substrate was removed from the solution, washed with water and dried. Part of the compositions and synthesis conditions used for the preparation of membrane from clear solution are listed in table 3.1.

Table 3.1 – Synthesis conditions for the membrane prepared from a clear solution

Sample	***Compositions ($Al_2O_3:SiO_2:Na_2O:H_2O$)***	***Time (h)***	***Temperature (°C)***	***Seed Crystals***	***Pore of support (nm)***	***Yield (mg/g)***
C1	1:9:80:5000	5	80	X20%	1800	3.34
C2				Y5%		8.26
C3		5+5*				9.84
C4				Y20%		6.80
C5				X20%		8.21
C6		5+5+5			1000	17.81
C7		5+5+5+5			1800	15.13
C8					70	6.67
C9					1000	10.82
C10	1:9:80:5000 + 1.0g PDMS in 100 mL n-heptane					18.51
C11	1:9:80:5000	5+5+5+5+5 +5			1800	15.46
C12					70	15.65
C13					1000	17.32
C14		5+5+5+5+5 +5+5+5			1800	21.76
C15		7				8.27
C16		24				8.78
C17		24+5				19.65
C18		24+24				22.90
C19					70	24.56
C20					1000	35.97
C21		24+24+24			1800	36.76
C22					70	24.57
C23					1000	32.84
C24		24+24+24+ 24			1800	36.12
C25		48				19.50
C26		48+24+24			1000	35.89

C27		24		Y20%	1800	8.16
C28		24+24				18.13
C29		5	100	X20%		7.73
C30		5+5				14.39
C31	1:9:45:5000	5	80			3.69
C32		5+5				3.61
C33	1:9:80:3000	5				10.68
C34	1:9:80:2000					12.97
C35	1:9:80:1000					19.94

* It represents the repeat synthesis.

3.3 Results and discussion

3.3.1 XRD analysis

The XRD pattern in figure 3.1 is the result obtained from the membrane synthesized at condition C18 in table 3.1. The formation of faujasite membrane can be clearly proved.

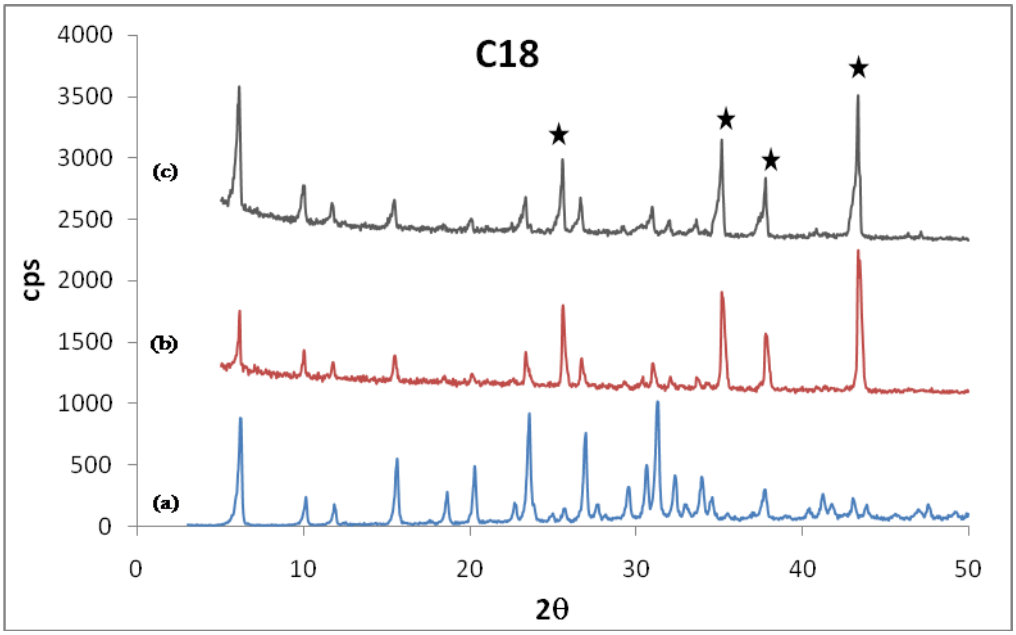

Figure 3.1 – XRD patterns collected from a powder sample (a); the inside (b) and outside (c) of a membrane synthesized at condition C18 in table 3.1. Stars depict the reflections from the α-alumina support.

3.3.2 SEM analysis

When using the clear solution as the starting mixture it was possible to obtain very well-defined faujasite crystals covering the surface of the support tube and forming a continuous and smooth zeolite layer, as is represented in figures 3.2-3.4.

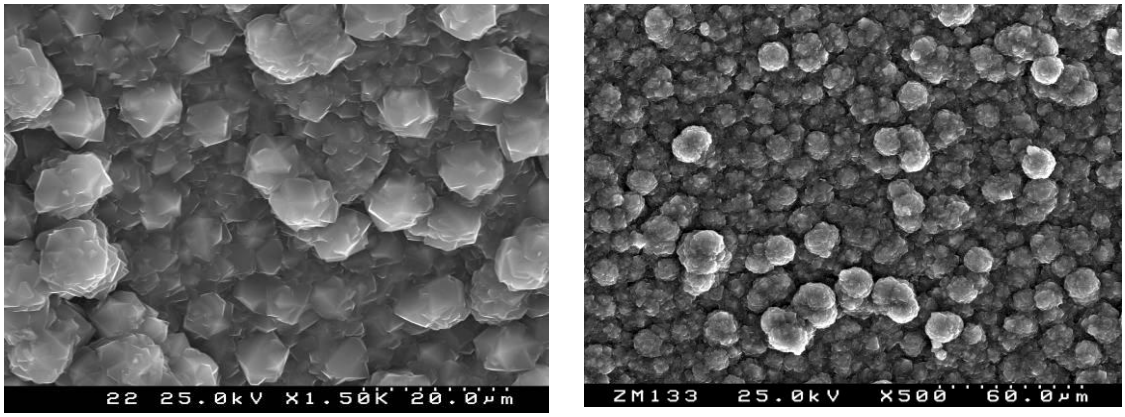

Figure 3.2 – The inside surfaces of the faujasite membranes synthesized at condition C19 (left) and C24 (right) in table 3.1.

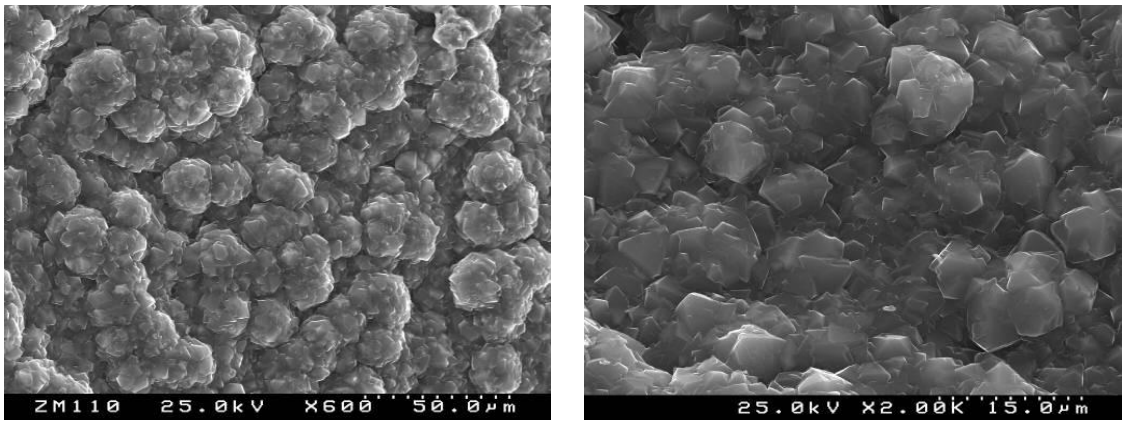

Figure 3.3 – The outside surfaces of the faujasite membranes synthesized at condition C21 (left) and C28 (right) in table 3.1.

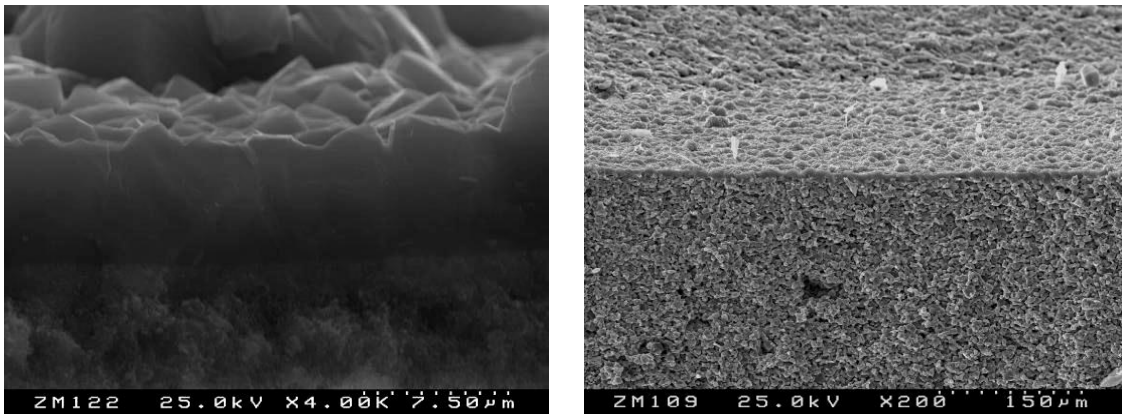

Figure 3.4 – The cross-section of the inside surface of the faujasite membrane synthesized at condition C22 (left) and C20 (right) in table 3.1.

3.3.2.1 Effect of seeding

Suspensions with 20 wt.% zeolite X or 5 and 20 wt.% zeolite Y crystals were used in seeding process in the synthesis with clear solution. Under some synthesis conditions there is no any difference in the final microstructure of the faujasite membranes (figures 3.5) when using zeolite X or Y seeds.

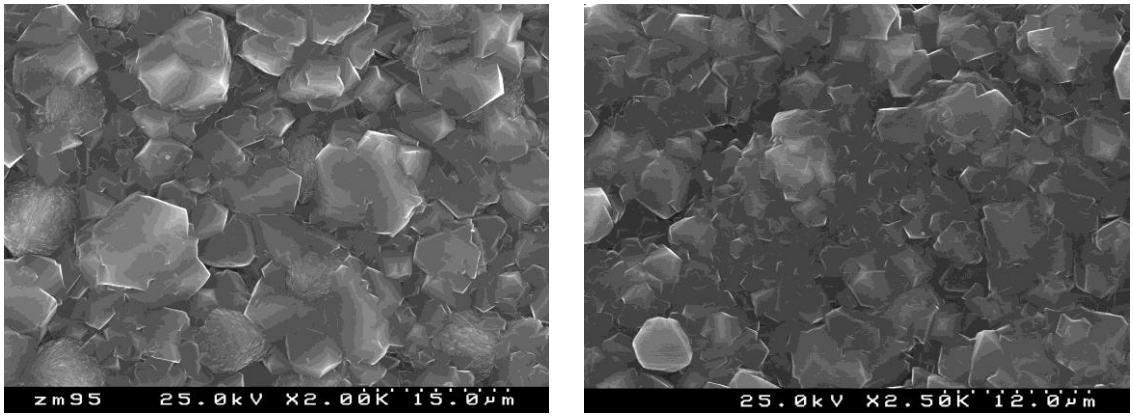

Figure 3.5 – The inside surface of the faujasite membranes synthesized at conditions C18 (left) and C28 (right) in table 3.1.

However, in general, the zeolite X seeding allows the formation of a continuous membrane, while with zeolite Y seeding the presence of a second phase was observed (figure 3.6). Although the formation of a second phase is not always observed when using zeolite Y, the coverage of the support is not well succeeded. In this regard, zeolite X should be the preferred seeding for the synthesis of faujasite membranes when using clear solutions as the starting batch.

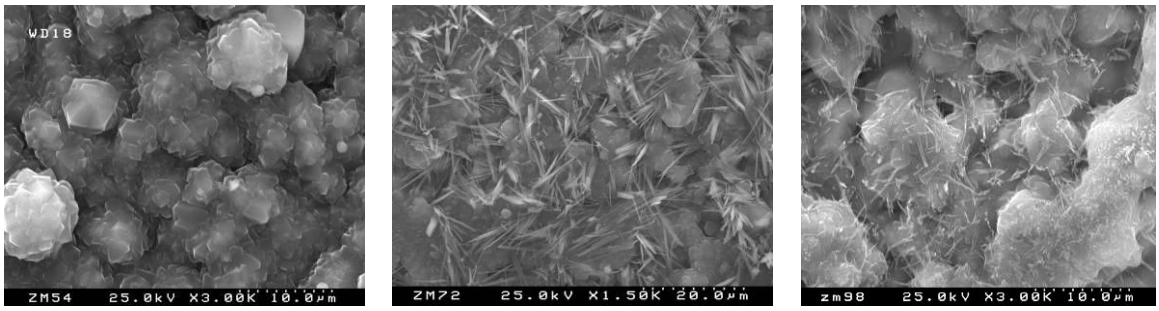

Figure 3.6 – The inside surface of membranes synthesized at conditions C5 (left), C3 (middle) and C4 (right).

3.3.2.2 Effect of time

The synthesis time was changed from 5 to 7 h (figure 3.7). No zeolite P, amorphous material and cracks were found and a single faujasite membrane was obtained although it seems that the pinholes

still existed. The quantity of crystals present was increased when raising the synthesis time to 7 h, but their morphology was maintained. Since the compositions used in the experiments has a higher water content any nucleation in solution will be eliminated, providing a better control of the phase formation.

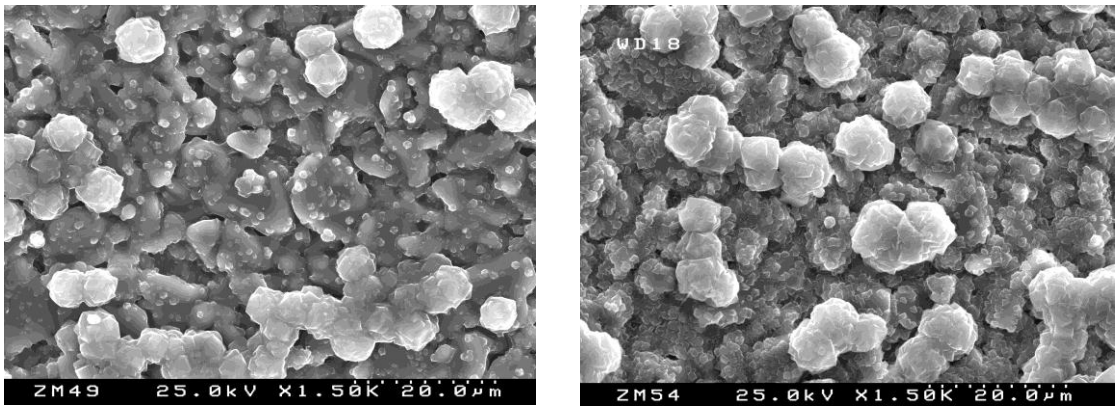

Figure 3.7 – The inside surface of membranes synthesized at conditions C1 (5h, left) and C15 (7h, right).

When the synthesis time was changed from 5 to 24 and 48 h in samples C1, C16 and C25, as illustrated in figures 3.8, pure faujasite membrane was obtained in all cases. The morphology was also maintained for every sample. The quantity of large crystals present increased significantly and the visible pinholes clearly decreased when increasing the time from 5 to 24 h. However, from 24 to 48 h they are very similar. Therefore, 24h is the suitable period for the synthesis of the faujasite membranes under these conditions.

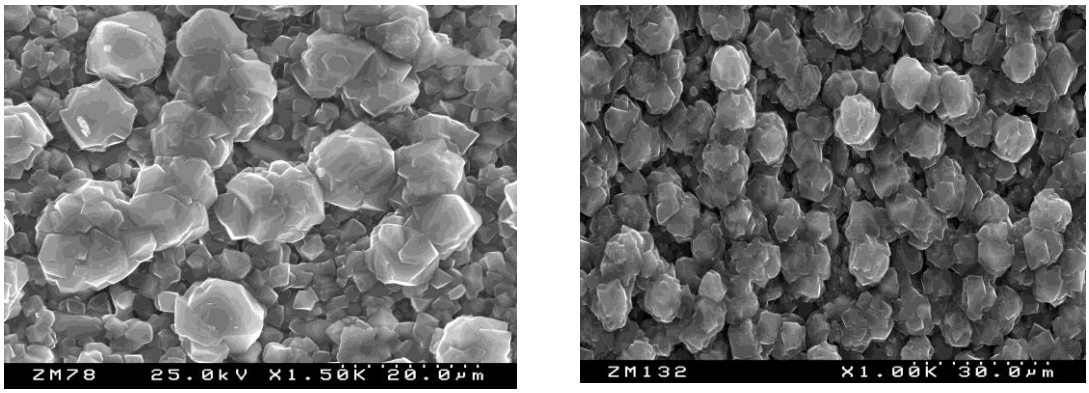

Figure 3.8 – The inside surface of a membrane synthesized at condition C16 (24h, left) and C25 (48h, right).

3.3.2.3 Effect of repeat synthesis

The repetition of the synthesis had the same effect as increasing the synthesis time (less than 24h). It was obtained crystals with typical faujasite morphology covering the support tube in a randomly oriented manner. The amount of crystals obtained was also enhanced comparing to a single synthesis.

When preparing the sample at 80°C for 5h, the faujasite phase was maintained after 8 time repeating syntheses without the presence of zeolite P and the crystals grew in an interlocking fashion covering the whole support surface (figures 3.9). Therefore, this composition and conditions are proved to be suitable for the synthesis of faujasite membranes since even after 8 times it is still possible to prepare pure phase. To date we have not reached the up-limit of the repetitious times of the synthesis that could be performed without second phase in the membrane.

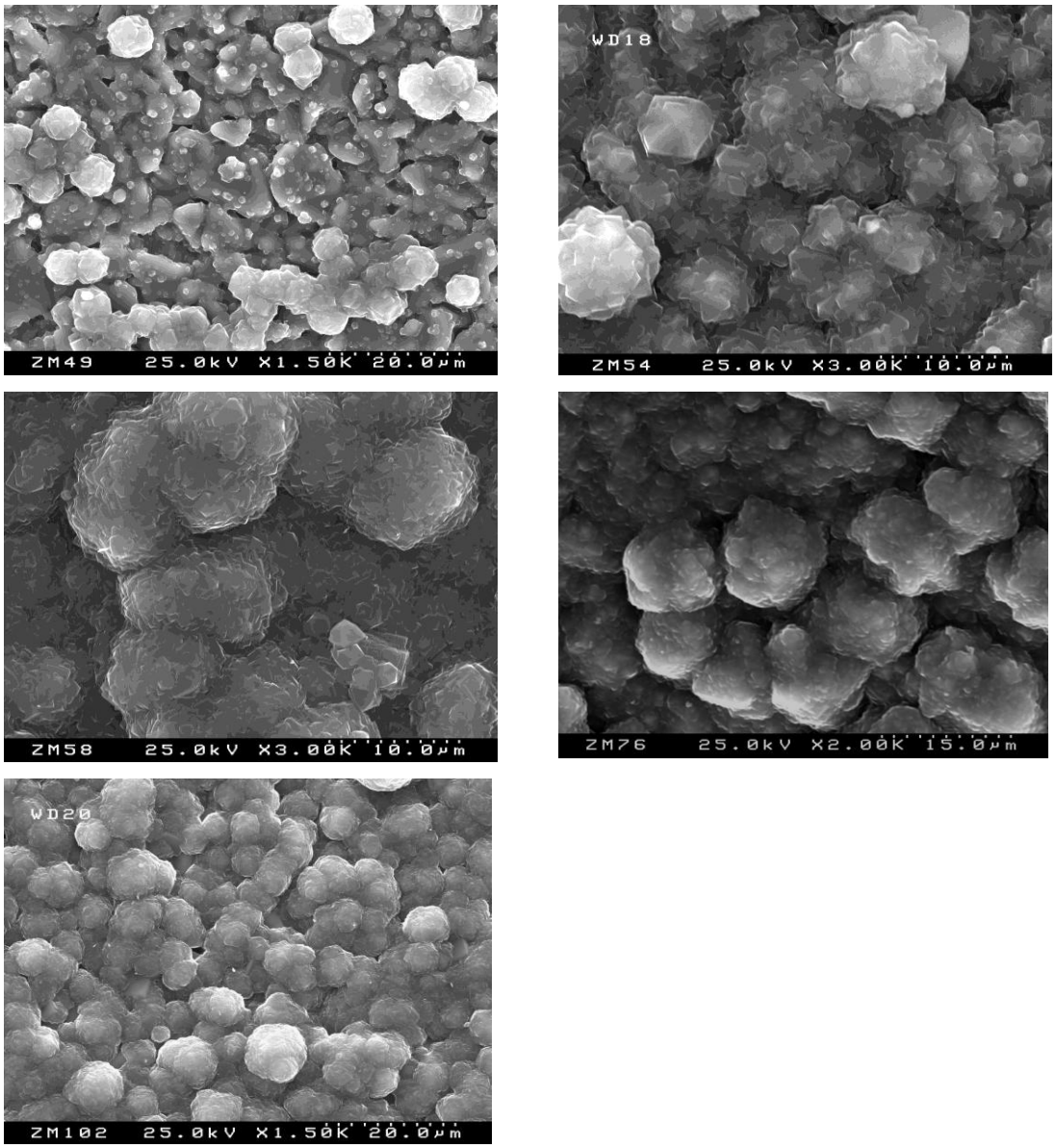

Figure 3.9 – The inside surface of membranes synthesized with different repletion times at conditions C1 (1 time, top left), C5 (2 times, top right), C7 (4 times, middle left) and C11 (6 times, middle right) and C14 (8 times, bottom). Each synthesis is 5h.

When the samples were prepared at 80°C for 24h, the repetition of the synthesis was made up to 4 times. There was an increase in the support coverage until three times the synthesis repetition, after which there was no observable change (figure 3.10). We also have not reached the up-limit of the repetitious times of the synthesis that could be performed without second phase in the membrane at this condition.

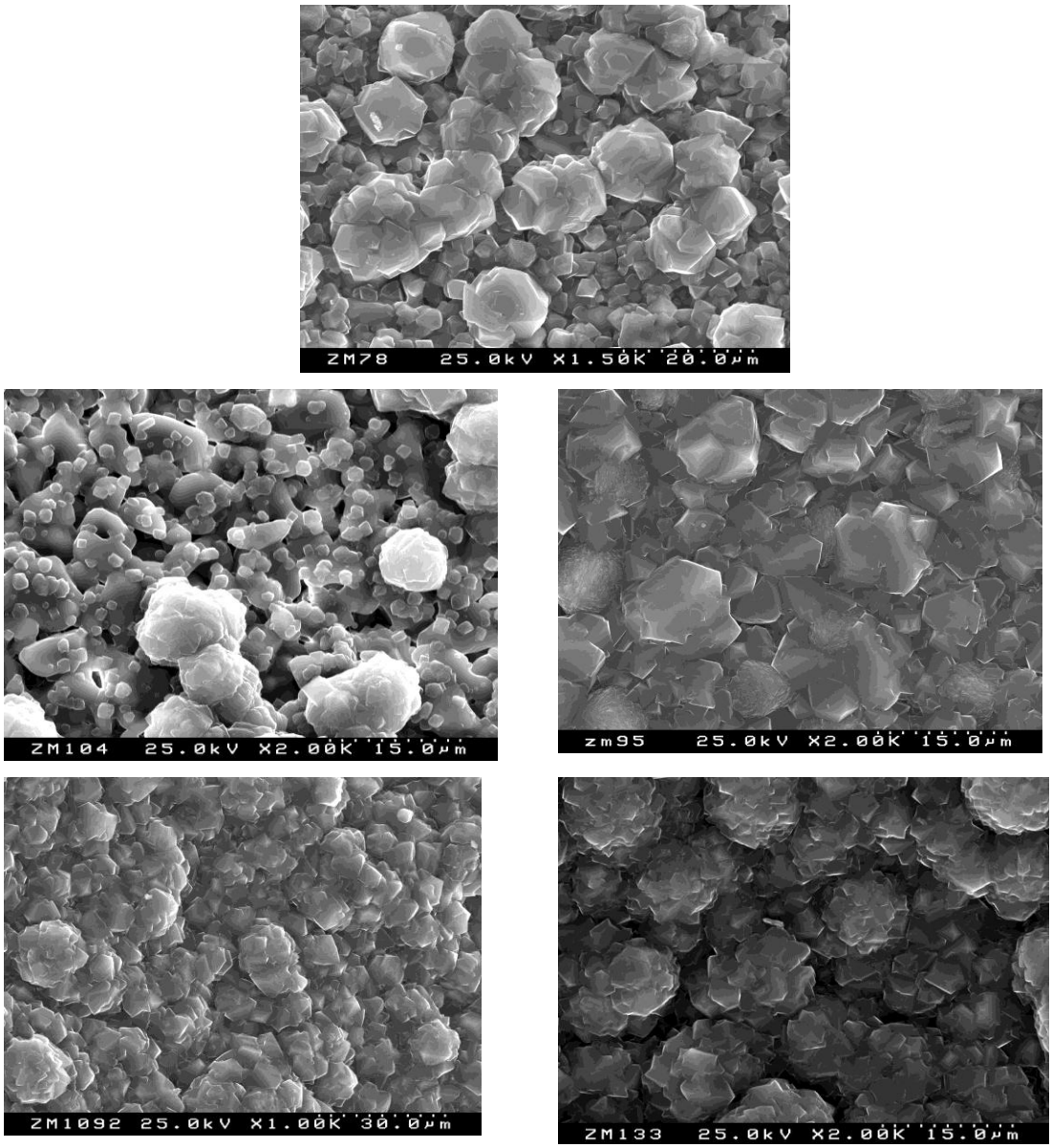

Figure 3.10 – The inside surfaces of membranes synthesized at conditions C16 (24h, top), C17 (24+5h, middle left), C18 (24+24h, middle right), C21 (3 times 24h, bottom left) and C24 (4 times 24h, bottom right).

Analyzing the cross-section images (figure 3.11) for the samples prepared at 80°C for 24h with a repetition up to 4 times, it is possible to conclude that the layer thickness increases from about 6 μm for the sample with a double synthesis up to about 8 μm when the synthesis was repeated three times. An enhancement of the layer's thickness was also observed for the sample with four repeated synthesis (ca. 12μm).

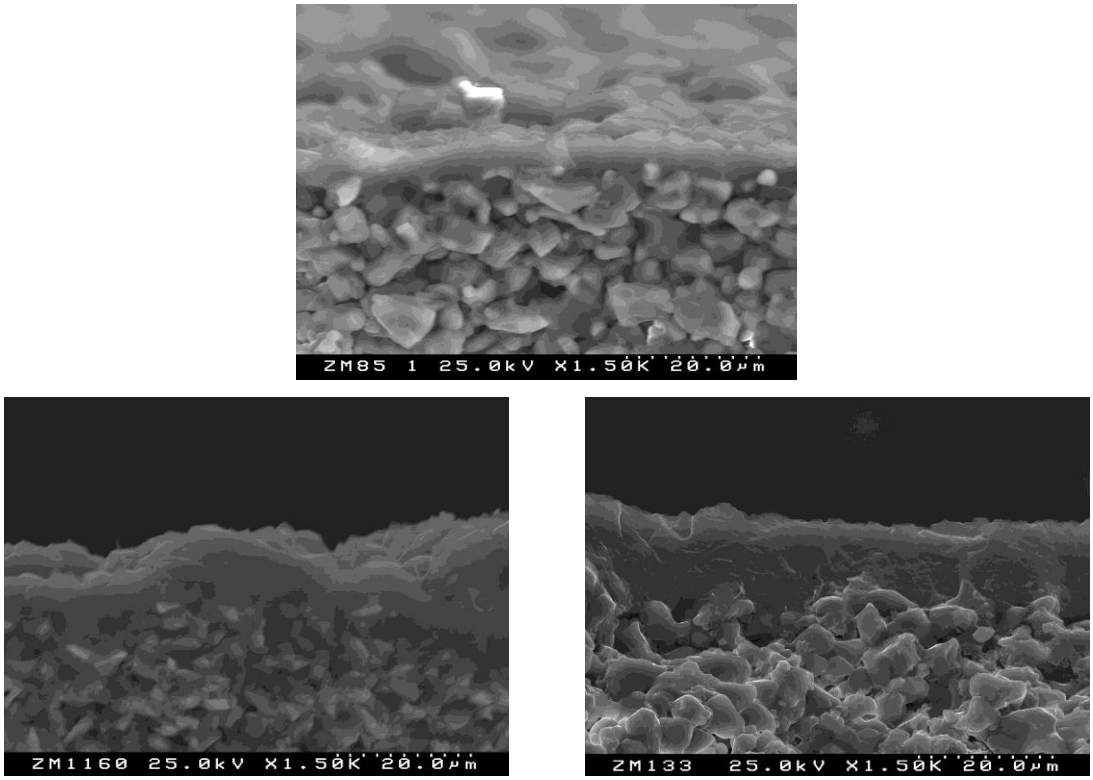

Figure 3.11 – Internal cross-section view of the membranes synthesized at conditions C18 (top), C21 (bottom left) and C24 (bottom right) corresponding, respectively, to 2, 3 and 4 repetitions of 24h each.

3.3.2.4 Effect of support

The effect of supports on the quality of membranes was tested using the ones with different porosities, namely: 70, 1000 and 1800 nm. The better results were obtained for the samples using 70 and 1000 nm, since the zeolite layer was thicker, forming a continuous and flat film, as shown in figures 3.12:

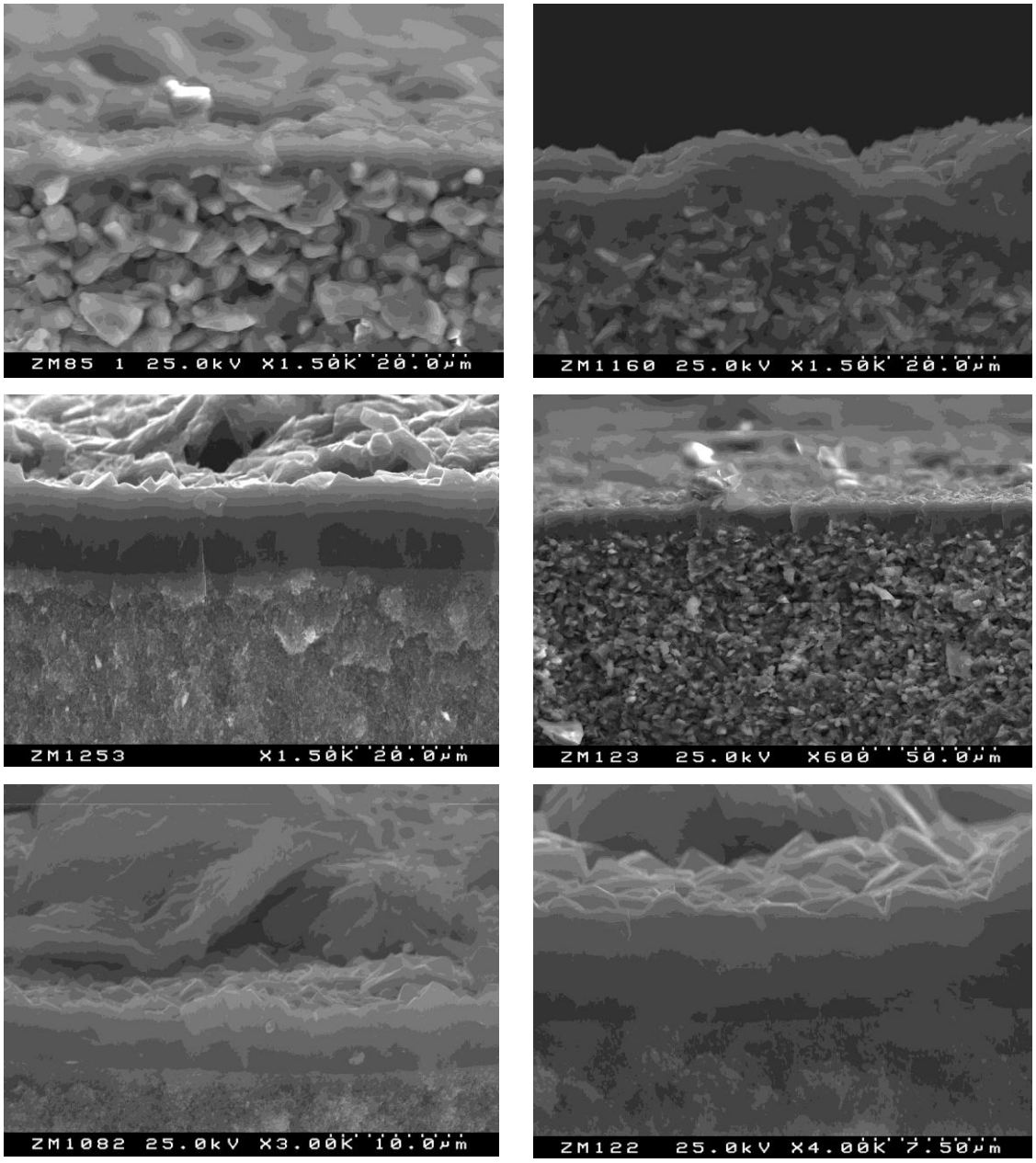

Figure 3.12 – The cross-sections of inside surface of membranes C18 and C21 (top images), C20 and C23 (middle images) and C19 and C22 (bottom images), corresponding to a support with 1800, 1000 and 70 nm pore, respectively.

3.3.2.5 Effect of composition

In this study, sodium hydroxide and the water content were both changed in the initial mixture. When the amount of sodium hydroxide was decreased the crystals form agglomerates in certain parts of the support providing an insufficient coverage in most of the support surface, as shown in figure 3.13.

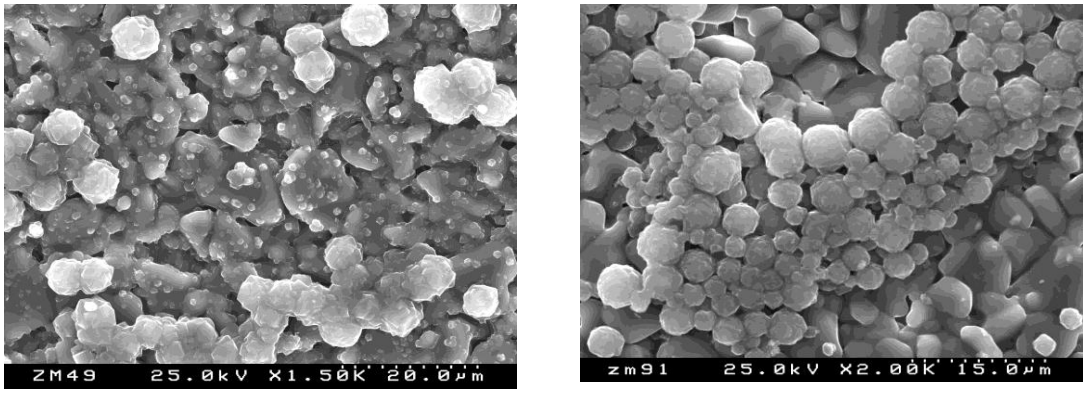

Figure 3.13 – The inside surfaces of membranes prepared at condition C1 (left) and with a lower sodium content at condition C31 (right).

When decreasing the water content from C1 (figure 3.13) to C33 (figure 3.14), it was observed an increase in the crystals size. A further decrease to condition C35 leads to the presence of a second phase.

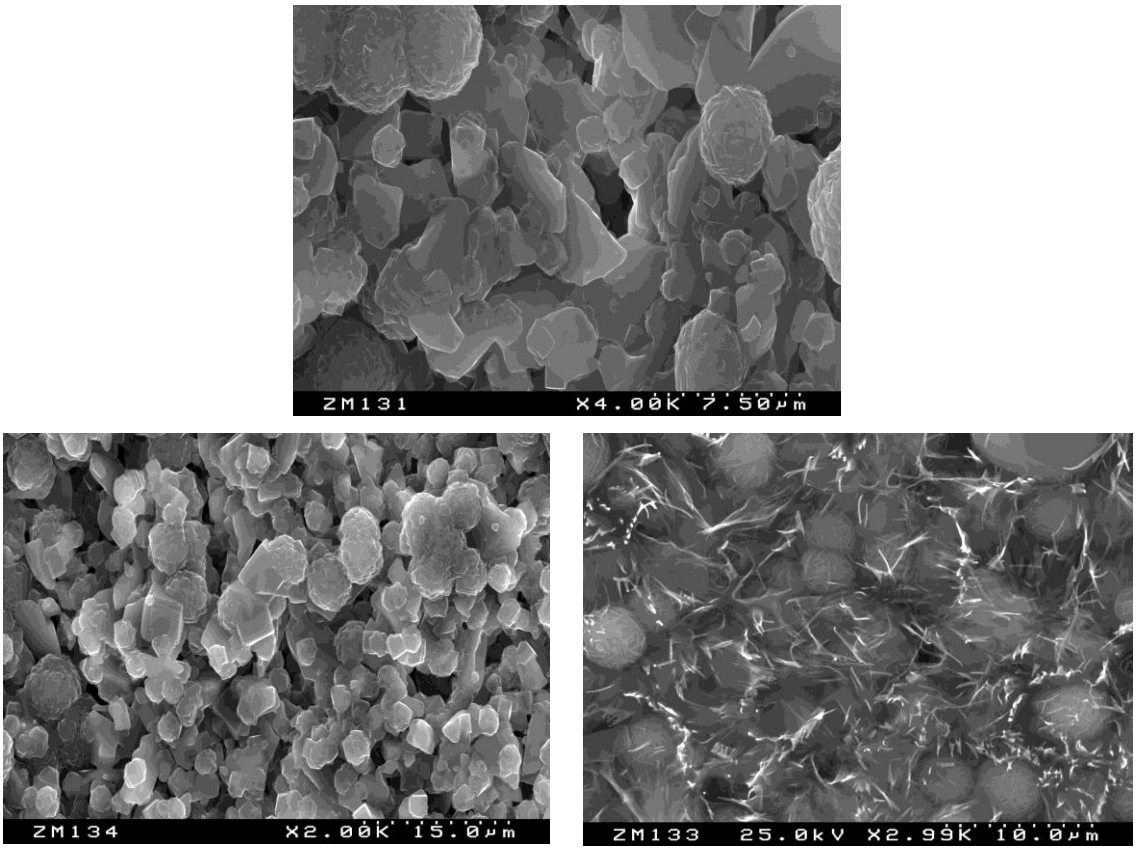

Figure 3.14 – The inside surfaces of membranes prepared at condition C33 (top), C34 (bottom left) and C35 (bottom right) corresponding to a H_2O/Al_2O_3 ratio of 3000, 2000 and 1000, respectively.

Therefore, the content of each components of the initial mixture is detrimental to obtain the faujasite membranes without the presence of a second phase and with the crystals well interconnected covering the whole support surface.

3.3.2.6 Effect of temperature

The preferred temperature was of 80°C since the synthesis at 100°C decreases the quality of the membrane due to the presence of defects, as illustrated in figure 3.15.

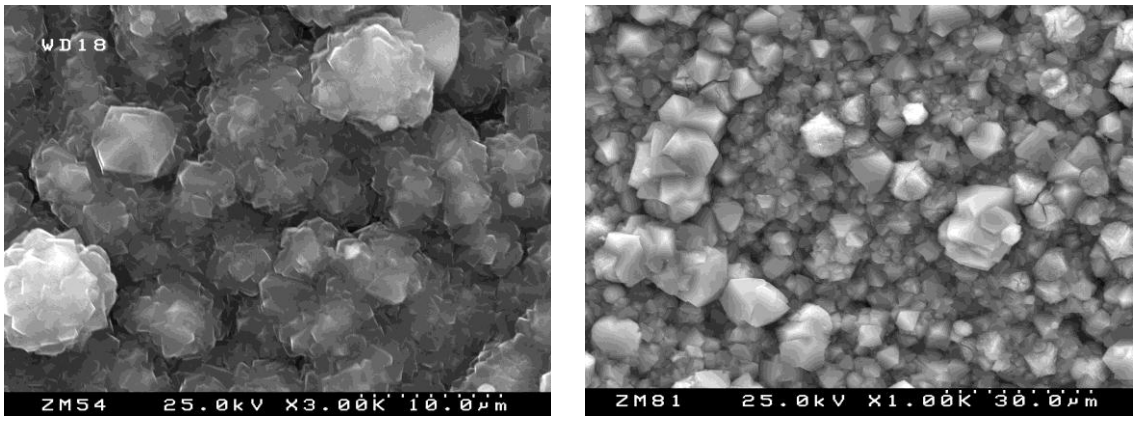

Figure 3.15 – The inside surface of membranes synthesized at condition C5 (left) and C30 (right), corresponding to 80°C and 100°C, respectively.

3.4 Conclusions

Several faujasite membranes were synthesized with clear solutions. A comparison between the seed crystals used makes it clear that zeolite X were preferred to zeolite Y. The use of this latter type of seeds may result in the presence of a second phase or in a lower degree of surface coverage. The optimum temperature was considered to be 80°C since when it was increased to 100°C the presence of defects was observed.

Using clear solutions as the starting materials a broader range of time was observed for the synthesis of pure, defect-free faujasite membranes, comparatively to the use of gels. Even after 48h the formation of zeolite P was not observed. This can be explained by the reduction of the rate of zeolite P nucleation when using clear solutions.

By repeating the synthesis several times one can conclude that there is an increase in the support coverage as well as in the layer thickness (12 μm for four repeated synthesis). Up to now, the up-limit of the repetitious times of the synthesis that could be performed without changing the membrane phase was not reached.

3.5 References

[1] L. R. A. Follens, A. Aerts, M. Haouas, T. P. Caremans, B. Loppinet, B. Goderis, J. Vermant, F. Taulelle, J. A. Martens and C. E. A. Kirschhock, Phys. Chem. Chem. Phys. 10 (2008) 5574–5583

[2] B. Tokay, M. Somer, A. Erdem-Şenatalar, F. Schüth, R.W. Thompson, Micropor. Mesopor. Mater. 118 (2009) 143–151

[3] B. Wang, H.Z. Ma, Q.Z. Shi, Chin. Chem. Lett. 13 (2002) 385-388

[4] T. Kyotani, T. Mizuno, Y. Katakura, S. Kakui, N. Shimotsuma, J. Saito, T. Nakane, J. Membr. Sci. 296 (2007) 162–170

[5] P. Frontera, F. Crea, F. Testa, R. Aiello, J. Porous Mater 14 (2007) 325–329

[6] Z. Wang, Y. Yan, Chem. Mater. 2001, 13, 1101-1107

[7] X. Xu, Y. Bao, C. Song, W. Yang, J. Liu, L. Lin, Micropor. Mesopor. Mater. 75 (2004) 173–181

[8] I. Kumakiri, T. Yamaguchi, S. Nakao, Ind. Eng. Chem. Res. 38 (1999) 4682-4688

[9] J. Padin, R.T. Yang, C.L. Munson, Ind. Eng. Chem. Res. 38 (1999) 3614-3621

4 Ion-exchanged membranes

4.1 Ion-exchange theory

The ability to exchange cations is probably one of the most apparent attributes of zeolites besides their adsorptive and catalytic properties. The ion-exchange properties of zeolites are caused by trivalent metal atoms, usually aluminum, that isomorphously substitute silicon atoms in the silicon oxide frameworks on the tetrahedra positions (T-sites), thus creating negative net-charges of the zeolite framework. The negative framework charges are compensated by cationic species that are extra framework ions. One of the most common ones is the Na^+ cation, which is usually found in as-synthesized zeolites. Depending on the synthesis conditions, other cations, such as for example K^+, NH_4^+, Ca^{2+}, Mg^{2+} or positively charged organic molecules, such as, tetraalkylammonium ions, might also be present in the as-synthesized materials. Whatever cationic species is present, it has to be located in the channels, cavities and/or cages of the respective zeolite structure. Not only cationic species are located in the channels and cavities of the as-synthesized zeolite but also solvent molecules, which are usually water molecules. According to Loewenstein's rule Si/Al ratios cannot be less than one to avoid Al-O-Al linkage, therefore the lowest Si/Al ratio is 1 although exception is known for sodalite. The compositions of zeolites range from those with Si/Al ratios of 1 in the low-silica zeolites A and X to pure siliceous forms, such as in silicalite-1. Since the amount of cations in a zeolite depends on the number of aluminum atoms in the framework, the ion-exchange capacity of different zeolites is also very variable. During an ion exchange the charge-compensating cation is replaced by another one, whereby the material remains neutral. Multivalent cations thus replace the respective number of monovalent cations in the zeolite [1]. The ion exchange process may be represented by the following equation [2]:

$$z_A\, B_{(z)}^{z_B^+} + z_B\, A_{(s)}^{z_A^+} \rightleftharpoons z_A\, B_{(s)}^{z_B^+} + z_B\, A_{(z)}^{z_A^+} \qquad \text{(eq. 4.1)}$$

where z_A, z_B are the charges of the exchange cations A and B and the subscripts z and s refer to the zeolite and solution, respectively.

The equivalent fractions of the exchanged cation in the solution (A_S) and zeolite (A_Z) are defined by:

$$A_s = \frac{z_A M_{A_S}}{z_A M_{A_S} + z_B M_{B_S}} \qquad \text{(eq. 4.2)}$$

$$A_z = \frac{z_A m_{A_Z}}{z_A m_{A_Z} + z_B m_{B_Z}} \qquad \text{(eq. 4.3)}$$

where M_{A_S} and M_{B_S} are the number of cations per unit volume of the solution and m_{A_Z} and m_{B_Z} are the molalities of the cations in zeolite. The expression in the denominator of eq. 4.3 is the total ion-exchange capacity of the zeolite.

The preference of the zeolite for one of two ions is expressed by the separation factor, α_B^A, defined by:

$$\alpha_B^A \equiv \frac{A_z B_s}{B_z A_s} \qquad \text{(eq. 4.4)}$$

If ion A is preferred, α_B^A is greater than unity. The separation factor depends on the total concentration of the solution, the temperature, and A_s. It is not affected by choice of concentration units.

Theoretically, the maximum degree of exchange is determined by the net-charge of the zeolite framework, e.g. the number of aluminum atoms per zeolite unit cell, and the number of positive charges of the respective cation. The negative charges of the framework and positive charges from the cations must be equal. However, there are some parameters that can significantly influence the maximum degree of exchange:

1) The size of the cation might be too large to fit into the zeolite pores and the cation is thus excluded from the zeolite pore system. This sieving effect is enhanced by water molecules that usually coordinate the cations in aqueous solutions.
2) In some zeolites cations are located in cages that are accessible only via cage windows confined by small rings. The access of a specific cation to these cages could be limited due to its size, thus leading to an incomplete exchange. Even if the entering cation could pass through the ring the coordination of the cation to be exchanged within the cage might be energetically more favorable, which also leads to an incomplete exchange.
3) For large cations the space inside the zeolite channels and cavities might be restricted, because the space needed for a complete charge compensation by these cations exceeds the available volume within the pores. In this case either some of the water molecules must be stripped from the cations - the cations may be coordinated by framework oxygen atoms - or the number of exchanged cations is less than the theoretically possible maximum number.
4) A factor that apparently increases the degree of exchange into the zeolite above the theoretically maximum value is salt imbibition, i.e. the transfer of not only cations into the zeolite but also of anions associated with the excess incorporation of cations needed for the charge compensation of the anions. This factor is usually neglected, but at very high salt

concentration in the exchange solution or at exchanges from salt melts salt imbibition might occur to significant extents.

5) A similar effect as from salt imbibition might occur when a salt or metal hydroxide/oxide layer is formed on the surface of the zeolite crystals during the ion exchange. The amount of metal cations caught from the solution is thus higher than expected from the maximum number of exchangeable cations (over-exchange). Finally, the resistance of the respective zeolite against exchange solution plays a crucial role. Especially low silica zeolites, such as zeolite A, X, or P, may suffer significant damages by alkaline or acidic exchange solutions, e.g. in some transition metal salt solutions. The zeolite may be damaged by dealumination and partial or complete structure collapse; it may even dissolve partly or completely.
6) A drying or calcination step after the ion exchange enhances the probability of obtaining an amorphous material, since a partly damaged zeolite structure is thermally less stable than an unaffected structure. This fact is often neglected and occasionally a more or less completely decomposed (amorphous) zeolite is used rather than an ion-exchanged zeolite for subsequent catalytic experiments or other investigations (especially for iron-, cobalt-, nickel- and/or copper-exchanged low-silica zeolites) [1].

4.2 Ion-exchanged faujasite for separation applications

Since the development of synthetic zeolites, adsorption has been playing an increasingly important role in gas separation. One of the most important areas for adsorption technology is olefin/paraffin separations. These separations represent a class of most important and also most costly operations in the chemical industry. Various petrochemical streams contain olefins and other saturated hydrocarbons, typically originated from steam cracking units (ethylene production), catalytic cracking units (motor gasoline production), or the dehydrogenation of paraffins [3]. These mixtures of light olefins and paraffins are often used as refinery fuel. Therefore, the recovery of olefins in these streams would be a substantial conservation of resources. Furthermore, federal environmental regulations will require reduction of hydrocarbon emissions from chemical processing facilities to low levels. Waste hydrocarbon streams from polyolefin processes and polymer storage facilities must be dealt with in an environmentally acceptable manner. Processing these small-volume hydrocarbon streams will require selective and economical separation technologies. Traditionally, these separations are performed by cryogenic distillation processes. Although it is reliable and essentially unchallenged for these separations, the necessary low temperatures and high pressures, due to the close relative volatilities of the compounds, make it an energy-intensive separation process [4]. Furthermore, high capital and operating costs are involved in a cryogenic distillation unit. These factors provided the motivation for research toward the development of alternative separation methods. Some processes have been exploited, namely, extractive distillation, molecular sieve adsorption, absorption and metal-based facilitated membrane transport [5]. Among them, the most promising approach to replace cryogenic

distillation is using a facilitated transport membrane (FTM). In these applications, a metallic salt solution is passed through the membrane interior, or the membrane is impregnated with a metallic salt. Metal ions complex olefins on the feed side of the membrane forming π-complexation bonds, the diffusion process is accelerated and the olefins are released on the permeate side [4]. π-complexation bonds are stronger than those formed by van der Waals forces alone. Therefore, it is possible to achieve high selectivity and high capacity for the component to be bound. At the same time, the bonds are still weak enough to be broken by using simple engineering operations such as raising the temperature or decreasing the pressure [6]. In addition, since adsorption would be accomplished at ambient temperature and pressure, success in this development would lead to a major advance in petroleum refining [7]. Therefore, metal-based facilitated transport membranes have been seriously considered for olefin/paraffin separation processes.

Several π-complexation sorbents have been studied, namely, CuCl [8], silver polymer electrolytes [9-10] and Ag^+ dispersed on γ-Al_2O_3 or SiO_2 [11]. In particular CuCl, can be disperse with ease on high-surface-area γ-Al_2O_3 to form nearly monolayer species, and this type of sorbent is already being used in industry for the separation of CO from CO-containing mixtures through π-complexation [12]. The adsorbents used for removal of olefins from a stream must follow some requisites, namely, (1) the active sites of the adsorbent should have a high adsorption selectivity for olefin; (2) the adsorbing bonds should be weak enough to be broken by simple engineering operations so that the regeneration of the adsorbent is possible; and (3) the active sites of the adsorbent should be relatively stable under operating conditions. As for olefin adsorbent, Ag^+ and Cu^+ have been commonly used as active species. But, since Cu^+ has a poor chemical stability and can be easily oxidized to Cu^{2+} in the presence of O_2, losing its adsorption capability, Ag^+ seems a more promising choice for this application. The ion-exchange properties of zeolites are interesting mainly due to the modification of selectivity characteristic exhibited by these materials. In addition, compared with active carbon, resin or carbon fiber, metal ion-modified zeolites can form stronger adsorptions with adsorbate and are usually used for purification [13]. Faujasite is particularly attractive for ion-exchange because of its large pore aperture (7.4Å), large pore volume (0.48 cm^3/g) and a wide range of Si/Al ratios (1 to ∝). Therefore, faujasite with silver ions might be preferred adsorbents to create a facilitated transport membrane for separation applications. Yang et al. [14] studied the effect of Ag content in Ag ion-exchanged Y-zeolite on 1,3-butadiene/1-butene adsorption using Ag-Y with different Si/Al ratios and different degrees of Ag^+/Na^+ exchange (AgNa-Y). AgNa-Y with a Ag content of 34 Ag/u.c. exhibited excellent adsorption performance in terms of both separation factor and uptake rate. Yang, Padin and Munson [15] found out that the purification of butene by removal of trace amounts of butadiene was superior for AgY zeolite than for sorbents based on physical adsorption (NaY). Yang et al. [7] also studied AgY zeolites as selective sorbents for the desulfurization of liquid fuels. They postulated that compared to NaY, AgY adsorbed significantly larger amounts of both thiophene and benzene at low pressures as a result of π-complexation with Ag^+. Guo et al. [13] investigated the removal of C_2H_4 from a CO_2 stream by using $AgNO_3$-modified Y-zeolites. The results show that NaY has poor adsorption selectivities of C_2H_4 from the

C_2H_4/CO_2 stream because of a stronger competition of CO_2 with C_2H_4 for the physical adsorption sites. By modification of zeolites with silver, it is possible to effectively remove C_2H_4 from CO_2 streams due to the strong chemical adsorption sites. The study of silver ion-exchanged faujasite membranes is much narrow than powder samples. Teramoto et al. [16] studied the ethylene/ethane separation by a facilitated transport membrane assigned bulk flow liquid membrane (BFLM), accompanied by permeation of aqueous silver nitrate solution. The selectivity of C_2H_4 over C_2H_6 was 1100, which is ~30 times higher than without the carrier solution. Marrero et al. [5] studied the propylene/propane separation by use of silver nitrate carrier and zirconia porous membranes. They found out that propylene production rate was as high as 3.4 cm^3(STP)/cm^2 min), a stable continuous separation process with silver utilization efficiency as high as 60% and propylene recovery ratio as high as 80%. Although the purity of the recovered propylene is high, it is not sufficient to make polymer grade material. Therefore, the process is envisioned as part of a hybrid system to reduce the energy consumption required by solely cryogenic distillation to separate propylene from mixtures of propane and propylene.

The use of zeolite membranes would be an interesting perspective since they may be coupled with a reactor and can be used for olefin/paraffin separations at a larger scale. Therefore, in this study, faujasite membranes were exchanged with silver ions for that separation. The results will be discussed in this chapter.

4.3 Olefins/metal complexation

The nature of the chemical bond between alkenes and some transition metals was first explained by Dewar in 1951. Applying the molecular orbital theory to silver-ethylene complexes, Dewar postulated that the stability of the metal-olefin complex derives from the interactions between the metal's atomic orbitals and the olefin's hybrid molecular orbitals. Later on, this explanation was enhanced by Chatt and Ducanson upon their study of platinum(II)-olefin complexes. The metal-olefin bonding described by the Dewar-Chatt model is commonly known as π-bond complexation [4]. The Dewar-Chatt description, as applied to Ag(I)-ethylene complexes is shown in figure 4.1.

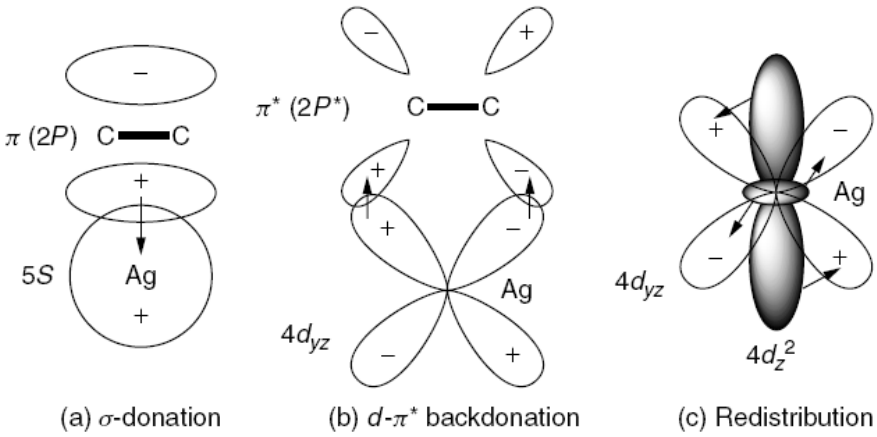

Figure 4.1 - Schematic representation of the C_2H_4-Ag interactions by π-complexation, showing (A) donation of the π-electrons of ethylene to the 5s orbital of Ag (B) backdonation of electrons from the d_{yz} orbitals of Ag to the antibonding π* orbitals of ethylene, and (C) redistribution. C also depicts the possible electron redistribution from the $4d_{z2}$ orbitals (the dumbbell and doughnut-shaped orbitals) to the $4d_{yz}$ orbitals [17].

When the adsorbate molecule approaches Ag^+, an overlap of the vacant outermost s atomic orbital of the metal with the C=C π orbital of the olefin occurs, resulting in a σ component of the bond. Simultaneously, electrons from the full outer d orbital of metal are back-donated to the symmetry-matched π* orbital of olefin, forming a π component of the metal-olefin bond.

The changes in electron populations of the five d orbitals of Ag upon olefin adsorption give further insight into the bonding between metal and olefin. The interactions of the five d orbitals with ethylene are skewed. Orbitals d_{xy}, d_{xz}, and d_{x2-y2} have almost no contribution to the overlap with the π* orbitals of the olefin, since there is no or little change in their electron population upon olefin adsorption. The main depopulation occurs in the d_{yz} and d_{z2} orbitals. This is because the three inactive orbitals (d_{xy}, d_{xz}, and d_{x2-y2}) are pointing in directions perpendicular to that of d_{yz} (in which the three-member ring C-C-M lies); there is little chance for them to overlap with the d_{yz} orbital. The depopulation in the d_{yz} orbital can be explained easily with the classic picture of π-complexation. However, the smaller amount of population decrease in the d_{z2} orbitals is not expected. This phenomenon can be understood with the concept of "electron redistribution". The dumbbell-and-doughnut-shaped d_{z2} orbitals are in the vicinity of the spatial directions of the d_{yz} orbitals and can overlap to some extent with the d_{yz} orbitals. This result indicates that there is considerable electron redistribution between the d_{yz} and d_{z2} orbitals during the metal-olefin bonding. Obviously, electron redistribution from the d_{z2} to the d_{yz} orbitals helped enhance the d-π* back-donation [17].

Several factors determine the tendency for formation of metal-olefin π complexes:

(1) nature of the facilitator – the electron/donor acceptor properties, solubility, and degree of ionization of the facilitator will affect the molar and absolute equilibrium capacity of the solution;

(2) nature of the solvent – the solvent structure and polarity will influence the solubility of both olefin and facilitator as well as the extent of ionization of the facilitator. This ultimately impacts the complexation capabilities of the system;
(3) concentration of the complexing agent – the concentration of the complexing agent influences the absorption capacity and olefin selectivity of the solution via salting in and salting out effects
(4) nature of the olefin – the olefin's electron donor/acceptor behavior, molecular weight, and steric hindrance about the double bond(s) dictate π complex stability
(5) additives to the solution – the chemical nature and concentration of additives can influence olefin-metal and/or solvent-metal interactions
(6) temperature and pressure – increased temperature discourages the exothermic π complexation reaction. Higher pressures increase molar and absolute absorptivity of the solution [4].

Due to reversibility of their complexes and relatively low cost, silver (I) and copper(I) are the most suitable transition metals for olefin/paraffin separations. Other transition metals such as Pd(II), Hg(II), and Pt(II) complex with olefins. However, these facilitators are impracticable due to safety concerns or expense. These agents also form comparatively stable complexes that are difficult to reverse.

4.4 Silver redox behavior

The redox behavior of the transition metal cations in various zeolites was reported earlier. Beyer et al. [18], Jacobs et al. [19], and Gellens et al. [20] studied the kinetics of hydrogen and oxygen uptake by Ag^{+}-Y and Ag^{0}-Y zeolites. Riekert [21] and Ono [22] showed that fully reduced AgY could be reoxidized to give back the original AgY, where the extent of oxidation could be controlled by the experimental conditions. Riekert [21] also studied the redox reaction equilibria in zeolites. According to his investigation, when proton-loaded zeolite was brought into contact with oxygen at 360°C, oxygen was consumed and water desorbed into gas phase. He also found that these redox reactions are reversible.

Jacobs et al. [23] have shown that the reduction of silver zeolites A and Y by vacuum thermal dehydration involves autoreduction of silver ions by intrazeolitic water and lattice oxygen in two clearly defined temperature regions:

(i) **autoreduction in the presence of zeolite water (25° - 250°C)**

$$2(Ag^{+}ZO^{-}) + H_2O \rightarrow 2Ag^{0} + \tfrac{1}{2}O_2 + 2ZOH \qquad \text{(eq. 4.5)}$$

(ii) **autoreduction by oxygen from the zeolite lattice (127-380°C)**

$$2(Ag^{+}ZO^{-}) \rightarrow 2Ag^{0} + \tfrac{1}{2}O_2 + ZO^{-} + Z^{+} \qquad \text{(eq. 4.6)}$$

From the quantitative measurements it was established that the oxidation of the Ag^0-Y zeolite follows the eq. 4.8 if the hydrogen uptakes is given by eq. 4.7

$$2Ag^+ + H_2 \rightarrow 2Ag^0 + 2H^+ \quad \text{(eq. 4.7)}$$

$$2Ag^0 + 2H^+ + \tfrac{1}{2}O_2 \rightarrow 2Ag^+ + H_2O \quad \text{(eq. 4.8)}$$

Depending on the initial silver ion exchange level the Ag^0 atoms so produced are either immobilized at their original sites or migrate and interact with other Ag^0 atoms or Ag^+ ions to form Ag_n^{q+} cationic silver clusters [24].

The interconversion between Ag^+ ions and Ag^0 metal particles became partially reversible from fully reversible with increasing degree of Ag^+ ion reduction. Adsorbed water molecules enhance the conversion of Ag^0 metal particles back into Ag^+ ions and also aid in the migration of cations [25].

4.5 Separation mechanisms

An ideal zeolite membrane can be considered as an infinite two-dimensional zeolite single crystal without any intercrystalline voids, stacking faults, pinholes or cracks. The separation can be achieved by two different mechanisms:

- *Molecular exclusion*, which is the simplest and most convincing mechanism if the components of the mixtures are smaller or larger than the pores of the molecular sieve. The selectivity of this molecular-sieving principle is independent of the loading of the zeolite membrane, i.e., independent of temperature and partial pressure;

- *Solution-diffusion mechanism*, which gives remarkable separation effects. At high pore loading of the zeolite membrane (low temperature, high partial pressures), the strongly adsorbed component fills the pores, and the weakly adsorbed component is excluded. The permeate is enriched in the strongly adsorbed component. At low pore filling (high temperatures, low partial pressures) the weakly adsorbed component, which usually has the higher diffusivity, is enriched in the permeate. The permeation behavior is, therefore, determined by the interplay of adsorption and diffusion effects.

In this study, zeolite Y was selected for separation of olefin/paraffin mixtures. Therefore, the understanding of the permeation process along this material is of utmost importance.

The permeation of hydrocarbons through the Y-type zeolite is known in the literature to proceed via the following five steps [27]:

1. adsorption on the external surface;
2. transport from the external surface into the pores;
3. diffusion between vacant sites;
4. transport out of the pores to the external surface;
5. desorption from the external surface

Both the adsorption and the diffusion processes control the net mass transport through the membrane depending on the polarity of the permeant molecules and the Y framework, on the relative size of the permeant molecules and the mean free volume of in the Y pores [28].

The permeability coefficient (P_A) of a particular gas is defined as the flux (N_A) normalized to the pressure difference across the membrane (ΔP_A), as well as the membrane thickness (l) [26].

$$P_A = N_A \frac{l}{\Delta P_A} \qquad \text{(eq. 4.9)}$$

However, the permeation properties of zeolite membranes are complicated since parallel permeation pathways often exist through intracrystal micropores (zeolitic micropores) and intercrystal gaps [27]. Permeation of molecules larger than the zeolitic pore size is sometimes observed; this suggests the existence of a nonzeolitic pathway having a larger diameter than the zeolite pore [30]. Several factors are also known to affect the permeance of zeolite membranes such Si/Al ratio, removal of adsorbed water and partial decomposition of membranes.

The selectivity (or separation factor) is defined as follows:

$$\alpha_{A/B} = \frac{(C_A/C_B)_{permeate\,side}}{(C_A/C_B)_{feed\ side}} \qquad \text{(eq. 4.10)}$$

where C_A and C_B represent, respectively, molar fractions of gases A and B at the permeate and feed sides of the membrane [31].

4.5.1 Diffusion

The diffusion of molecules in pores can be classified in a number of different regimes depending on the pore diameter (figure 4.2). For large pore diameters, of the order of 1 µm or larger, collisions between the molecules occur much more frequently than collisions with the wall, and *molecular diffusion* is the dominant mechanism. Typically, the diffusion constants of gases are around

10^{-5} $m^2 \cdot s^{-1}$. As the size of the pores decreases, the probability of collisions with the wall increases until the pore size finally becomes smaller than the mean free path (the average distance travelled by a molecule between two collisions) of the gas molecules. At this point, *Knudsen diffusion* prevails and the mobility starts to depend on the dimensions of the pore. When pore size decreases to the range of 20Å and smaller it becomes comparable to the size of the molecules, which will continuously undergo the interaction with the walls. Diffusion in the micropores of a zeolite usually takes place in this regime, and is called *configurational* diffusion [32].

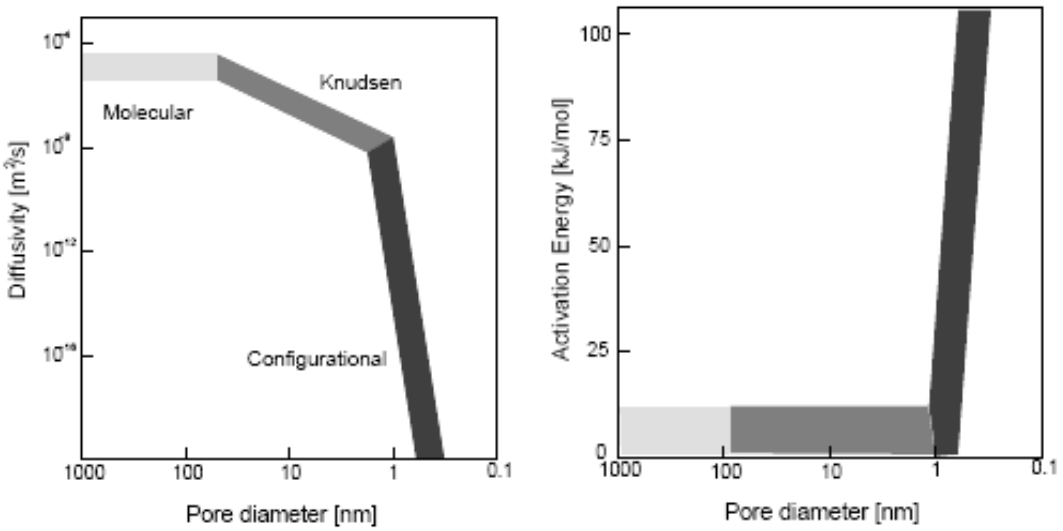

Figure 4.2 - Effect of pore size on the diffusivity and activation energy of diffusion [32].

4.5.2 Diffusion in zeolites

The diffusion pathways in zeolite membranes are defined by the pore structure, channel interconnectivity and tortuosity, and therefore, these are the characteristics responsible for the transport resistance and separation properties of the membranes [33].

The mechanism by which the molecules move through the pores in the configurational regime is comparable to that of surface diffusion of adsorbed molecules on a surface. This is due to the small distance between the molecules and the pore wall and, therefore, the molecules are more or less physically bonded to it. The diffusivity in this regime will depend strongly on the pore structure and size, the interactions between the surface atoms and the diffusing molecules, the shape of the diffusing molecules and the way the channels are connected. As a result, it is very difficult to derive generalized equations relating the aforementioned properties to the diffusion coefficient that one finds for these systems. In fact, the values of these coefficients span in an enormous range from 10^{-8} to as low as 10^{-20} $m^2 \cdot s^{-1}$ [32].

In Knudsen diffusion (without considering porosity and tortuosity terms to simplify) the

coefficient of diffusivity (D_k) is given by:

$$D_k = \frac{2}{3} r_p \sqrt{\frac{8\Re T}{\pi M}} \qquad \text{(eq. 4.11)}$$

where r_p is the radius of the pore, R is the gas constant, T is the temperature and M is the gas molecular weight.

The Knudsen flux, $N_{k,}$ can be expressed by using Fick's law:

$$N_k = -D_k \frac{dC}{dz} = \frac{2}{3} r_p \sqrt{\frac{8\Re T}{\pi M}} \frac{P_h - P_l}{l\Re T} \qquad \text{(eq. 4.12)}$$

where C is the concentration, z is the length, P_h and P_l are the partial pressures on the feed and permeate side, respectively.

The permeability of a membrane due exclusively to Knudsen diffusion, L_k, can then be written as:

$$L_k = \frac{N_k l}{\left(P_h - P_l\right)} = \frac{2}{3\Re T} r_p \sqrt{\frac{8\Re T}{\pi M}} \qquad \text{(eq. 4.13)}$$

where l is the thickness of the membrane.

Therefore, the permeability due exclusively to Knudsen diffusion is independent of feeding pressure. On the other hand, the expression for molecular diffusion, considering unidirectional transport in an isotropic and homoporous medium [34], can be written as:

$$N_v = \frac{r_p{}^2 (P_h^2 - P_l^2)}{16\mu_m \Re T l} \qquad \text{(eq. 4.14)}$$

where μ_m is the dynamic viscosity.

By the definition of permeability (eq. 4.13) and equation (eq. 4.14) we obtain that:

$$L_v = \frac{r_p{}^2}{16\mu_m \Re T} (P_h + P_l) \qquad \text{(eq. 4.15)}$$

i.e., the permeability of a system only with molecular diffusion (L_v) is directly proportional to the feeding pressure.

When both mechanisms are present, the representation of total permeance, L_G, as a function of feeding pressure, P_h, can be represented by the following equation:

$$L_G = aP_h + b \qquad \text{(eq. 4.16)}$$

The parameters *a* and *b* have the following physical meaning:

a – term associated to molecular diffusion.

b – term associated with Knudsen diffusion.

Usually, membranes with a ratio *b/(a+b)* higher than 0.9 can be considered for separation study (the predominant contribution is therefore Knudsen diffusion, typical of small pores). Therefore, this is one of parameters to be used in order to evaluate the quality of the zeolite membranes.

The diffusive and adsorptive properties of alkanes in zeolite molecular sieves have been the focus of numerous experimental and theoretical studies. Not only are these properties important from a fundamental point of view, but also because zeolites are used in a number of important petroleum refining processes such as hydro-isomerization and catalytic cracking. Furthermore zeolites are increasingly used for separation processes. For all these applications the dynamic behavior of the molecules inside the zeolite micropores plays an essential role in determining its catalytic and separating properties. A thorough understanding of this behavior will thus help the design and efficient operation of catalysts [30].

4.6 Experimental

Zeolite membranes for the permeability measurements were synthesized on the surface of porous cylindrical α-Al_2O_3 supports of 6 cm long. The endings of the support tube were sealed with enamel and further covered with Teflon tape to prevent the dissolution of the enamel in the synthesis. The support tubes were then sustained vertically with a Teflon holder in an autoclave, which was filled with aluminosilicate precursor. The parameters of the syntheses are described in table 4.1, where in parenthesis are the labels related to the samples described in tables 2.1 and 3.1 in the previous chapters. Some samples were prepared at the same conditions in order to evaluate the effect of ion exchange. The ion-exchange was performed by contacting the faujasite membranes with an excess amount of 0.1 M aqueous $AgNO_3$ solution, for 1h. This solution contained a cation content that permits the achievement of a 100% exchange. After ion-exchange, the membrane was thoroughly washed with distilled water. The silver-exchanged sample was dried at room temperature and atmospheric conditions. The process is represented in figure 4.3:

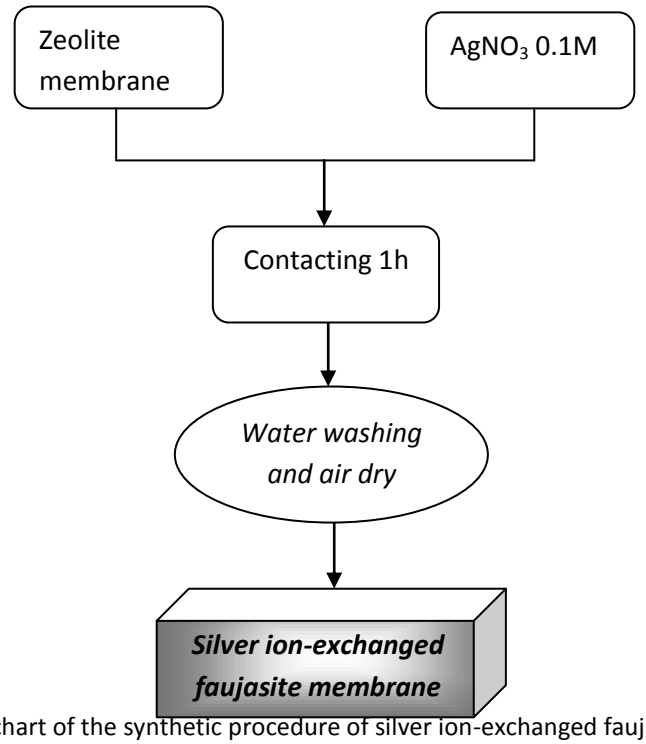

Figure 4.3 – Flow chart of the synthetic procedure of silver ion-exchanged faujasite membranes.

Table 4.1 – Synthesis conditions of the membranes for permeability measurements

Sample	*Compositions (Al_2O_3:SiO_2:Na_2O:H_2O)*	*Temperature (°C)*	*Time (h)*	*Seed Crystals*	*Support (nm)*	*Modification*
S1 (G6)	1:10:14:829	100	5+5*	X20%	1800	-
S2 (G41)	1:19:25:1575					
S3 (G49)	1:5:7:415		5			
S4 (G54)				Y20%		
S5 (G52)					1000	
S6 (G56)			5+5	X20%	1800	
S7 (G57)			5+5+5+5			
S8 (G59#)					1000	
S9 (G62)	1:5:7:415 + 1:9:80:5000	2×100 + 2×80			1800	
S10						
S11						$m_{Ag} = 0.4\ m_Z$
S12						$m_{Ag} = 0.4\ m_Z$ (×2)
S13 (G61)					70	-
S14 (G60)					1000	
S15 (C7)	1:9:80:5000	80			1800	
S16						
S17						
S18						$m_{Ag} = 2\ m_Z$
S19			24+24	Y20%	1000	$m_{Ag} = 0.1\ m_Z$
S20 (C18)				X20%	1800	-
S21 (C20)					1000	
S22 (C23)			24+24+24			
S23						
S24						
S25						$m_{Ag} = 0.1 m_Z$

S26						$m_{Ag} = 0.086$ m_Z
S27						$m_{Ag} = 10\ m_Z$

* It represents the repeat synthesis; # synthesis with rotation

4.7 Results

The Ag^+-exchanged membranes were studied by scanning electron microscopy (SEM) (Hitachi, S-4100) coupled with energy dispersive X-ray spectroscopy (EDS). The membranes were mounted in a holder using carbon glue and a carbon layer was deposited on the surface by sputtering. The SEM analysis gave the images of the faujasite membranes so it was possible to confirm if after exchange they maintained the desired morphology. The EDS analysis gave the elements present in the membranes and, therefore, it was possible to prove the presence of silver in the samples.

The permeability and selectivity of the membranes were tested in Faculty of Engineering of the University of Porto (FEUP) where an experimental unit was setup. It consists in a thermostatic bath in which the membrane cell is placed. The bath is used for high temperature stability and a wider range of operation (between 0 and 150°C). The dimensions of the membrane cell are 12.8 mm internal diameter, 21 mm external diameter and 60 mm length. It has three openings: one for the entrance of the feeding stream, another one for the exit of the adsorbed material and a last one for the exit of permeated material. The temperature is recorded on the membrane's surface under the control of a thermocouple. A vacuum pump was used to attain pressures until 20 mbar on permeate side and it makes possible to collect the permeated gas under a low pressure and its feeding for GC analysis. When it is necessary to evacuate all or part of the unit a rotating vacuum pump is used, since it can reach pressures lower than 1 mbar.

4.7.1 SEM

The silver ion-exchanged membranes were analyzed by SEM and EDS. The images represented in figures 4.4 and 4.5 show that the crystals preserved their morphology.

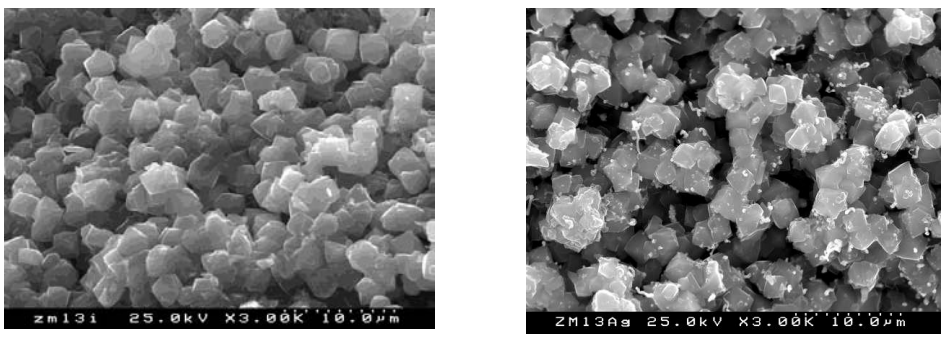

Figure 4.4 - The outside surface of a faujasite membrane prepared at condition S3 in Table 4.1 before (left) and after (right) ion-exchange with silver in a 0.1M $AgNO_3$solution.

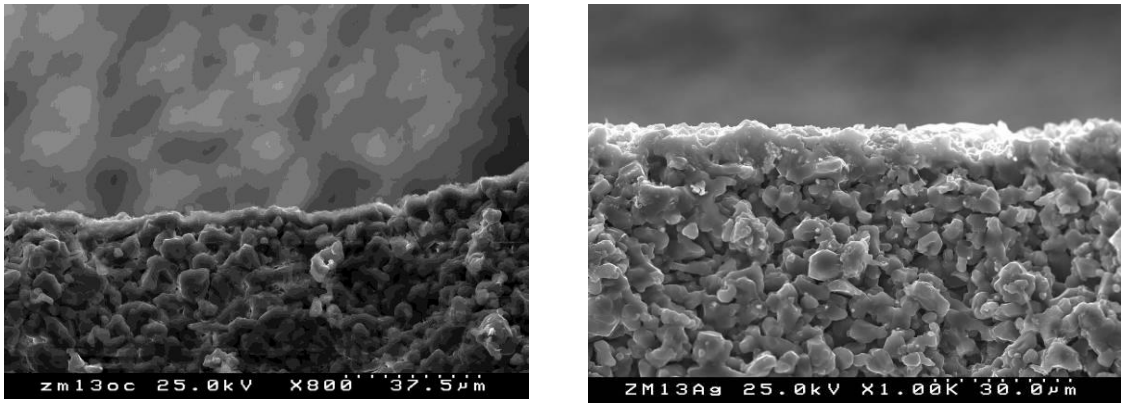

Figure 4.5 - The cross-section of outside surface of a faujasite membrane prepared at condition S3 in Table 4.1 before (left) and after (right) ion-exchange with silver in a 0.1M $AgNO_3$solution.

4.7.2 EDS

EDS results also show the existence of silver in the membrane (figure 4.6).

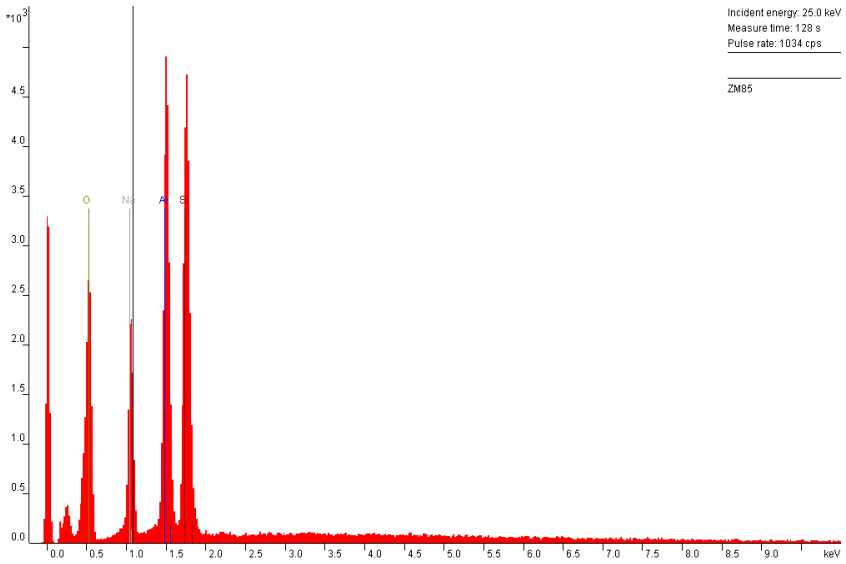

Figure 4.6 – EDS of sample S20.

When the membrane was ion-exchanged with silver it was also observed a reduction of sodium proportionally to silver ions (figures 4.7-4.8). In figure 4.7, the ion-exchange was made by using the same amount of silver as the weight of the zeolite. According to the EDS results, all the sodium was exchanged. When, the amount of silver was reduced to 1/2 of the zeolite weight (figure 4.8), some sodium remained in the membrane.

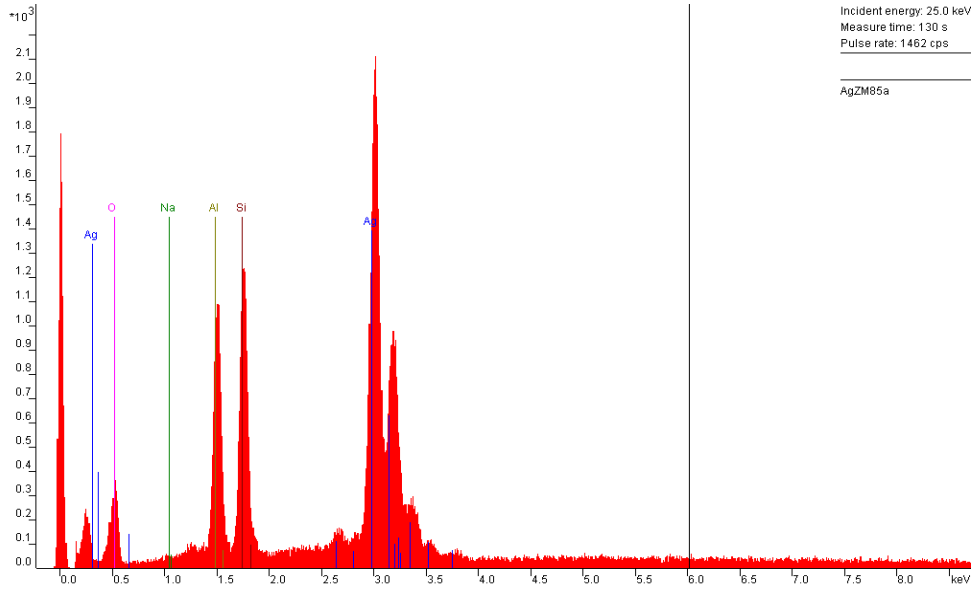

Figure 4.7 – EDS of sample S20 after ion-exchange with 0.1M $AgNO_3$.

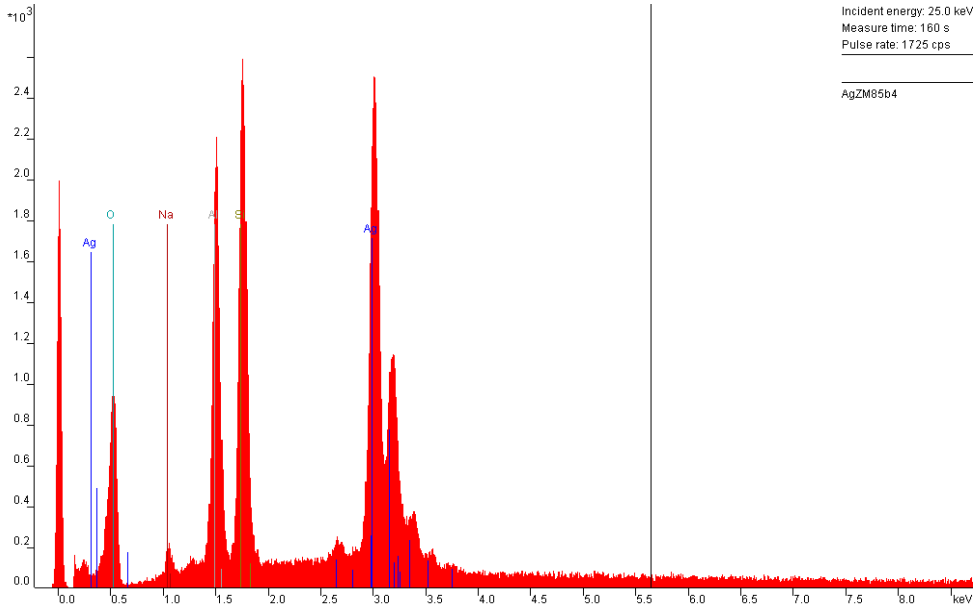

Figure 4.8 – EDS of sample S20 after ion-exchange with 0.1M $AgNO_3$ with less Ag content.

4.7.3 Permeability and selectivity

The quality of the membranes was evaluated by Knudsen diffusion and values as high as 99.5% were obtained. Therefore, it was possible to conclude that high-quality membranes were synthesized. The bi-component selectivity and permeances for streams of propane and propene were measured and were achieved values of 1.0-2.4 and 10^{-6}-10^{-8}, respectively. The results are displayed in Table 4.2.

Table 4.2 – Summary of the results for some of the most promising faujasite membranes synthesized without silver exchange.

			Bi-component selectivity (C_3H_6/C_3H_8)			Permeances (25°C) mol·m^{-2}·s^{-1}·Pa^{-1}		
Membrane	**Nº of layers**	**Knudsen Diffusion (%)**	**20°C**	**40°C**	**70°C**	**N_2**	**C_3H_6**	**C_3H_8**
α-Al_2O_3 support	0		-			2.0×10^{-5}	-	-
S2	2	72.0	1.0			3.5×10^{-6}	3.1×10^{-6}	2.8×10^{-6}
S7	4	91.0	1.3	-	-	3.6×10^{-6}	9.2×10^{-6}	5.0×10^{-6}
S16	4	98.0	1.3	1.2	-	5.5×10^{-6}	-	-
S19	2	99.5	1.9	1.7	2.0	-	-	-
S21	2	93.0	1.2	-	-	1.6×10^{-7}	1.3×10^{-7}	9.0×10^{-8}
S25	3	99.0	1.3	1.2	-	2.6×10^{-7}	1.4×10^{-7}	2.4×10^{-7}
S26	3	99.5	2.4	1.2	1.2	3.2×10^{-7}	1.6×10^{-7}	3.4×10^{-7}
S27	3	99.0	1.3	1.2	-	3.8×10^{-7}	5.4×10^{-7}	1.8×10^{-7}

4.7.3.1 Effect of Ag^+ on bi-component selectivity

The effect of silver ion-exchange on the permeability and selectivity of the high-quality, defect-free membranes was analyzed for a feed with equimolar composition of propane and propylene. The results are summarized in table 4.3, showing that the presence of silver led to an increase in the selectivity.

Table 4.3 – Bi-component selectivity (C_3H_6/C_3H_8) results for faujasite membrane before and after silver ion-exchange, at 25°C.

	Before Ag-exchange Feed: 50% C_3H_6/50%C_3H_8		**After Ag-exchange Feed: 50% C_3H_6/50%C_3H_8**	
Membrane	**Bicomponent permeance** mol·m^{-2}·s^{-1}·Pa^{-1}	**Bicomponent selectivity**	**Bicomponent permeance** mol·m^{-2}·s^{-1}·Pa^{-1}	**Bicomponent selectivity**
S19	1.8×10^{-7}	1.9	-	-
S25	-	1.3	9.0×10^{-8}	1.7
S26	1.5×10^{-6}	2.4	6.2×10^{-7}	6.3

With time, silver ions are reduced and the membrane loses the ability to perform facilitated transport. The use of diluted feeds with small amounts of oxygen was investigated since the presence of

oxygen should minimize silver(I) reduction. Also, diluting propylene/propane mixtures in helium allowed carrying out bi-component selectivity experiments in a much broader pressure driving force range. The use of lower driving forces should minimize viscous flow and increase the membrane performance. The results (Table 4.4) show that using a diluted feed with a very small amount of oxygen, higher selectivities are obtained. Particularly, the membrane prepared in condition S26 has reached a promising selectivity of 8.0.

Table 4.4 – Bi-component selectivity (C_3H_6/C_3H_8) results of silver functionalized membranes for a feed composition of 10%C_3H_6/10%C_3H_8/1%O_2/79%He, at 25°C.

	After Ag-exchange **Feed: 10%C_3H_6/10%C_3H_8/1%O_2/79%He**	
Membrane	**Bicomponent permeance** $mol \cdot m^{-2} \cdot s^{-1} \cdot Pa^{-1}$	**Bicomponent selectivity**
S19	5.0×10^{-8}	4.2
S25	4.2×10^{-8}	3.4
S26	6.2×10^{-7}	8.0

Membranes S19, S25 and S26 all managed to sustain the selectivity values reported on table 4.4 for long periods of time (more than one week of continuous mixture exposure), something that did not occur in previous functionalized membranes (where experiments were always carried out with non-diluted feeds). Bi-component permeability decreased and this was not expected. However, this can be attributed to the fact that Ag^+ might decrease the effective pore size, thus blocking some pores to the hydrocarbons, or to the bonding between Ag^+ and the component on the gas phase.

4.8 Conclusions

Faujasite membranes were ion-exchanged with Ag^+ for propane/propene separation. The EDS analysis proved the presence of silver and the consequent variation on the Na content in the zeolite framework. The SEM analysis showed that the morphology of the faujasite membranes remained after the ion-exchange.

The quality of faujasite membranes was evaluated by Knudsen diffusion and values as high as 99.5% were obtained, which suggests that high quality and defect-free membranes were synthesized.

The permeability and selectivity for propane/propane was studied for samples with and without silver in order to understand the influence of exchange in those parameters. For samples without silver the values measured for bi-component selectivity and permeance were 1.0-2.4 and 10^{-6}-10^{-8}, respectively. After silver exchange and for streams of equimolar composition of propane and propene was observed an increase in selectivity up to 6.3.

With time, due to the reduction of silver ions, the membranes lose the ability to perform facilitated transport. This can be minimized by using diluted feeds in which were present small amounts of oxygen and helium. Under these conditions, the selectivity was increased and was obtained a promising value of 8.0 for sample S26. The selectivity was also maintained for longer periods of time when using diluted feeds. The bi-component permeance was reduced and this can possibly be explained by the decrease in the effective pore size due to the presence of Ag^+. Another reason can be the bonding of Ag^+ and the component on the gas.

4.9 References

[1] F. Schuth, K.S.W. Sing, J. Weitkamp, *Handbook of porous solids*, Vol. 4, Wiley-VCH, 2002, p. 1058

[2] D.W. Breck, *Zeolite Molecular Sieves*, John Wiley & Sons Inc, 1974, New York & London

[3] R.L. Burns, W.J.Koros, J. Membr. Sci. 211 (2003) 299-309

[4] D.J. Safark, R.B. Eldridge, Ind. Eng. Chem. Res. 37 (1998) 2571-2581

[5] J.W. Chang, T.R. Marrero, H.K. Yasuda, J. Membr. Sci. 205 (2002) 91-102

[6] H.Y. Huang, J. Padin, R.T. Yang, J. Phys. Chem B 103 (1999) 3206-3212

[7] R.T. Yang, A. Takahashi, F.H. Yang, Ind. Eng. Chem. Res. 40 (2001) 6236-6239

[8] H.Y. Huang, J. Padin, R.T. Yang, Ind. Eng. Chem. Res. 38 (1999) 2720-2725

[9] J.H. Kim, J. Won, Y. S. Kang, J. Membr. Sci. 237 (2004) 199-202

[10] J.H. Kim, S.M. Park, J. Won, Y.S. Kang, J. Membr. Sci. 236 (2004) 209-212

[11] J. Padin, R.T. Yang, Chem. Eng. Sci. 55 (2000) 2607-2616

[12] J.P. Chen, R.T. Yang, Langmuir 11 (1995) 3450-3456

[13] J. Zhou, Y. Zhang, X. Guo, A. Zhang, X. Fei, Ind. Eng. Chem. Res. 45 (2006) 6236-6242

[14] A. Takahashi, R.T. Yang, C.L. Munson, D. Chinn, Ind. Eng. Chem. Res. 40 (2001) 3979-3988

[15] J. Padin, R.T. Yang, C.L. Munson, Ind. Eng. Chem. Res. 38 (1999) 3614-3621

[16] M. Terramoto, N. Takeuchi, T. Maki, H. Matsuyama, Sep. Purif. Technol. 28 (2002) 117-124

[17] N. Chen, R. T. Yang, Ind. Eng. Chem. Res. 35 (1996) 4020-4027

[18] H. Beyer, P.A. Jacobs, J.B. Uytterhoeven, J. Chem Soc., Faraday Trans., 72 (1976) 674

[19] P.A. Jacobs, J.B. Uytterhoeven, H. Beyer, J. Chem. Soc., Chem. Commun. (1977) 128

[20] L.R. Gellens, W.J. Mortier, J.B. Uytterhoeven, Zeolites 1 (1981) 85

[21] L. Riekert, Ber. Bunsenges. Phys. Chem. 73 (1973), 331

[22] T. Baba, N. Akuiaka, M. Nomura, T. Ono, J. Chem. Soc., Faraday Trans. 89 (1993) 595

[23] P.A. Jacobs, J.B. Uytterhoeven, H. Beyer, J. Chem. Soc., Faraday Trans. 75 (1979) 56-64

[24] G.A. Ozin, M.D. Baker, J. Godber, J. Phys. Chem. 88 (1984) 4902-4904

[25] A. Jayaraman, R.T. Yang, C.L. Munson, D. Chinn, Ind. Eng. Chem. Res. 40 (2001) 4370-4376

[26] R.L. Burns, W.J. Koros, J. Membr. Sci. 211 (2003) 299-309

[27] B. Jeong, Y. Hasegawa, K. Sotowa, K. Kusakabe, Shigeharu, J. Membr. Sci. 213 (2003) 115-124

[28] J. Padin, R.T. Yang, C.L. Munson, Ind. Eng.Chem. Res. 38 (1999) 3614-3621

[29] K. Kusakabe, T. Kuroda, S. Morooka, J. Membr. Sci. 148 (1998) 13-23

[30] I. Kumakiri, T. Yamaguchi, S. Nakao, Ind. Eng. Chem. Res. 38 (1999) 4682-4688

[31] Y. Li, T. Chung, S. Kulprathipanja, AIChE Journal 53 (2007) 610-616

[32] D. Schuring, *Diffusion in Zeolites: Towards a Microscopic Understanding*, Eindhoven: Technische Universiteit Eindhoven, Netherlands (2002) p. 13-15

[33] W.C. Wong, L. T. Y. Au, C.T. Ariso, K.L. Yeung, J. Membr. Sci. 191 (2001) 143-163

[34] A. Mendes, *Laboratórios de Engenharia Química. Reactores em Fase Homogénea, Reactores Catalíticos, Separações Não Convencionais e Tecnologia dos Sólidos Divididos*, FEUP Edições 2002

5 General conclusions and future work

Several faujasite membranes were prepared using gels or clear solutions as starting mixtures. In both approaches pure faujasite membranes were obtained with well-defined and intergrown crystals covering the α-Al_2O_3 support. It was possible to conclude that for both them a suspension of 20% zeolite X crystals was considered to be better for seeding instead of zeolite Y. The use of this latter type of seeds may result in the presence of a second phase or in a lower degree of surface coverage. In addition, the supports of 70 and 1000 nm produced better and thicker membranes relatively to 1800 nm due to the lower porosity.

The effect of each component in the gel was also studied. Since the influence of every constituent is strictly dependent on the other parameters used, its effect was not clear identified. Nevertheless, the composition $1Al_2O_3{:}5SiO_2{:}7Na_2O{:}415H_2O$ resulted in a wider range of variable conditions for the production of defect-free, well intergrown, faujasite membranes.

When gels were used, a prolonged hydrothermal treatment would lead to the formation of zeolite P. Therefore, a suitable time and temperature of synthesis must be selected in order to avoid its formation and produce pure faujasite membranes. A better way to control the layer thickness and phase formation consists in repeating the synthesis. When using only gels, no more than two syntheses could be performed without the presence of zeolite P. However, when using mixed gels and clear solutions at least four syntheses could be performed with an increase in the layer thickness and without reducing the quality and purity of the membrane.

The use of clear solutions as starting mixtures for the preparation of faujasite membranes is preferable to gels. This conclusion is supported by the avoidance of phase transformation to zeolite P and, therefore, the conditions for the preparation of pure membranes with the required phase are broader. This means that longer times and more synthesis could be performed without changing the purity and quality of the membranes. Furthermore, thicker layers of about ~12 μm were obtained comparatively to the use of gels (~10 μm).

Membranes with Knudsen diffusion higher than 98.0% were obtained, therefore, we can prove that the membranes were with high quality and could be used for permeability and selectivity measurements. They exhibited separations factors for a propane/propylene mixture of 1.2-2.4 and permeabilities in the range 1.5×10^{-6} – 1.8×10^{-7}. Ion-exchanging the membranes with silver resulted in an increase in the selectivity (1.7-6.3) as well as a decrease in the permeability (9.0×10^{-8}- 7.7×10^{-7}). Changing the composition of the feed mixture resulted in an improvement in the selectivity of the membranes for propane/propylene mixtures and a value as high as 8.0 was obtained. Therefore, faujasite membranes modified by ion-exchanged with silver are a promising alternative for the separation of olefin/paraffin mixtures.

To explore the potentialities of faujasite membranes to separate mixtures of olefin and paraffins some studies need be performed in future. They are listed below:

1. Fully understand the mechanisms involved in the silver behavior in faujasite membranes, the identification of the oxidation state of silver and verify the presence of silver clusters. Since, only Ag^{+} and not metallic silver has affinity for olefin and forms π-complexation bonds, the reduction of ionic silver might decrease the selectivity of the material for the separation process.
2. Study the optimum amount of silver that must be ion-exchanged to obtain the highest selectivity values.